

UNRAVELLING THE NITROGEN CYCLE IN A PERIODICALLY HYPOXIC ESTUARY

Keryn L. Roberts

Bachelor of Environmental Science (Hons)

A thesis submitted in total fulfilment of the requirements for the degree
of Doctor of Philosophy

Water Studies Centre, School of Chemistry, Faculty of Science



MONASH University

Clayton, Victoria, 3800

January 2014

Under the Copyright Act 1968, this thesis must be used only under the normal conditions of scholarly fair dealing. In particular no results or conclusions should be extracted from it, nor should it be copied or closely paraphrased in whole or in part without the written consent of the author. Proper written acknowledgement should be made for any assistance obtained from this thesis.

Table of Contents

Table of Contents	1-3
Abstract	1-9
Statement of Authorship	1-11
Acknowledgements	1-13
List of Figures	1-15
List of Tables.....	1-19
1. Introduction	1-21
1.1 The Nitrogen Cycle	1-26
1.1.1 Nitrification.....	1-27
1.1.2 Denitrification.....	1-28
1.1.3 Dissimilatory nitrate reduction to ammonium (DNRA)	1-29
1.1.4 Anaerobic Ammonium Oxidation (Anammox)	1-31
1.2 Review of the current literature on hypoxia in coastal waters	1-33
1.3 Project aims, hypotheses and thesis structure	1-36
1.4 References	1-38
2. Hypoxic events stimulate nitrogen recycling in a shallow salt-wedge estuary: The Yarra River estuary, Australia	2-45
2.1 Declaration for Thesis Chapter Two	2-47
2.2 Abstract	2-49
2.3 Introduction	2-51
2.4 Methods	2-54
2.4.1 Site description.....	2-54
2.4.2 Sampling protocol.....	2-54
2.4.3 Light and sediment chlorophyll a.....	2-55
2.4.4 Sediment flux.....	2-56

2.4.5	<i>Denitrification and DNRA</i>	2-57
2.4.6	<i>Sediment profiles</i>	2-59
2.4.7	<i>Analytical methods</i>	2-59
2.4.8	<i>Constituent deviations</i>	2-60
2.4.9	<i>Statistical analysis</i>	2-61
2.5	Results	2-62
2.5.1	<i>Verification of the isotope pairing technique assumptions</i>	2-62
2.5.2	<i>The behaviour of oxygen in the Yarra River estuary</i>	2-63
2.5.3	<i>Light and sediment chlorophyll a</i>	2-65
2.5.4	<i>Sediment fluxes and nutrient behaviour</i>	2-66
2.5.5	<i>Denitrification and DNRA</i>	2-70
2.6	Discussion	2-74
2.6.1	<i>Development of hypoxia in the Yarra River estuary</i>	2-74
2.6.2	<i>DON production during hypoxia</i>	2-74
2.6.3	<i>Net efflux of NH_4^+ during hypoxia</i>	2-76
2.6.4	<i>Denitrification and DNRA in the Yarra River estuary</i>	2-77
2.7	Concluding Remarks	2-82
2.8	Acknowledgements	2-83
2.9	References	2-84

3. Denitrification and DNRA in sediment profiles combining the isotope pairing technique and diffusive equilibrium in thin layer gels
..... **3-91**

3.1	Abstract	3-93
3.2	Introduction	3-95
3.3	Methods	3-98
3.3.1	<i>Site Description</i>	3-98
3.3.2	<i>Sampling</i>	3-98
3.3.3	<i>Intact core incubations</i>	3-98

3.3.4	<i>Micro-profiles of nitrate reduction pathways</i>	3-100
3.3.5	<i>Analytical methods</i>	3-103
3.3.6	<i>Modelling Fe and S profiles</i>	3-107
3.4	Results	3-110
3.4.1	<i>Intact core experiments</i>	3-110
3.4.2	<i>Micro-profiles in intact cores - September 2012</i>	3-110
3.4.3	<i>Micro-profiles in intact cores - January 2013</i>	3-113
3.4.4	<i>Comparison of N₂O and ¹⁵N-N₂ method</i>	3-116
3.4.5	<i>Modelling Fe and S</i>	3-118
3.5	Discussion	3-119
3.5.1	<i>Long-term oxygen treatment in intact cores</i>	3-119
3.5.2	<i>Sediment profiles of denitrification and DNRA</i>	3-119
3.5.3	<i>Comments on the combined ¹⁵N-N₂ and ¹⁵N-NH₄⁺ DET gels</i>	3-122
3.5.4	<i>Comparison of the N₂O and ¹⁵N-N₂ denitrification methods</i>	3-126
3.6	Concluding Remarks	3-129
3.7	Acknowledgements	3-130
3.8	References	3-131

4. Increased rates of dissimilatory nitrate reduction to ammonium (DNRA) under aerobic conditions in a periodically hypoxic estuary are linked to the availability of iron 4-137

4.1	Abstract	4-139
4.2	Introduction	4-141
4.3	Methods	4-144
4.3.1	<i>Site description and sampling</i>	4-144
4.3.2	<i>Slurry preparation</i>	4-144
4.3.3	<i>NO₃⁻ slurries</i>	4-144
4.3.4	<i>pH adjusted slurries</i>	4-145
4.3.5	<i>NO₃⁻ storage and Sulfur oxidising bacteria</i>	4-145

4.3.6	<i>Fe²⁺ and S²⁻ slurries</i>	4-146
4.3.7	<i>Fe²⁺ long term slurries</i>	4-147
4.3.8	<i>Analytical methods</i>	4-148
4.3.9	<i>Statistical analyses</i>	4-149
4.4	Results	4-150
4.4.1	<i>NO₃⁻ slurries</i>	4-150
4.4.2	<i>pH adjusted slurries</i>	4-151
4.4.3	<i>NO₃⁻ storage and Sulfur oxidising bacteria</i>	4-152
4.4.4	<i>Fe²⁺ and S²⁻ slurry experiments</i>	4-152
4.4.5	<i>Fe²⁺ long term slurries</i>	4-154
4.5	Discussion	4-157
4.5.1	<i>The influence of NO₃⁻ on DNRA</i>	4-157
4.5.2	<i>pH influence on nitrate reduction pathways</i>	4-157
4.5.3	<i>NO₃⁻ storage and Sulfur oxidising bacteria</i>	4-159
4.5.4	<i>Fe²⁺ and S²⁻</i>	4-160
4.5.5	<i>DNRA linked to availability of Fe²⁺</i>	4-160
4.6	Concluding Remarks	4-164
4.7	References	4-165
5.	Discussion and Concluding Remarks	5-171
5.1	Chapter summaries	5-173
5.1.1	<i>Chapter Two: Hypoxic events stimulate nitrogen recycling in a shallow salt-wedge estuary: The Yarra River estuary, Australia</i>	5-173
5.1.2	<i>Chapter Three: Denitrification and DNRA in sediment profiles combining the isotope pairing technique and diffusive equilibrium in thin layer gels</i>	5-175
5.1.3	<i>Chapter Four: Increased rates of dissimilatory nitrate reduction to ammonium (DNRA) under aerobic conditions in a periodically hypoxic estuary are linked to the availability of iron</i>	5-176
5.2	Nitrogen cycling in the Yarra River estuary during hypoxia	5-178
5.3	Recommendations for Future Research	5-183

5.4 References	5-185
6. Appendix	6-187

Abstract

The incidences of hypoxia ($O_2 < 100 \mu\text{mol-O}_2 \text{ L}^{-1}$) in coastal waters have been increasing in recent decades, largely due anthropogenic induced eutrophication. Hypoxia not only has a detrimental impact on aquatic life it can also lead to a shift in nutrient transformation pathways. To date, several studies have focused on hypoxia in deep coastal waters, such as, Chesapeake Bay ($> 10 \text{ m}$) and the Baltic Sea ($> 60 \text{ m}$) or oxygen minimum zones ($100 - 1000 \text{ m}$). To my knowledge no studies currently exist on the influence of hypoxia on nitrogen cycling in a shallow ($3 - 5 \text{ m}$) salt wedge estuary. The Yarra River estuary, Australia, the study site for this research, is a shallow salt wedge estuary prone to periods of hypoxia during low freshwater inflow events. The estuary is a conduit for the transport of nitrogen into Port Phillip Bay; a nitrogen limited system. This research investigated the influence of hypoxia on nitrogen cycling within the Yarra River estuary through two means;

- 1) an observational survey of *in situ* nitrogen behaviour in addition to the measurement of nitrate (NO_3^-) reduction pathways, denitrification and dissimilatory NO_3^- reduction to ammonium (DNRA) using the ^{15}N isotope pairing technique.
- 2) an in depth experimental study on the behaviour of denitrification and DNRA under changing oxygen conditions alongside availability of reductants using microelectrodes combined with diffusive equilibrium in thin layer (DET) gels and slurries.

The observational survey of the Yarra River estuary was carried out from September 2009 through to March 2011. The estuary was a source of dissolved organic nitrogen (DON) and ammonium (NH_4^+) during hypoxic conditions using deviations from conservative mixing (Δ). Dissolved inorganic carbon (DIC) was used as a proxy for mineralisation and comparison of the *in situ* nutrient measurements (whole system) and DIC and NH_4^+ fluxes from intact core incubations showed that NH_4^+ was regenerated more efficiently relative to DIC under hypoxic conditions. For the whole system, mean $\Delta\text{DIC} : \Delta\text{NH}_4^+$ ratios under oxic (85 ± 33) and hypoxic (20 ± 3) conditions were significantly different. The more efficient NH_4^+ regeneration during hypoxia was due to a disconnect between mineralisation and nitrogen removal via nitrification-denitrification coupling due the cessation of nitrification; DNRA was not a significant contributor.

Unexpectedly, DNRA increased in the presence of oxygen in the water column; the mean DNRA rate under oxic conditions ($124 \pm 31 \mu\text{mol m}^{-2} \text{h}^{-1}$) was significantly higher than rates during hypoxia ($0.6 \pm 0.1 \mu\text{mol m}^{-2} \text{h}^{-1}$). High DNRA rates led to a significant decrease in the denitrification : DNRA ratio under oxic (19 ± 18) conditions compared to the ratio during hypoxia (144 ± 48).

In contradiction to the current paradigm, the increased DNRA rates can be explained by the presence of Fe^{2+} in the sediment supported by data from both intact cores and slurries. The coupling of Fe^{2+} oxidation and NO_3^- reduction to NH_4^+ has been observed in a bacterial study Weber *et al.* (2006) however to our knowledge this is the first study to observe this process in intact estuarine sediments. The absence of DNRA under hypoxic conditions was explained by the presence of high S^{2-} concentrations and the binding of FeS, removing available Fe^{2+} for DNRA.

This study identified the impact of hypoxia on the nitrogen removal capacity of a shallow estuarine system; the nitrogen removal capacity of the Yarra River estuary was low with $< 4 \%$ of the dissolved inorganic nitrogen load removed when compared to 20 - 50 % removal presented for other estuarine systems. During hypoxia the removal of NO_3^- via denitrification was minimal compared with the efflux of NH_4^+ from the sediment due to the disconnect between NH_4^+ removal via nitrification-denitrification coupling and mineralisation.

Importantly, this study observed DNRA under conditions not considered to be conducive toward this process; Fe^{2+} oxidation coupled to NO_3^- reduction to NH_4^+ . The Yarra River estuary is prone to high inputs of iron both filterable and colloidal, and as such has high concentrations of Fe^{2+} in the porewaters under oxic conditions. In large rivers such as the Amazon and Mississippi, significant amounts of iron may be deposited on the continental shelf, leading to high rates of iron reduction and Fe^{2+} accumulation within the porewaters. It is therefore possible that Fe-driven DNRA observed in the Yarra River estuary may occur at globally significant rates within these diagenetic hotspots.

Statement of Authorship

I hereby declare that this thesis contains no material which has been accepted for the award of any other degree or diploma at any university or academic institution. To the best of my knowledge, this thesis contains no material previously published or written by another person, except where due reference is made in the text of the thesis.

I certify that I have made reasonable efforts to secure copyright permissions for third-party content included in this thesis and have not knowingly added copyright content to my work without the owner's permission.

This thesis includes one manuscript (Chapter Two) that has been published in the peer reviewed journal the '*Journal of Limnology and Oceanography*.' In addition, parts of Chapters Three and Four have been compiled and submitted for review in the peer reviewed journal '*Geochimica et Cosmochimica Acta*.' The ideas, development, field work, experiments and writing of the thesis and manuscripts were the responsibility of myself, the candidate, under the supervision of Dr. Perran Cook, Associate Professor Michael Grace and Professor Bradley Eyre in the Water Studies Centre at Monash University.

The inclusion of co-authors on the manuscripts reflects work that came from collaboration between researchers and acknowledges the input into team-based research. A declaration of authorship for the published manuscript outlining the contribution of the principle author (myself) and co-authors is given for Chapter Two. I have re-numbered sections of the published manuscript (Chapter Two) to generate consistent presentation in the thesis. Moreover, additional figures have been included to justify the mention of unpublished data in the manuscript.

Signed:

A solid black rectangular box used to redact the author's signature.

Dated: 28-01-2014

Acknowledgements

The completion of my doctoral research would not have been possible without the assistance and support of a number of people.

Firstly, I would like to thank my principal supervisor Dr. Perran Cook for his support throughout my project. I would like to thank him for introducing me to estuarine science and throughout my project for questioning, discussing, reading, re-reading and advising when needed. Despite some scatterbrain moments and his trademark 'Perran' hover in the lab, his endless enthusiasm for biogeochemistry has been an asset during my PhD. I would also like to acknowledge the support of my associate supervisors Assoc. Prof Mike Grace and Prof. Bradley Eyre for their guidance and helpful advice when called upon.

I am very grateful for the assistance of Vera Eate in the field and laboratory in the early stages of my project. I would also like to thank Adam Kessler, Michael Bourke, Erinn Richmond, Lawton Shaw, Wei Wen Wong, Todd Scicluna and David Kerr for their assistance in the field under all weather conditions. Victor Evrard and the analytical laboratory staff Keralee Browne and Tina Hines provided invaluable assistance and guidance with regard to laboratory work. I would like to acknowledge Ryan Woodland for his assistance with the more complicated statistical analyses.

Importantly, I would like to thank the lunch time crew who all helped me maintain balance and sanity (in part) throughout my PhD for which I am very grateful. I am thankful for the support and friendship of my fellow colleagues throughout my PhD; Vera Eate, Keralee Browne, Wei Wen Wong, Adam Kessler, Erinn Richmond, Michael Bourke, Terry Chan, Doug Russell, Yassir Arafat, Daryl Holland, Peter Faber, Todd Scicluna, Samantha Imberger, Fiona Warry, Chuyen Phung, Ryan Woodland, Victor Evrard and Kellie Vanderkruk.

Last but not least, I would like to acknowledge the support of my family and friends. I appreciate the time taken to critically review presentations, manuscripts and the final thesis. In particular, I would like to thank Richard Roberts for his assistance with a number of unusual projects that I brought home when the science workshop were not able to help. Without the respite my family and friends provided throughout my PhD I would not have been able to finish. *Thanks Keryn*

List of Figures

- Figure 1.1** Map of the global spread of coastal hypoxia and oxygen minimum zones Source: <http://www.wri.org/project/eutrophication/map>, Diaz and Breitburg (2009)_____ 1-21
- Figure 1.2** The impact of oxygen depletion in coastal waters adapted from Diaz *et al.* (2013)_____ 1-22
- Figure 1.3** The Yarra River Catchment, land use and tributaries. Map sourced from the ‘Yarra River Action Plan’ - Melbourne Water Corporation_____ 1-24
- Figure 1.4** Simplified representation of a salt wedge estuary under stratified and mixed conditions_____ 1-25
- Figure 1.5** Simplified representation of the nitrogen cycle_____ 1-26
- Figure 1.6** Study design and thesis structure_____ 1-35
- Figure 2.1** The Yarra River estuary, Australia. Sampling of the estuary extended from (A) the Johnston St Bridge to (E) the Bolte Bridge. The fixed sites are located at the upstream extent of the salt wedge (B) at Bridge Road, (C) Scotch College, and (D) Morell Bridge_____ 2-56
- Figure 2.2** Assumptions of the isotope pairing technique - validation____ 2-62
- Figure 2.3** Temporal variation in total inflow (ML day⁻¹), salinity, temperature (°C), and dissolved oxygen (µmol L⁻¹) in 2008_____ 2-63
- Figure 2.4** Spatial variation in salinity and dissolved oxygen saturation (%) in the bottom waters of the Yarra River estuary_____ 2-64
- Figure 2.5** Euphotic depth (Zeu; m) with respect to turbidity (NTU) in the water column_____ 2-65
- Figure 2.6** Deviations from conservative mixing of ΔNH_4^+ , ΔNO_x and ΔDON with respect to oxygen concentration (µmol L⁻¹)_____ 2-67
- Figure 2.7** Sediment-water nutrient fluxes from September 2009 to March 2011. DIC, O₂, NH₄⁺ and NO_x flux (±SE; µmol m⁻² h⁻¹). Denitrification and DNRA (± SE; µmol m⁻² h⁻¹)_____ 2-68
- Figure 2.8** (A) Ratio of $\Delta\text{DIC} : \Delta\text{NH}_4^+$ with respect to dissolved oxygen concentration (µmol L⁻¹) in the bottom water of the Yarra River estuary, (B) Ratio of DIC flux : NH₄⁺ flux ± SE from the sediment_____ 2-69

- Figure 2.9** Mean NH_4^+ and DIC (\pm SE; $\mu\text{mol L}^{-1}$) with respect to sediment depth (cm) at (A) Morell Bridge, (B) Scotch College, and (C) Bridge Road; (D) DIC with respect to NH_4^+ _____ 2-70
- Figure 2.10** DNRA, denitrification (\pm SE; $\mu\text{mol m}^{-2} \text{h}^{-1}$) and the denitrification : DNRA ratio in response to dissolved oxygen concentration ($\mu\text{mol L}^{-1}$) _____ 2-72
- Figure 2.11** ^{15}N -DNRA potential (\pm SE; $\mu\text{mol m}^{-2} \text{h}^{-1}$) with respect to salinity, bottom water oxygen and DIC flux _____ 2-73
- Figure 2.12** Conceptual diagram of the Yarra River estuary when conditions are: (A) a hypoxic stratified salt wedge, and (B) oxic where the salt and freshwater are mixed _____ 2-75
- Figure 3.1** The gel sampler preparation before re-hydration, insertion into the sediment and removal and slicing _____ 3-103
- Figure 3.2** Denitrification, DNRA ($\mu\text{mol m}^{-2} \text{h}^{-1}$) and the denitrification : DNRA ratio for the control oxic treatment and the treated cores represented by open shapes for the first 11 days hypoxic (\circ) and subsequent oxic duration (\square) _____ 3-111
- Figure 3.3** September 2012 micro-profiles denitrification (N_2O), DNRA ($^{15}\text{N-NH}_4^+$), NO_3^- , NH_4^+ , S^{2-} , and O_2 with respect to depth (cm) for anoxic, sub-oxic and oxic conditions _____ 3-112
- Figure 3.4** January-February 2013 micro-profiles of DNRA ($^{15}\text{N-NH}_4^+$), denitrification ($^{15}\text{N-N}_2$), denitrification : DNRA ratio ($^{15}\text{N-N}_2$: $^{15}\text{N-NH}_4^+$), NO_3^- , NH_4^+ , Fe_{tot} , S^{2-} and O_2 with respect to sediment depth (cm) for long-term anoxic conditions, short-term oxic conditions and oxic conditions _____ 3-114
- Figure 3.5** Calibration of $^{15}\text{N-N}_2$ in DET gels after exposure to air, (A) calibration standards of starting $^{15}\text{N-N}_2$ standards (B) Actual $^{15}\text{N-N}_2$ and calculated $^{15}\text{N-N}_2$ from the equation _____ 3-116
- Figure 3.6** Comparison of the $^{15}\text{N-N}_2$ ($\mu\text{mol L}^{-1}$) and N_2O ($\mu\text{mol L}^{-1}$) method under oxic and anoxic conditions _____ 3-117
- Figure 3.7** Modelled profiles of S^{2-} , FeOOH , Fe^{2+} and FeS with respect to depth under oxic and anoxic conditions _____ 3-118
- Figure 3.8** Conceptual model of denitrification and DNRA in the Yarra River estuary under (A) oxic and (B) anoxic conditions _____ 3-122

- Figure 3.9** Lateral diffusion of an analyte into a gel from the sediment. (A) Lateral diffusion in a single gel sheet and (B) lateral diffusion into a gel separated into discrete slices before deployment. 3-123
- Figure 3.10** Figure 5 from Harper *et al.* (1997). Concentration changes over time in a DET gel for the diffusive case. 3-124
- Figure 3.11** (A-B) Gel sampler design used in the present study and (C-D) modified sampler design to include discrete slices and reduce peak flattening. 3-126
- Figure 4.1** Denitrification, DNRA ($\mu\text{mol L-slurry h}^{-1}$) and denitrification : DNRA ratio with respect to NO_3^- concentration ($\mu\text{mol L}^{-1}$). 4-150
- Figure 4.2** Denitrification, DNRA ($\mu\text{mol L-slurry h}^{-1}$) and the denitrification : DNRA ratio for the control and pH treatment. 4-151
- Figure 4.3** NO_3^- concentration profiles and ^{15}N -DNRA with sediment depth for February, April, May and June 2010 for (A-B) Bridge Road, (C-D) Scotch College and (D-E) Morell Bridge. 4-153
- Figure 4.4** Denitrification, DNRA ($\mu\text{mol L-slurry h}^{-1}$) and the denitrification : DNRA ratio for the control, Fe^{2+} and S^{2-} treatments. 4-154
- Figure 4.5** $^{15}\text{N-NH}_4^+$, NO_x , NO_2^- , $^{15}\text{N-N}_2$ ($\mu\text{mol L-slurry}^{-1}$) with respect to time. Dissolved Fe^{2+} ($\mu\text{mol L}^{-1}$) in the water column and 0.5 mol L^{-1} HCl-extractable Fe^{2+} ($\mu\text{mol L-slurry}^{-1}$) over time (h) in 5 % estuarine slurries. 4-156
- Figure 4.6** pH range in the bottom waters of the Yarra River estuary over the observational period from September 2009 to March 2011 (Chp. 2) with respect to salinity. 4-158
- Figure 4.7** Formation of Fe^{3+} (Fe(III) oxy-hydroxides; $\mu\text{mol L-slurry}^{-1}$) with respect to time for the control and Fe treatments. 4-162
- Figure 5.1** Conceptual model of the nitrogen cycle in the Yarra River estuary under stratified hypoxic conditions and well mixed oxic conditions. 5-174
- Figure 5.2** The influence of freshwater inflow on nutrient loads entering the estuary; NO_x ($\text{NO}_3^- + \text{NO}_2^-$), NH_4^+ and Total nitrogen (TN; kg-N day^{-1}). Data from Melbourne Water Corporation. 5-179
- Figure 5.3** Simplified pathways in the iron and sulfur cycles linked to DNRA. a) DNRA, b) Fe^{2+} oxidation, c) Fe^{3+} reduction, d) FeS precipitation, e) sulfur oxidation, f) sulfate reduction. 5-180

List of Tables

Table 3.1	Outline of methods used in bulk measurements and sediment profiles including sample pre-treatment, standards and analysis techniques	<u>3-106</u>
Table 3.2	Kinetic reactions included in the model	<u>3-108</u>
Table 3.3	Parameters used to model Fe and S under varying oxygen conditions	<u>3-109</u>
Table 5.1	Summary of common hypotheses described in the literature that explain the behaviour of DNRA. The reasoning is provided for the exclusion (×) or supported (□) hypothesis with respect to the behaviour of DNRA in the Yarra River estuary and (?) represents a plausible or indirect predictor of DNRA	<u>5-182</u>

1. Introduction

The incidence of hypoxia ($< 100 \mu\text{mol-O}_2 \text{ L}^{-1}$) in coastal and marine waters has increased in recent decades on a global scale (Fig 1.1; Diaz and Breitburg, 2009). In a mixed or partially mixed system, dissolved oxygen in the surface waters is mixed throughout the water column. However, when a system becomes stratified or is over enriched in nutrients (eutrophic) oxygen can become depleted (Diaz, 2001). Stratification induced hypoxia is caused by the isolation of dense bottom waters (driven by either salinity or temperature differences in the water column) minimising exchange with oxygen rich surface waters (Diaz, 2001). Alternatively, eutrophication-induced hypoxia occurs when the consumption of oxygen by rapid rates of organic matter decomposition exceed the rate of oxygen replenishment (Diaz, 2001). Coastal waters heavily impacted by anthropogenic eutrophication can experience these hypoxic events as a result of increased primary productivity and respiration that are coincident with an enrichment of nutrients (Diaz and Rosenberg, 2008; Paerl *et al.*, 1998). The depletion of oxygen to levels below $\sim 60 \mu\text{mol-O}_2 \text{ L}^{-1}$ (or $2 \text{ mg-O}_2 \text{ L}^{-1}$) can have a detrimental impact on aquatic life, and can lead to mass mortality of aquatic organisms and a decrease in the overall biodiversity within coastal waters (Fig 1.2; Diaz *et al.*, 2013; Herbert, 1999; Ritter and Montagna, 1999). Aside from the biological pressures of hypoxia or anoxia ($0 \mu\text{mol-O}_2 \text{ L}^{-1}$) on these environments, oxygen depletion can alter physio-chemical processes resulting in a shift in nutrient transformation pathways (Herbert, 1999).



Figure 1.1 Map of the global spread of coastal hypoxia (●) and oxygen minimum zones (grey shading). *Source:* <http://www.wri.org/project/eutrophication/map>, Diaz and Breitburg (2009).

Estuarine systems are transitional zones between freshwater and marine environments and are highly productive habitats (Bianchi, 2007). The convergence of fresh and saline waters make these environments prone to hypoxia; in estuarine systems where freshwater inflow dominates mixing, stratification can occur and saline bottom waters can become isolated and depleted in oxygen. Estuaries are of great significance for marine environments as they can act as a nutrient filter preventing further transport of excess nutrients into coastal waters (Bianchi, 2007; Paerl *et al.*, 1998). Our interest in nutrient sinks, particularly in marine environments, has increased in recent years due to the pressure of anthropogenic nutrient inputs on coastal waters (Kemp *et al.*, 1992; Martin *et al.*, 2010). Nutrient transformation processes are heavily influenced by oxygen concentration and the depletion of oxygen in these environments can alter bioavailable nutrient budgets. The impacts of hypoxia on aquatic flora and fauna has been studied extensively, however, the influence of these conditions on nutrient cycling and removal processes is not well understood (Fig. 1.2; Paerl *et al.*, 1998).

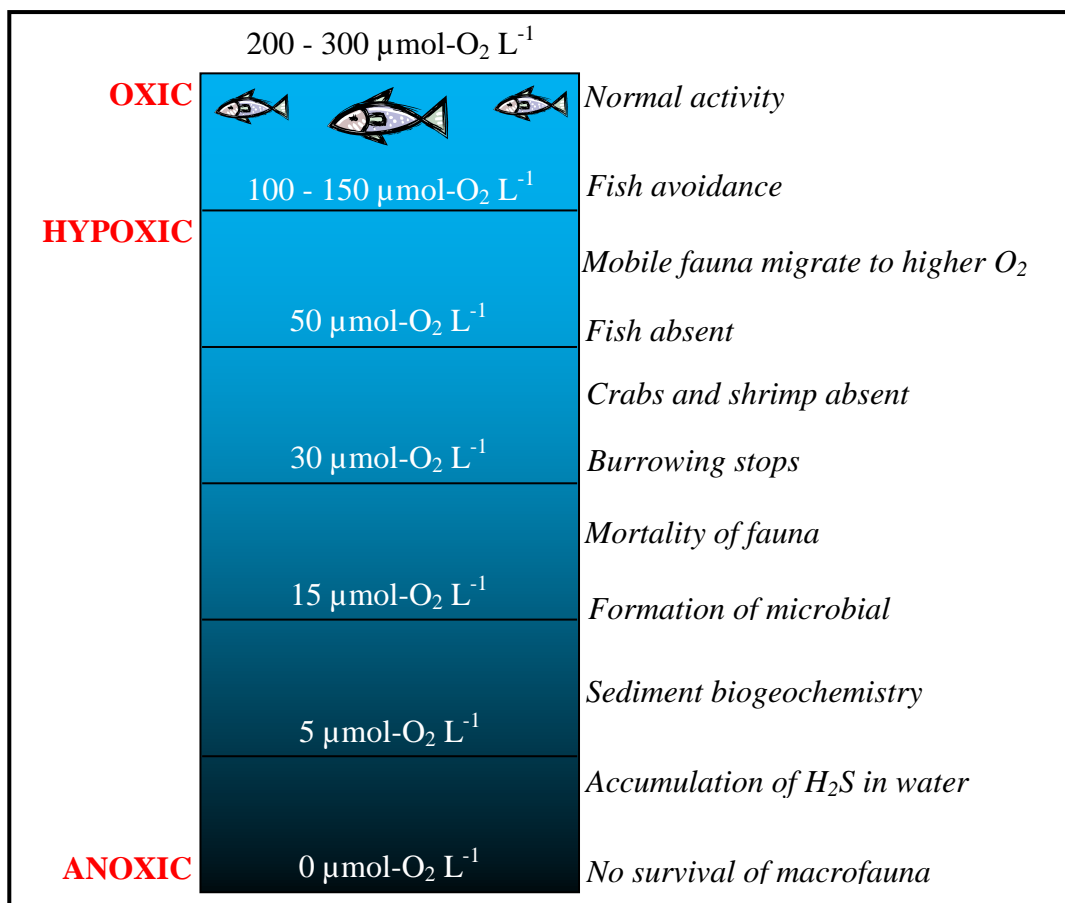


Figure 1.2 The impact of oxygen depletion in coastal waters adapted from Diaz *et al.* (2013).

Nitrogen is an abundant gas in the atmosphere and can be found in nature in a variety of forms, many of which are bioavailable; however, anthropogenic sources of inorganic nitrogen have significantly increased in recent years (Canfield *et al.*, 2005). Because many marine systems are nitrogen limited (cellular growth is constrained by bioavailable nitrogen), increased nitrogen loads from anthropogenic sources can result in eutrophication, enhanced primary productivity and subsequent anoxia of the water column (Bianchi, 2007; Howarth and Marino, 2006). Nitrogen processing within an estuarine system can potentially reduce the amount of bioavailable nitrogen reaching coastal waters (Soetaert and Herman, 1995). However, the effectiveness of an estuary to act as a sink is dependent on a number of factors such as the residence time of the water, oxygen concentrations and mixing of the water column (Bianchi, 2007).

The Yarra River estuary, Melbourne, Australia was the study site for this research and is the area of convergence between the Yarra River Catchment and Port Phillip Bay (Fig. 1.3). For most of the year the Yarra River estuary exhibits a 'salt wedge' structure (Fig 1.4; Beckett *et al.*, 1982). A salt wedge estuary develops through density stratification where a dense layer of salt water is present on the bottom and the seaward freshwater flow remains on the surface, characterised by a strong salinity gradient both vertically and horizontally (Fig. 1.4; Bianchi, 2007; Dyer, 1973). A small amount of mixing occurs at the interface between the fresh and salt water due to the convergence of the two water bodies. Freshwater outflow from the river and, to a lesser extent, tidal movements determine the magnitude of the salt wedge within the estuary and its residence time, particularly in the case of the study site (Beckett *et al.*, 1982; Ibanez *et al.*, 1997).

Estuaries like the study site are particularly prone to hypoxia in the summer due to decreased rainfall and reduced freshwater inflows. These conditions decrease the resistance between the fresh and salt water layers leading to the isolation of the saline bottom waters and reduced oxygen transfer (Diaz and Rosenberg, 2008; Ritter and Montagna, 1999). Unlike oxygen minimum zones estuarine systems are generally shallow (< 10 m) and oxygen consumption and nutrient cycling, in addition to water column processes, are heavily influenced by sediment biogeochemistry. In the presence of high nutrient and organic carbon concentrations, respiration in both the sediment and water column is enhanced leading to further

depletion of oxygen and eventually resulting in hypoxia (Diaz and Rosenberg, 2008; Martin *et al.*, 2010; Paerl *et al.*, 1998). In far South Eastern Australia, freshwater flows are predicted to decrease, because a rise in global temperatures will increase evaporation from the catchment, reducing the amount of run off reaching stream environments (Hughes, 2003). Reduced freshwater inflows and increased severity of drought in this region will lengthen the residence time of salt water within the estuary (Hughes, 2003; Ibanez *et al.*, 1997), in addition to the pressure of anthropogenic eutrophication the incidences and duration of hypoxia will increase. Biological and chemical processes are governed by oxygen availability, therefore it is important to understand the physical drivers of oxygen dynamics in an estuarine system to completely understand nitrogen cycling.

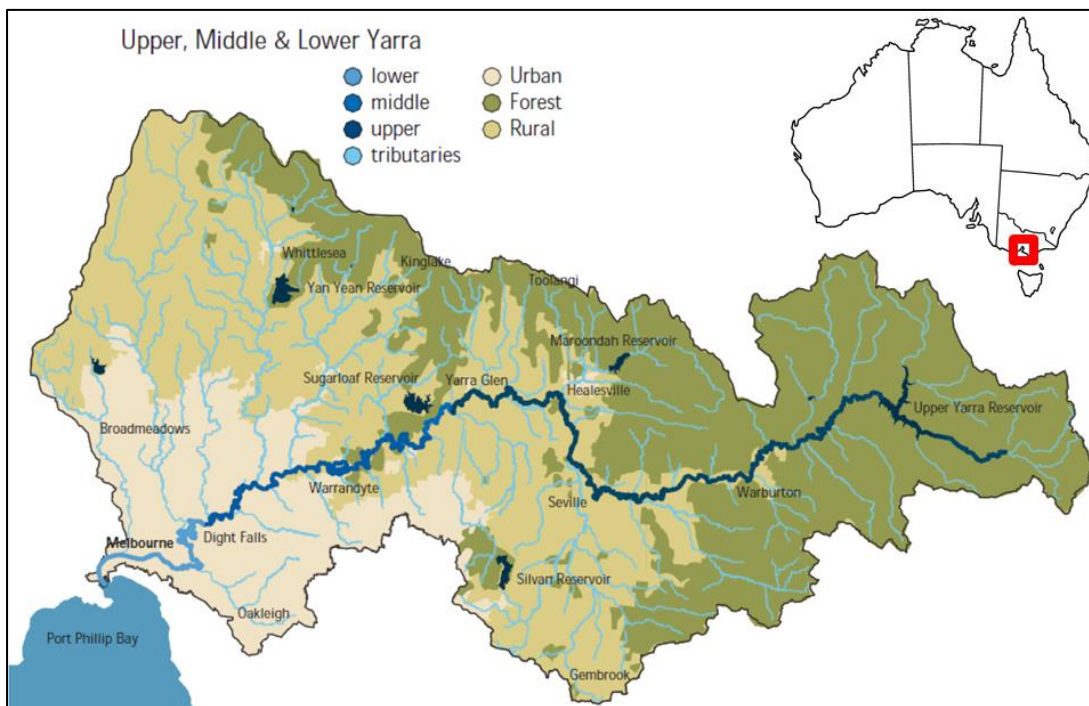


Figure 1.3 The Yarra River Catchment, land use and tributaries are described in the key. The study site, in South Eastern Australia, is in the lower reach of the river where the river meets saline water (mid-upper estuary) from Port Phillip Bay. Map sourced from the ‘Yarra River Action Plan’ - Melbourne Water Corporation.

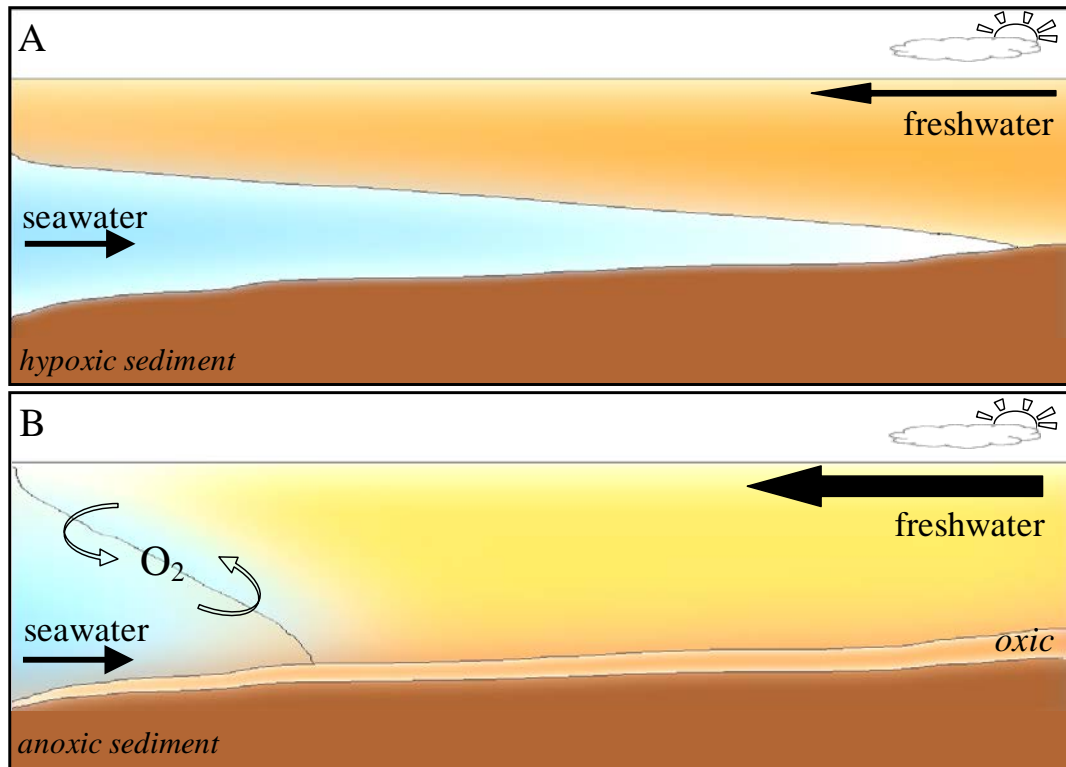


Figure 1.4 Simplified representation of a salt wedge estuary (A) low freshwater inflow induced stratification and (B) high freshwater inflow induced mixing.

This introductory chapter summarises the nitrogen cycle with particular focus on nitrate (NO_3^-) reduction pathways: denitrification, dissimilatory NO_3^- reduction to ammonium (DNRA) and anammox. In addition, a review of the current literature is provided on nitrogen processing in oxygen-depleted environments and importantly how this research will fill important, current knowledge gaps. Finally, the research aims and hypotheses are presented in addition to an outline of the thesis and the approach taken to address these research aims in the Yarra River estuary.

bioavailable (Bianchi, 2007). Nitrogen remineralisation occurs when dissolved or particulate organic nitrogen is broken down into inorganic forms through the decay of organisms with the assistance of heterotrophic bacteria (Bianchi, 2007). In contrast, biological assimilation is an important process in the immobilisation of nitrogen because nitrogen is taken up by the organism and incorporated into its cellular material. Assimilation can occur under both oxic and anoxic conditions (Canfield *et al.*, 2005). Although these processes are important stages of the nitrogen cycle, they were not the focus of this research. Four processes are commonly referred to throughout the thesis and are described in detail in this introductory chapter; nitrification (a precursor to NO_3^- reduction), denitrification (N-removal), DNRA (N-recycling) and anammox (N-removal).

1.1.1 Nitrification

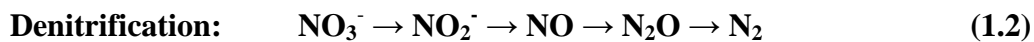
There are two main sources of NO_3^- for NO_3^- reduction pathways; NO_3^- in the overlying water column and NO_3^- produced via nitrification within the sediment. Nitrification is the conversion of NH_4^+ (derived from external inputs, DNRA or remineralisation) to NO_3^- in the presence of oxygen (Eq. 1.1, Fig. 1.5; Bianchi, 2007; Canfield *et al.*, 2005; Herbert, 1999). The aerobic process proceeds via a stepwise reaction that is bacterially mediated by species such as *Nitrosomonas* sp. and *Nitrobacter* sp. (Eq. 1.1; Wetzel, 2001). Although nitrification is typically an aerobic process it can occur at oxygen concentrations as low as $\sim 10 \mu\text{mol L}^{-1}$; however, under these conditions the process is inefficient and it can lead to the production of nitrous oxide (N_2O^1), a strong greenhouse gas, via the breakdown of the hydroxylamine intermediate (Toyoda *et al.*, 2009; Wetzel, 2001). Nitrification is an important precursor to NO_3^- reduction pathways such as denitrification, anammox and DNRA.



¹ The behaviour of N_2O is not described in this thesis, however N_2O data can be found in the attached Appendix.

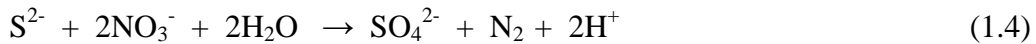
1.1.2 Denitrification

Heterotrophic denitrification, the conversion of NO_3^- to N_2 gas via a number of intermediates, utilises organic carbon as an electron acceptor and the N_2 produced is lost to the atmosphere and effectively removed from the system (Eq. 1.2, 1.3, Fig. 1.5). The anaerobic process is carried out by a number of bacteria such as *Paracoccus* sp., *Pseudomonas* sp. and *Bacillus* sp. (Bianchi, 2007; Canfield *et al.*, 2005; Wetzel, 2001). The main enzymes involved in the denitrification process are nitrogen reductases which require cofactors of iron and molybdenum that are catalytically reduced and oxidised throughout the reaction (Shah and Brill, 1977). The end product of denitrification is most commonly N_2 ; however, under changing environmental conditions, for example O_2 or pH, the process can be incomplete and the end product may be N_2O (Canfield *et al.*, 2005; Wetzel, 2001). Although denitrification is an anaerobic process, the production of N_2 is observed under aerobic conditions in the water column due to a strong coupling between nitrification and denitrification at the oxic-anoxic boundary layer.

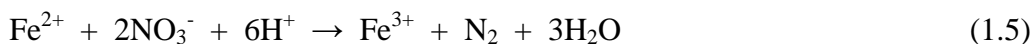


Alternatively, chemoautotrophic denitrification is the reduction of NO_3^- to N_2 gas using sulfur or ferrous iron (Fe^{2+}) as the electron donor (Eq. 1.4, 1.5; Fossing *et al.*, 1995; Reyes-Arila *et al.*, 2004; Straub *et al.*, 1996). Prolonged periods of hypoxia can lead to the development of sulfide (S^{2-}) in the water column and sediment; S^{2-} is toxic to many aquatic microorganisms leading to the inhibition of conventional NO_3^- reduction pathways (Reyes-Arila *et al.*, 2004). Under reducing conditions, sulfur oxidising bacteria reduce NO_3^- to N_2 gas concurrently with the oxidation of toxic hydrogen sulfide to sulfate (SO_4^{2-}), effectively reducing sulfide toxicity and removing nitrogen (Eq. 1.4; Jensen *et al.*, 2009; Lavik *et al.*, 2009). Species of sulfur oxidising bacteria involved in chemoautotrophic denitrification

include *Thiobacillus denitrifican* sp. and *Sulfurimonas denitrifican* sp. which can also survive over a wide range of temperatures and pH conditions (Shao *et al.*, 2010). Under reducing conditions nitrification-denitrification coupling is unlikely to occur due to the inhibitory effects of S^{2-} on nitrification, and low (no) oxygen that typically causes reducing conditions (Joye and Hollibaugh, 1995).

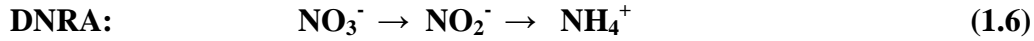


A number of heterotrophic denitrifiers can utilise Fe^{2+} as an energy source in the absence of organic carbon (Eq. 1.5, Fig. 2; Benz *et al.*, 1998; Straub *et al.*, 1996). In addition, *Thiobacillus denitrifican* sp. are able to oxidise FeS as an energy source for denitrification (Straub *et al.*, 1996). Currently there is limited research on the involvement of Fe^{2+} in NO_3^- reduction and the majority of the work in this field has been based on isolating and understanding the role of the bacteria in this process (Benz *et al.*, 1998; Burgin and Hamilton, 2007; Straub *et al.*, 1996). If organic carbon becomes depleted under low oxygen conditions an existing denitrifying community could continue to remove nitrogen from the system via Fe^{2+} oxidation.



1.1.3 Dissimilatory nitrate reduction to ammonium (DNRA)

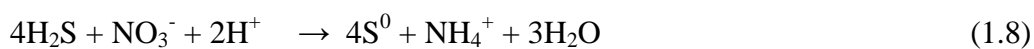
DNRA, an alternative NO_3^- reduction pathway to denitrification, converts NO_3^- to NH_4^+ under hypoxic or anoxic conditions. Consequently, the nitrogen remains bioavailable in the system (Eq. 1.6, Fig. 1.5; An and Gardner, 2002). In a system with low bioavailable nitrogen inputs, DNRA may be an important supply mechanism of NH_4^+ for marine communities (An and Gardner, 2002). Alternatively, the retention of bioavailable nutrients within the system could enhance eutrophication and result in the estuarine system acting as a nitrogen source (Paerl *et al.*, 1998; Zopfi *et al.*, 2001).



Heterotrophic DNRA is carried out by fermentative bacteria (*E. coli* sp.) and is observed in environments with high labile organic carbon availability (Tiedje, 1988; Yin *et al.*, 2002). Cole and Brown (1980) observed the accumulation of acetate and formate, by-products of glucose fermentation, with NO_2^- reduction to NH_4^+ in strains of *E. coli* sp., a pathway later confirmed by Bonin (1996) (Eq. 1.7). Moreover, several studies have observed an increase in heterotrophic DNRA when NO_3^- concentrations are low and labile carbon concentrations are high. For example, Fazzolari *et al.* (1998) observed an increase in DNRA after the addition of labile organic carbon increasing from 2 to 25 % of total NO_3^- reduction owing to the increase in the C/N ratio.



Alternatively, chemoautotrophic DNRA is important in highly reducing environments and is largely controlled by available reductants such as S^{2-} and Fe^{2+} (Eq. 1.8, 1.9). A number of sulfur-oxidizing bacteria, for example *Thioploca* sp. and *Beggiatoa* sp., can store and reduce NO_3^- to NH_4^+ as a secondary metabolic pathway (Otte *et al.*, 1999; Schulz and Jorgensen, 2001). Some of these sulfur oxidising bacteria involved in DNRA are motile and can store NO_3^- in large vacuoles then move into the S^{2-} zone to carry out DNRA (Fossing *et al.*, 1995; Hinck *et al.*, 2007; Zopfi *et al.*, 2001). The role of these bacteria in DNRA was evident in a study in Aarhus Bay, Denmark, where DNRA only occurred in the presence of sulfur oxidising bacteria (Sayama *et al.*, 2005).



Although Fe^{2+} oxidation has been previously linked to denitrification, studies on its involvement in NH_4^+ production via DNRA are limited. In wetland sediments Weber *et al.* (2006) showed that *Geobacter* sp. could both reduce Fe^{3+} and couple the oxidation of Fe^{2+} with the reduction of NO_3^- to NH_4^+ (Eq. 1.10). Hou *et al.* (2012) postulated that Fe^{2+} could be a controlling factor on DNRA, inferred through a strong correlation of NH_4^+ production and reactive iron oxide concentrations in Texas coastal sediments. However, to my knowledge, to date there have been no reports of direct measurements of this process in the natural environment and there is no information on whether estuaries receiving high inputs of available Fe^{2+} can support Fe-driven DNRA.



1.1.4 Anaerobic Ammonium Oxidation (Anammox)

Anammox is the anaerobic oxidation of NH_4^+ to form N_2 gas. Anammox bacteria use NO_2^- as an electron acceptor in the conversion of NH_4^+ to N_2 via hydroxylamine and hydrazine (toxic intermediates; Eq. 1.11, Fig. 1.5; Kuypers *et al.*, 2003). A number of anammox bacteria have been identified, including *Ca. Brocadia* sp., *Ca. Kuenenia* sp and *Ca. Scalindua* sp., and can be found in a number of environments including waste water treatment plants and in marine and estuarine sediments (Dale *et al.*, 2009). Generally temperature and NO_2^- supply (regulated by organic carbon or NO_3^- in the overlying water column) regulate rates of anammox (Nicholls and Trimmer, 2009; Risgaard-Petersen *et al.*, 2004; Trimmer *et al.*, 2003). This anaerobic process has been identified in several estuarine environments including, but not limited to, the Thames and Colne estuaries, England, and Randers Fjord, Denmark (Nicholls and Trimmer, 2009; Risgaard-Petersen *et al.*, 2004; Trimmer *et al.*, 2003).



Although many of these processes (nitrification, denitrification, DNRA and anammox) have been studied extensively in estuarine environments, there is limited research on the impacts of oxygen depletion on NO_3^- reduction pathways, particularly in shallow estuarine environments. In addition, the relative rates of these processes can potentially determine whether nitrogen is removed or recycled within an estuary. Hence, understanding the mechanism behind a shift in NO_3^- reduction pathways from denitrification to DNRA, for example, will assist in the future management of nitrogen loads in periodically hypoxic estuaries, like the Yarra River estuary.

1.2 Review of the current literature on hypoxia in coastal waters

Hypoxia has been observed naturally in a number of environments including lakes, estuaries and oceans. However, occurrences of anthropogenic induced hypoxia have been increasing in coastal waters, driven by eutrophication (Diaz, 2001). Although nutrient enrichment is often the cause of hypoxia, it can also change the way in which nutrients are cycled within these zones, further compounding the issue.

Mineralisation, and the production of NH_4^+ , occurs under all oxygen conditions; in the presence of oxygen, the NH_4^+ produced via mineralisation may be removed via nitrification-denitrification coupling (Kemp *et al.*, 2005; Kemp *et al.*, 1990). However, hypoxic conditions lead to the cessation of nitrification and an efflux of NH_4^+ from the sediment resulting in a shift in the main form of nitrogen from NO_3^- to NH_4^+ (Christensen *et al.*, 2000; Rysgaard *et al.*, 1994). In addition, less NO_3^- is removed due to the breakdown of nitrification-denitrification coupling (Diaz, 2001). Several studies have observed the increase in recycling of NH_4^+ during hypoxia in coastal environments (Childs *et al.*, 2002; Christensen *et al.*, 2000; Kemp *et al.*, 2005; Rysgaard *et al.*, 1996; Soetaert and Herman, 1995).

A shift in the main form of nitrogen from NO_3^- to NH_4^+ can reduce NO_3^- removal and increase competition for available NO_3^- by alternate NO_3^- reduction pathways. A shift from removal processes such as denitrification and anammox to DNRA under hypoxic conditions could lead to further recycling. The Baltic Sea, for example, is prone to hypoxia in ~20 % of the bottom waters (> 60 m) due to salinity stratification (Conley *et al.*, 2002; Jantti and Hietanen, 2012). In a study of the Baltic Sea, a shift was observed in the relative contribution of denitrification and DNRA, where DNRA dominated at low oxygen conditions due to the development of sulfide and inhibition of denitrification and the presence of sulfur oxidising bacteria (*Beggiatoa* sp.) (Jantti and Hietanen, 2012).

Oxygen minimum zones occur at depths of 100 - 1000 m below productive surface waters (Lam and Kuypers, 2011; Wyrski, 1962). The largest zones are located in the North and South Pacific, the Arabian Sea and the South Atlantic (Diaz and Rosenberg, 2008; Lam and Kuypers, 2011). In addition, hypoxia has also been observed on continental shelves such as the Baltic Sea, Kattegat Sea, Black Sea, Bay of Bengal, Gulf of Mexico, Chesapeake Bay and East China Sea (Diaz, 2001; Diaz

and Rosenberg, 2008). Although oxygen minimum zones make up only a small percentage of the ocean volume (~1 %) they are responsible for 30 -50 % of the nitrogen lost from the world's oceans via processes such as denitrification or anammox (Lam and Kuypers, 2011). In the past, denitrification was considered to be the dominant NO_3^- reduction pathway in these hypoxic environments. However, more recent studies of the eastern tropical South Atlantic and the eastern tropical South Pacific oxygen minimum zones have identified anammox to be a more important process (Kuypers *et al.*, 2005; Lam and Kuypers, 2011; Thamdrup *et al.*, 2006). Most of the nitrogen removed in oxygen minimum zones is sourced from NO_3^- in deep, upwelling water masses and through mineralisation of organic material from overlying surface waters (Lam and Kuypers, 2011; Lam *et al.*, 2009).

Bottom water hypoxia has been observed in several estuaries including the Pamlico River and Neuse River estuaries in North Carolina, America (Buzzelli *et al.*, 2002; Paerl *et al.*, 1998; Stanley and Nixon, 1992). However, to date, studies of nitrogen cycling in hypoxic zones have focused on deep coastal waters or oxygen minimum zones in oceans (Jantti and Hietanen, 2012; Kuypers *et al.*, 2005; Lam and Kuypers, 2011). The behaviour of nitrogen in these deep waters is unlikely to be reflected in a shallow estuarine system, like the Yarra River estuary, due to the long residence time of the hypoxic waters within deep coastal systems and the reduced role of sediment biogeochemistry. In Australia, more than 50 % of the population live < 150 kilometres from the coastline (<http://www.ga.gov.au/marine/coasts-estuaries.html>), a statistic reflected globally (Hinrichsen, 1998), making these environments particularly prone to anthropogenic eutrophication. To my knowledge there is no detailed information on the impact of hypoxia on nitrogen cycling in a shallow estuarine system. Although further investigations are essential to fully understand nitrogen cycling in hypoxic estuaries, the research presented in this thesis provides the first insight into the behaviour of nitrogen cycling in a periodically hypoxic estuary, the Yarra River estuary.

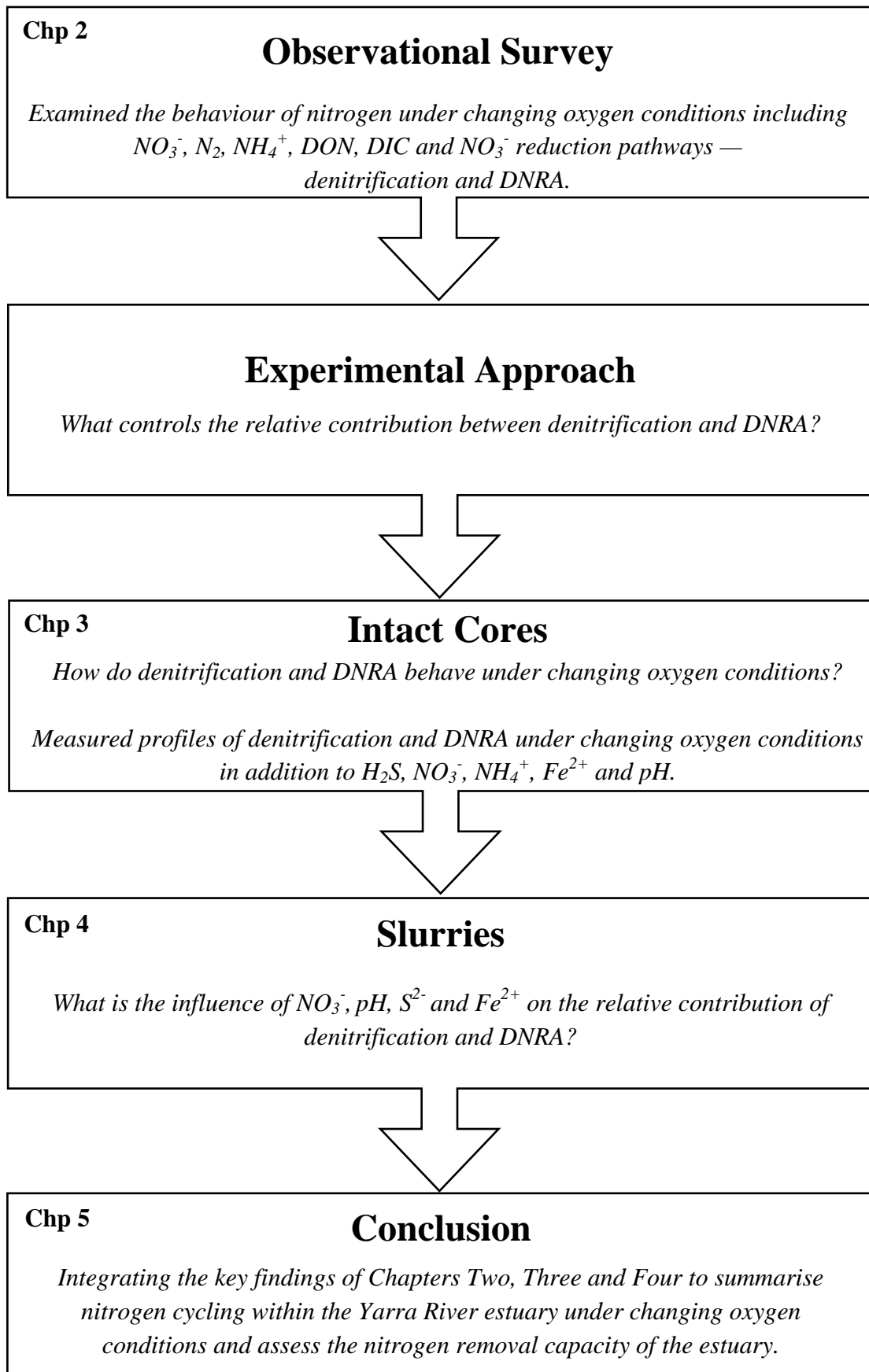


Figure 1.6 Study design and thesis structure, highlighting key points of research addressed in each chapter.

1.3 Project aims, hypotheses and thesis structure

An outline of the thesis structure is provided in Figure 1.6 and will be referred to in the proceeding discussion. This research aimed to determine the impact of hypoxia on the nitrogen cycle in the periodically hypoxic estuary, the Yarra River estuary, Australia. Three specific research questions are addressed in this thesis:

- (1) Does bottom water hypoxia within the Yarra River estuary promote the recycling or removal of nitrogen?
- (2) What are the main mechanisms of nitrogen removal or recycling during hypoxic conditions?
- (3) Does oxygen concentration influence the relative contribution of NO_3^- reduction pathways within the estuary, and if so, what is the controlling mechanism behind this shift?

Chapter Two addresses research questions (1) and (2) through investigating the behaviour of nitrogen under *in situ* conditions. An observational survey of the estuary was performed from September 2009 through to March 2011 (Chp. 2, Fig 1.6). *In situ* concentrations of nutrients were measured and rates of denitrification and DNRA determined at three fixed sites using the ^{15}N isotope pairing technique (Nielsen 1992, Dalsgaard 2000). It was hypothesised that hypoxic events would lead to the recycling of nitrogen through two mechanisms:

- (i) The breakdown of nitrification-denitrification coupling, leading to less nitrogen removed as N_2 and more nitrogen released into the water column as NH_4^+ due to the cessation of nitrification.
- (ii) DNRA would be an important process during a hypoxic event, promoted by reducing and NO_3^- limited conditions resulting in more NH_4^+ recycled than N_2 removed.

Unexpectedly the observational study yielded interesting findings that contradict the current literature on the behaviour of denitrification and DNRA under hypoxic conditions (Fig 1.6, 2.10). As a result of these observations, Chapters Three and Four are focused on understanding the cause of this shift between denitrification and DNRA under changing oxygen conditions, yielding research question (3).

Chapter Three aimed to replicate the behaviour of denitrification and DNRA in the observational study (Chp. 2) under laboratory conditions via long term oxygen experiments. In addition, denitrification ($^{15}\text{N-N}_2$ or N_2O), DNRA ($^{15}\text{N-NH}_4^+$), NO_3^- , $\text{NH}_4^+_{\text{tot}}$ ($^{14}\text{N-NH}_4^+ + ^{15}\text{N-NH}_4^+$), O_2 , S^{2-} and Fe^{2+} were measured in profiles, using diffusive equilibrium in thin layer gels or microelectrodes, under different oxygen conditions. Profiles were measured in September 2012 and January-February 2013. During this time, two denitrification methods were used, and as such, a comparison of these methods and a method for measuring denitrification in profile is provided in this chapter.

Chapter Four describes the behaviour of denitrification and DNRA in slurries, which enabled manipulation of the availability of NO_3^- and reductants such as S^{2-} and Fe^{2+} , in addition to environmental conditions such as pH. An alternate hypothesis was formulated from the results of Chapters Three and Four to explain the unexpected behaviour of denitrification and DNRA in the Yarra River estuary identified in Chapter Two (Fig. 1.6).

Finally, Chapter Five summarises the major findings of this thesis, describes the impact of hypoxia on the nitrogen cycle and the potential implications of these findings in similar environments (Fig. 1.6). This chapter also discusses recommendations for future research in the Yarra River estuary and this field.

1.4 References

- An S. and Gardner W.S. (2002) Dissimilatory nitrate reduction to ammonium (DNRA) as a nitrogen link, versus denitrification as a sink in a shallow estuary (Laguna Madre/ Baffin Bay, Texas). *Marine Ecology Progress Series* **237**, 41-50.
- Beckett R., Easton A.K., Hart B.T., and McKelvie I.D. (1982) Water movement and salinity in the Yarra and Maribyrnong Estuaries. *Australian Journal of Marine and Freshwater Research* **33**, 401-415.
- Benz M., Brune A., and Schink B. (1998) Anaerobic and aerobic oxidation of ferrous iron at neutral pH by chemoheterotrophic nitrate reducing bacteria. *Archives of Microbiology* **169**, 159-165.
- Bianchi T.S. (2007) *Biogeochemistry of Estuaries*. Oxford University Press, New York.
- Bonin P. (1996) Anaerobic nitrate reduction to ammonium in two strains isolated from coastal marine sediment: A dissimilatory pathway. *FEMS Microbiology Ecology* **19**, 27-38.
- Burgin A.J. and Hamilton S.K. (2007) Have we overemphasized the role of denitrification in aquatic ecosystems? A review of nitrate removal pathways. *Frontiers in Ecology and the Environment* **5**, 89-96.
- Buzzelli C.P., Luettich Jr. R.A., Powers S.P., Peterson C.H., McNinch J.E., Pinckney J.L., and Paerl H.W. (2002) Estimating the spatial extent of bottom-water hypoxia and habitat degradation in a shallow estuary. *Marine Ecology Progress Series* **230**, 103-112.
- Canfield D.E., E K., and Thamdrup B. (2005) *Aquatic Geomicrobiology*. Elsevier Academic Press, San Diego.
- Childs C.R., Rabalais N.N., Turner R.E., and Proctor L.M. (2002) Sediment denitrification in the Gulf of Mexico zone of hypoxia. *Marine Ecology Progress Series* **240**, 285-290.
- Christensen P.B., Rysgaard S., Sloth N.P., Dalsgaard T., and Schwaerter S. (2000) Sediment mineralization, nutrient fluxes, denitrification and dissimilatory nitrate reduction to ammonium in an estuarine fjord and sea cage trout farms. *Aquatic Microbial Ecology* **21**, 73-84.
- Cole J.A. and Brown C.M. (1980) Nitrite reduction to ammonia by fermentative bacteria: a short circuit in the biological nitrogen cycle. *FEMS Microbiology Letters* **7**, 65-72.

- Conley D.J., Humborg C., Rahm L., Savchuk O.P., and Wulff F. (2002) Hypoxia in the Baltic Sea and basin-scale changes in phosphorus biogeochemistry. *Environmental Science and Technology* **36**, 5315-5320.
- Dale O.R., Tobias C.R., and Song B. (2009) Biogeographical distribution of diverse anaerobic ammonium oxidizing (anammox) bacteria in Cape Fear River Estuary. *Environmental Microbiology* **11**, 1194-1207.
- Diaz R.J. (2001) Overview of hypoxia around the world. *Journal of Environmental Quality* **30**, 275-281.
- Diaz R.J. and Breitburg D.L. (2009) The Hypoxic Environment, in: Richards, J.G., Farrell, A.P., Brauner, C.J. (Eds.), *Hypoxia*. Academic Press, London, pp. 1–23.
- Diaz R.J., Eriksson-Hägg H., and Rosenberg R. (2013) Hypoxia, in: Noone, K.J., Sumaila, U.R., Diaz, R.J. (Eds.), *Managing ocean environments in a changing climate - Sustainability and economic perspectives*. Elsevier, San Diego.
- Diaz R.J. and Rosenberg R. (2008) Spreading dead zones and consequences for marine ecosystems. *Science* **321**, 926-929.
- Dyer K.R. (1973) *Estuaries: a physical introduction*. Wiley, New York.
- Erisman J.W., Sutton M.A., Galloway J., Klimont Z., and Winiwarter W. (2008) How a century of ammonia synthesis changed the world. *Nature Geoscience* **1**, 636-639.
- Fazzolari E., Nicolardot B., and Germon J.C. (1998) Simultaneous effects of increasing levels of glucose and oxygen partial pressures on denitrification and dissimilatory nitrate reduction to ammonium in repacked soil cores. *European Journal of Soil Biology* **34**, 47-52.
- Fossing H., Gallardo V.A., Jorgensen B.B., Huttel M., Nielsen L.P., Schulz H., Canfield D.E., Forster S., Glud R.N., Gundersen J.K., Kuver J., Ramsing N.B., Teske A., Thamdrup B., and Ulloa O. (1995) Concentration and transport of nitrate by the mat-forming sulphur bacterium *Thioploca*. *Letters to Nature* **374**, 713-715.
- Herbert R.A. (1999) Nitrogen cycling in coastal marine ecosystems. *FEMS Microbiology Reviews* **23**, 563-590.
- Hinck S., Neu T.R., Lavik G., Musmann M., De Beer D., and Jonkers H.M. (2007) Physiological adaptation of a nitrate-storing *Beggiatoa* sp. to diel cycling in a

- phototrophic hypersaline mat. *Applied and Environmental Microbiology* **73**, 7013-7022.
- Hinrichsen D. (1998) *Coastal waters of the world: trends, threats, and strategies*. Island Press, Washington.
- Hou L., Liu M., Carini S.A., and Gardner W.S. (2012) Transformation and fate of nitrate near the sediment-water interface of Copano Bay. *Continental Shelf Research* **35**, 86-94.
- Howarth R.W. and Marino R. (2006) Nitrogen as the limiting nutrient for eutrophication in coastal marine ecosystems: evolving views over three decades. *Limnology and Oceanography* **51**, 364-376.
- Hughes L. (2003) Climate change and Australia: trends, projections and impacts. *Austral Ecology* **28**, 423-443.
- Ibanez C., Pont D., and Prat N. (1997) Characterization of the Ebre and Rhone estuaries: A basis for defining and classifying salt-wedge estuaries. *Limnology and Oceanography* **42**, 89-101.
- Jantti H. and Hietanen S. (2012) The effects of hypoxia on sediment nitrogen cycling in the Baltic Sea. *Ambio* **41**, 161-169.
- Jensen M., Petersen J., Dalsgaard T., and Thamdrup B. (2009) Pathways, rates, and regulation of N₂ production in the chemocline of an anoxic basin, Mariager Fjord, Denmark. *Marine Chemistry* **113**, 102-113.
- Joye S.B. and Hollibaugh J.T. (1995) Influence of sulfide inhibition of nitrification on nitrogen regeneration in sediments. *Science* **270**, 623-625.
- Kemp W.M., Boynton W.R., Adolf J.E., Boesch D.F., Boicourt W.C., Brush G., Cornwell J.C., Fisher T.R., Glibert P.M., Hagy J.D., Harding L.W., Houde E.D., Kimmel D.G., Miller W.D., Newell R.I.E., Roman M.R., Smith E.M., and Stevenson J.C. (2005) Eutrophication of Chesapeake Bay: historical trends and ecological interactions. *Marine Ecology Progress Series* **303**, 1-29.
- Kemp W.M., Caffrey S.J., Mayer M., Henriksen K., and Boynton W.R. (1990) Ammonium recycling versus denitrification in Chesapeake Bay sediments. *Limnology and Oceanography* **35**, 1545-1563.
- Kemp W.M., Sampou P.A., Garber J., Tuttle J., and Boynton W.R. (1992) Seasonal depletion of oxygen from bottom waters of Chesapeake Bay: roles of benthic and planktonic respiration and physical exchange processes. *Marine Ecology Progress Series* **85**, 137-152.

- Kuypers M.M.M., Lavik G., Woebken D., Schmid M., Fuchs B.M., Amann R., Jorgensen B.B., and Jetten M.S.M. (2005) Massive nitrogen loss from the Benguela upwelling system through anaerobic ammonium oxidation. *Proceedings of the National Academy of Sciences* **102**, 6478-6483.
- Kuypers M.M.M., Sillekers A.O., Lavik G., Schmid M., Jorgensen B.B., Kuenen J.G., Damste J.S.S., Strous M., and Jetten M.S.M. (2003) Anaerobic ammonium oxidation by anammox bacteria in the Black Sea. *Letters to Nature* **422**, 608-611.
- Lam P. and Kuypers M.M.M. (2011) Microbial nitrogen cycling processes in oxygen minimum zones. *Annual Review of Marine Science* **3**, 317-345.
- Lam P., Lavik G., Jensen M.M., Van de Vossenberg J., Schmid M., Woebken D., Gutierrez D., Amann R., Jetten M.S.M., and Kuypers M.M.M. (2009) Revising the nitrogen cycle in the Peruvian oxygen minimum zone. *Proceedings of the National Academy of Sciences* **106**, 4752-4757.
- Lavik G., Stuhmann T., Bruchert V., Van Der Plas A., Mohrholz V., Lam P., Mussmann M., Fuchs B.M., Amann R., Lass U., and Kuypers M.M.M. (2009) Detoxification of sulphidic African shelf waters by blooming chemolithotrophs. *Nature* **457**, 581-585.
- Martin G.D., Muraleedharan K.R., Vijay J.G., Rejomon G., Madhu N.V., Shivaprasad A., Haridevi C.K., Nair M., Balachandran K.K., Revichandran C., Jayalakshmy K.V., and Chandramohanakumar N. (2010) Formation of anoxia and denitrification in the bottom waters of a tropical estuary, southwest coast of India. *Biogeosciences Discussions* **7**, 1751-1782.
- Nicholls J.C. and Trimmer M. (2009) Widespread occurrence of the anammox reaction in estuarine sediments. *Aquatic Microbial Ecology* **55**, 105-113.
- Otte S., Kuenen J.G., Nielsen L.P., Paerl H.W., Zopfi J., Schulz H., Teske A., Strotmann B., Gallardo V.A., and Jorgensen B.B. (1999) Nitrogen, carbon, and sulfur metabolism in natural *Thioploca* samples. *Applied and Environmental Microbiology* **65**, 3148-3157.
- Paerl H.W., Pinckney J.L., Fear J.M., and Peieris B.L. (1998) Ecosystem responses to internal watershed organic matter loading: consequences for hypoxia in the eutrophying Neuse River Estuary, North Carolina, USA. *Marine Ecology Progress Series* **166**, 17-25.
- Reyes-Arila J., Razo-Florez E., and Gomez J. (2004) Simultaneous biological removal of nitrogen, carbon and sulfur by denitrification. *Water Research* **38**, 3313-3321.

- Risgaard-Petersen N., Meyer R.L., Schmid M., Jetten M.S.M., Enrich-Prast A., Rysgaard S., and Revsbech N.P. (2004) Anaerobic ammonium oxidation in an estuarine sediment. *Aquatic Microbial Ecology* **36**, 293-304.
- Ritter C. and Montagna P.A. (1999) Seasonal hypoxia and models of benthic response in a Texas Bay. *Estuaries* **22**, 7-20.
- Rysgaard S., Risgaard-Petersen N., and Sloth N.P. (1996) Nitrification, denitrification, and nitrate ammonification in sediments of two coastal lagoons in Southern France. *Hydrobiologia* **329**, 133-141.
- Rysgaard S., Risgaard-Petersen N., Sloth N.P., Jensen K., and Nielsen L.P. (1994) Oxygen regulation of nitrification and denitrification in sediments. *Limnology and Oceanography* **39**, 1643-1652.
- Sayama M., Risgaard-Petersen N., Nielsen L.P., Fossing H., and Christensen P.B. (2005) Impact of bacterial NO_3^- transport on sediment biogeochemistry. *Applied and Environmental Microbiology* **71**, 7575-7577.
- Schulz H.N. and Jorgensen B.B. (2001) Big Bacteria. *Annual review of Microbiology* **55**, 105-137.
- Shah V.K. and Brill W.J. (1977) Isolation of an iron-molybdenum cofactor from nitrogenase. *Proceedings of the National Academy of Sciences* **74**, 3249-3253.
- Shao M., Zhang T., and Fang H.H. (2010) Sulfur-driven autotrophic denitrification: diversity, biochemistry, and engineering applications. *Applied Microbiology and Biotechnology* **88**, 1027-1042.
- Soetaert K. and Herman P.M.J. (1995) Nitrogen dynamics in the Westerschelde estuary (SW Netherlands) estimated by means of the ecosystem model MOSES. *Hydrobiologia* **311**, 225-246.
- Stanley D.W. and Nixon S.W. (1992) Stratification and bottom-water hypoxia in the Pamlico River Estuary. *Estuaries* **15**, 270-281.
- Straub K.L., Benz M., Shinck B., and Widdel F. (1996) Anaerobic, nitrate-dependent microbial oxidation by ferrous iron. *Applied and Environmental Microbiology* **62**, 1458-1460.
- Thamdrup B., Dalsgaard T., Jensen M.M., Ulloa O., Farias L., and Escobedo R. (2006) Anaerobic ammonium oxidation in the oxygen-deficient waters off northern Chile. *Limnology and Oceanography* **51**, 2145-2156.

- Tiedje J.M. (1988) Ecology of denitrification and dissimilatory nitrate reduction to ammonium, in: Zehnder, A.J.B. (Ed.), *Biology of Anaerobic Microorganisms*. Wiley, New York, pp. 179-244.
- Toyoda S., Iwai H., Koba K., and Toshida N. (2009) Isotopomeric analysis of N₂O dissolved in a river in the Tokyo metropolitan area. *Rapid Communications in Mass Spectrometry* **23**, 809-821.
- Trimmer M., Nicholls J.C., and Deflandre B. (2003) Anaerobic ammonium oxidation measured in sediments along the Thames Estuary, United Kingdom. *Applied and Environmental Microbiology* **69**, 6447-6454.
- Weber K.A., Urrutia M.M., Churchill P.F., Kukkadapu R.V., and Roden E.E. (2006) Anaerobic redox cycling of iron by freshwater sediment microorganisms. *Environmental Microbiology* **8**, 100-113.
- Wetzel R.G. (2001) *Limnology: lake and river ecosystems*. Academic Press, San Diego.
- Wyrski K. (1962) The oxygen minima in relation to ocean circulation. *Deep-Sea Research* **9**, 11-23.
- Yin S.X., Chen D., Chen L.M., and Edis R. (2002) Dissimilatory nitrate reduction to ammonium and responsible microorganisms in two Chinese and Australian paddy soils. *Soil Biology and Biogeochemistry* **34**, 1131-1137.
- Zopfi J., Kjaer T., Nielsen L.P., and Jorgensen B.B. (2001) Ecology of *Thioploca* spp.: nitrate and sulfur storage in relation to chemical microgradients and influence of *Thioploca* spp. on the sedimentary nitrogen cycle. *Applied and Environmental Microbiology* **67**, 5530-5537.

2. Hypoxic events stimulate nitrogen recycling in a shallow salt-wedge estuary: The Yarra River estuary, Australia

Keryn L. Roberts^a

Vera M. Eate^a, Bradley D. Eyre^b, Daryl P. Holland^a and Perran L. M. Cook^a

^aWater Studies Centre, Monash University, Clayton, Victoria, Australia

^bCentre for Coastal Biogeochemistry, School of Environmental Science and Management, Southern Cross University, Lismore, New South Wales, Australia



Published version:

Roberts, K.L, Eate, V.M, Eyre, B.D, Holland, D.P and Cook, P.L.M (2012) 'Hypoxic events stimulate nitrogen recycling in a shallow salt-wedge estuary: The Yarra River estuary, Australia' *Journal of Limnology and Oceanography*, 57 (5), 1427-1442 doi:10.4319/lo.2012.57.5.1427

The published version of this chapter was amended to include additional data on the behaviour of dissolved organic nitrogen within the Yarra River estuary. In addition, 'unpublished data' from the manuscript has been included in the thesis.

2.1 Declaration for Thesis Chapter Two

Declaration by candidate

In the case of Chapter Two, the nature and extent of my contribution to the work was the following:

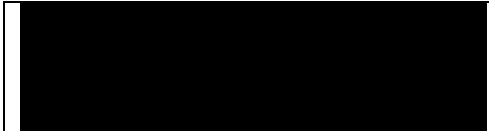
Nature of contribution	Extent of contribution (%)
I designed the field campaign, performed the majority of the field work and laboratory measurements. I completed all of the data and statistical analyses and was the primary author.	80

The following co-authors contributed to the work. If co-authors are students at Monash University, the extent of their contribution in percentage terms must be stated:

Name	Nature of contribution	*Extent of contribution (%)
Perran L.M. Cook	Assisted with study design and concept and provided guidance and manuscript editing.	10
Vera M. Eate	Assisted with field and laboratory work and review of the final manuscript.	5
Bradley D. Eyre	Provided guidance with study design and manuscript editing.	2.5
Daryl P. Holland	Collected the oxygen logger data in 2008 and review final manuscript.	2.5

The undersigned hereby certify that the above declaration correctly reflects the nature and extent of the candidate's and co-authors' contributions to this work*.

**Candidate's
Signature**

	<p>Date 28-01-2014</p>
-------------------------------------------------------------------------------------	-----------------------------------

**Main
Supervisor's
Signature**

	<p>Date 28-01-2014</p>
--------------------------------------------------------------------------------------	-----------------------------------

*Co-authors are not students of Monash University

2.2 Abstract

The Yarra River estuary is a salt wedge estuary prone to periods of stratification-induced anoxia ($0 \mu\text{mol-O}_2 \text{ L}^{-1}$) and hypoxia ($< 100 \mu\text{mol-O}_2 \text{ L}^{-1}$) during low flow events. Nitrate reduction pathways were examined using the ^{15}N isotope pairing technique in intact sediment cores, emulating *in situ* conditions, to evaluate the fate of NO_3^- during changing oxygen concentrations. Water column concentrations of dissolved inorganic carbon (DIC), O_2 , NH_4^+ , NO_x ($\text{NO}_3^- + \text{NO}_2^-$) and dissolved organic nitrogen (DON) were also measured to examine any deviation from conservative behaviour (denoted as Δ) in response to oxygen variability within the estuary.

The estuary was a source of DON and NH_4^+ in the hypoxic bottom waters. Whole system estimates using deviations from conservative behaviour and core incubations were in good agreement and showed that NH_4^+ was regenerated more efficiently relative to DIC under hypoxic conditions. For the whole system, mean $\Delta\text{DIC} : \Delta\text{NH}_4^+$ ratios under oxic (85 ± 33) and hypoxic (20 ± 3) conditions were significantly different. The more efficient NH_4^+ regeneration during hypoxia was attributed to rapid mineralisation rates and cessation of nitrification; dissimilatory nitrate reduction to ammonium (DNRA) was not a significant contributor. Unexpectedly, the denitrification : DNRA ratio was significantly higher under hypoxic (144 ± 48) than oxic (19 ± 18) conditions, with denitrification contributing $99.1 \pm 0.3 \%$ of total NO_3^- reduction. DNRA rates were significantly higher during oxic conditions ($123.5 \pm 30.7 \mu\text{mol m}^{-2} \text{ h}^{-1}$) when compared with rates during hypoxia ($0.6 \pm 0.1 \mu\text{mol m}^{-2} \text{ h}^{-1}$). The increase in DNRA in the presence of oxygen in the water column was attributed to the alleviation of NO_3^- limitation.

2.3 Introduction

Estuaries are transitional zones between freshwater and marine environments and play an important role in nitrogen cycling (Bianchi, 2007; Paerl *et al.*, 1998). In recent decades, anthropogenic activities have substantially increased eutrophication, through land use change and alteration of flow regimes, leading to enhanced primary productivity in coastal environments (Kemp *et al.*, 2005). Many coastal waters are nitrogen limited and hence the nitrogen removal or recycling ability of an estuary is an important determinant of the nutrient status of the receiving waters (Howarth and Marino, 2006). Two main competing NO_3^- reduction pathways, dissimilatory nitrate reduction to ammonium (DNRA) and denitrification, recycle or remove nitrogen, respectively (Chp. 1 Fig. 1.5). DNRA reduces NO_3^- to NH_4^+ under hypoxic conditions and conserves bioavailable nitrogen within the system (An and Gardner, 2002). Alternatively, denitrification is an anaerobic process in which NO_3^- , sourced from the water column or nitrification, is reduced to dinitrogen gas (N_2), reducing the bioavailable nitrogen load (Bianchi, 2007). The relative contribution of each of these processes in nitrogen cycling is important because this determines how much nitrogen is lost from the system and how much remains bioavailable (Bonin *et al.*, 1998).

Oxygen concentrations strongly regulate nitrogen transformation pathways including nitrification, denitrification and DNRA (Bianchi, 2007). Eutrophication and stratification-induced hypoxia ($< 100 \mu\text{mol-O}_2 \text{ L}^{-1}$) or anoxia have increased in recent decades in many coastal environments (Diaz, 2001). Hypoxic events are triggered by the isolation of bottom waters via stratification and subsequent depletion of oxygen through respiration of organic matter (Diaz, 2001; Ritter and Montagna, 1999). Conley *et al.* (2007) observed oxygen depletion in the coastal waters off Denmark and identified a shift in the form of inorganic nitrogen from NO_3^- to NH_4^+ during hypoxic events. Prolonged hypoxia or anoxia has the potential to shift nitrogen transformation processes from removal to recycling within a coastal environment. For example, hypoxia in the bottom waters of Chesapeake Bay, USA, caused a decrease in denitrification and inhibition of nitrification leading to less N_2 gas removed and an efflux of NH_4^+ from the sediment (Kemp *et al.*, 2005). An anoxic or hypoxic event may increase nitrogen recycling and maintain bioavailable nitrogen in the system through two mechanisms: first, the suppression of nitrification

during hypoxia leading to a reduction in nitrification-denitrification coupling and less nitrogen removed as N_2 resulting in accumulation of NH_4^+ ; and second, the promotion of DNRA.

In the Etung de Prost Lagoon, Rysgaard *et al.* (1996) observed an increase in NH_4^+ efflux from the sediment due to a disconnection between nitrogen removal (via nitrification-denitrification coupling) and mineralisation. Denitrification can remove in excess of 50 % of the nitrogen mineralised within the sediment via nitrification-denitrification coupling, but this efficiency can decrease rapidly as mineralisation rates increase (Eyre and Ferguson, 2009; Soetaert *et al.*, 2000). Nitrification of NH_4^+ is a critical step in this process, and the inhibition of nitrification through lowered oxygen concentrations within the water column will thus increase the amount of NH_4^+ released from the sediment relative to N_2 .

Further recycling of nitrogen may occur during hypoxia if DNRA is favoured over denitrification leading to the formation of NH_4^+ in preference to N_2 . Several studies have noted the importance of DNRA when NO_3^- concentrations are low. Nitrate ammonifiers produce more energy per mole of NO_3^- and thus have a higher affinity for NO_3^- than denitrifying bacteria (Childs *et al.*, 2002; Dong *et al.*, 2011; Nizzoli *et al.*, 2010). Hypoxic events often occur when the bottom water becomes isolated, and at these times NO_3^- will not be replenished from surface waters, potentially favouring DNRA over denitrification. In the Laguna Madre and Baffin Bay estuaries, high DNRA rates were attributed to sulfate reduction within the sediment and subsequent sulfide inhibition of nitrification and denitrification (An and Gardner, 2002), and studies from other estuaries support this (Jorgensen, 1989; Rysgaard *et al.*, 1996; Sayama *et al.*, 2005). Alternatively, Christensen *et al.* (2000) noted the importance of high organic carbon loading in the promotion of DNRA over denitrification beneath fish cages in Horsens Fjord, Denmark. Yin *et al.* (2002) hypothesised that high carbon loading can support large populations of heterotrophic nitrate ammonifiers. However, high carbon loading provides the ideal environment for sulfate reduction to occur; a predictor variable such as carbon is therefore difficult to isolate as a control on DNRA. Because DNRA occurs under highly reducing and low NO_3^- conditions, it has the potential to outcompete denitrification during a hypoxic event, leading to an increase in bioavailable nitrogen being transported to the ocean.

Several studies have examined the nitrogen cycle in detail and observed the co-occurrence of denitrification and DNRA (An and Gardner, 2002; Bonin *et al.*, 1998; Nizzoli *et al.*, 2010). To date, however, there have been no studies on the occurrence and relative importance of denitrification and DNRA during hypoxic events in estuaries. The incidence of estuarine hypoxia is increasing (Diaz, 2001), and understanding how this affects the cycling of nitrogen, the limiting nutrient in coastal waters, is important. The aim of this study was to quantify nitrogen recycling and removal processes within the sediments of a periodically hypoxic estuary and provide further insight into the behaviour of DNRA in estuarine systems. The specific research questions addressed were:

- (1) Do low oxygen conditions reduce nitrogen removal through the breakdown of nitrification-denitrification coupling?
- (2) Do low oxygen, reducing conditions promote DNRA, resulting in further recycling of nitrogen in the system?
- (3) What is the relative importance of (1) and (2)?

2.4 Methods

2.4.1 Site description

Sediment fluxes and water quality were investigated on 14 occasions in the Yarra River estuary, Australia, between September 2009 and March 2011. On 6 of these occasions NO_3^- reduction pathways were quantified. The Yarra River estuary flows through a highly urbanised area of Melbourne, Victoria, Australia and discharges into Port Phillip Bay, a nitrogen limited coastal embayment (CSIRO, 1996). The estuary exhibits a typical 'salt wedge' structure that extends up to 22 km from the estuary mouth to an artificial barrier called Dights Falls (Beckett *et al.*, 1982). The catchment area is approximately 4000 km² and is highly urbanised in the lower reaches, with ~2 million residents. The Lower Yarra River Catchment is subject to direct stormwater drainage, whereas the upper and middle reaches are dominated by agricultural, farming and park land (Melbourne Water Corporation, Fig 1.3).

Sites for sediment sampling were selected to include 'always oxic' through to periodically hypoxic sites. The high turbidity of the inflowing Yarra River water (24-192 nephelometric turbidity units (NTU)) means that the sediment surface below the salt wedge is aphotic in the section of the estuary studied. Three fixed sediment sampling sites were chosen: Bridge Rd (55°32'52.73''E, 58°12'40.2''N), Scotch College (55°32'63.48''E, 58°10'85.4''N) and Morell Bridge (55°32'27.25''E, 58°11'38.5''N; Fig. 2.1). From September 2009 until July 2010, water quality parameters were measured at three additional sites, the location of which depended on the position of the salt wedge within the estuary. These sites ranged from as far downstream as the Bolte Bridge (55°31'81.97''E, 58°12'17.0''N) up to the Johnston St Bridge (55°32'41.03''E, 58°14'01.3''N), ~1 km downstream of Dights Falls (Fig. 2.1).

2.4.2 Sampling protocol

In 2008, the extent of hypoxia through time was measured using temperature, oxygen (Greenspan, Australia) and salinity (Odyssey, Australia) loggers placed 0.5 m off the bottom at the Scotch College site (Fig. 2.1). Loggers were retrieved every

three to four weeks and replaced with clean, freshly calibrated loggers. Dissolved oxygen (DO) concentrations were corrected for drift and salinity. River flow data (gauged at Chandler highway) were obtained from the Melbourne Water Corporation.

At the fixed and additional sampling sites, water quality parameters including temperature, DO, pH, conductivity, salinity, and turbidity were measured at 0.5 m depth intervals through the water column using a calibrated multimeter (U-10 Horiba multimeter, Japan, or DS5X Hydrolab, USA). A 5 L Niskin bottle was used to collect water samples from the surface and bottom waters. Samples for analysis of total dissolved nitrogen (TDN), NO_x ($\text{NO}_3^- + \text{NO}_2^-$) and NH_4^+ were filtered (0.45 μm ; 30 mm polypropylene housing; Bonnet) and stored in 50 mL high density polyethylene sample bottles. Samples collected in the field were kept on ice and then frozen at -18°C until analysis.

At the three fixed sediment sampling sites (Fig. 2.1), using a coring apparatus intact sediment cores were collected in 27.5 (depth) \times 6.6 (diameter) cm polyethylene cylinders and stoppered. Five cores were collected from each site, one for porosity and four for the measurement of sediment fluxes of DO, dissolved inorganic carbon (DIC), NH_4^+ and NO_x , and rates of denitrification and DNRA. In addition, ~ 10 L of bottom water was collected for the sediment incubations.

2.4.3 Light and sediment chlorophyll *a*

Chlorophyll *a* was used to indicate the presence of microphytobenthos. In February 2012 three cores were collected at each of the three fixed core sites, and maintained in a dark, cool environment until analysis. Two subsamples were collected from the surface of the core using a 30 mL cut off syringe down to 1.0 cm depth. The sediment was then extracted for chlorophyll *a* using the Lorenzen (1967) acidification method. On two additional occasions (March 2010 and 2011) the euphotic depth was surveyed along the estuary using a Secchi disk. Seven replicate measurements were taken at 15 sites in the estuarine region including the three fixed core sites. Secchi depth (Z_{sd}) was converted to euphotic depth (Z_{eu}) using the principles described by Kirk (1994) (Eq. 2.1).

$$Z_{\text{eu}} = 4.6 / K_d \quad \text{where the attenuation coefficient } (K_d) = 1.44/Z_{\text{sd}} \quad (2.1)$$

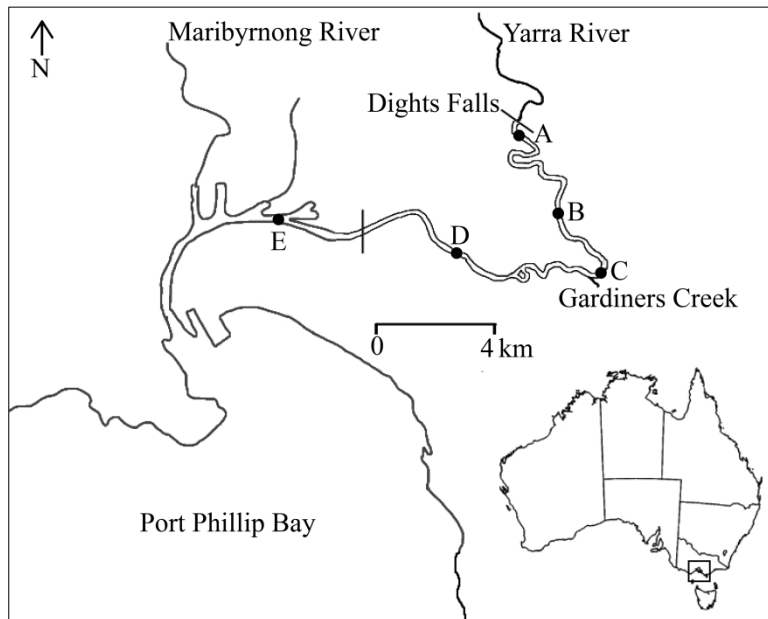


Figure 2.1 The Yarra River estuary, Australia. Sampling of the estuary extended from (A) the Johnston St Bridge to (E) the Bolte Bridge. The fixed sites are located at the upstream extent of the salt wedge (B) at Bridge Road, (C) Scotch College, and (D) Morell Bridge. Distances are measured from the Bolte Bridge (E). Below this site, the shipping channel is thoroughly mixed and saline. The shipping channel and Port Phillip Bay is represented by the dark line, grey lines represent the estuarine region.

2.4.4 Sediment flux

The sediment cores were transferred to a temperature controlled water bath and circulated overnight with site bottom water at *in situ* temperature and oxygen concentration. The cores were stirred continuously throughout the incubation period by a suspended magnetic bar, with the stirring rate kept below the rate that would cause sediment disturbance (~40 rpm). Prior to and throughout the flux incubation, DO and pH were measured using a HQ-40d Hach multimeter (Germany). The incubation was only carried out when the DO was within $\pm 30 \mu\text{mol L}^{-1}$ of the *in situ* oxygen concentration. If necessary, the circulating water was bubbled with argon or air to achieve the required DO. When the oxygen concentration was within the acceptable range, the core was sealed and isolated. DO and pH were measured, and 25 mL of water for nutrient (NH_4^+ , NO_x) and alkalinity analysis was collected and filtered (0.45 μm ; 30 mm polypropylene housing; Bonnet) at approximately 1, 3, 5,

and 7 hours, by which time the DO had dropped by ~20 %. Nutrient samples were frozen and alkalinity samples refrigerated until analysis. The water that was removed was replaced with bottom water collected from the site at *in situ* oxygen concentration.

Sediment-water nutrient fluxes were calculated as the concentration change of the analyte over time. The water volume and the surface area of the sediment were taken into consideration along with the correction for the addition or dilution of constituents by the replacement of reservoir water (Dalsgaard *et al.*, 2000).

2.4.5 Denitrification and DNRA

After the flux incubation, sediment cores used for the flux experiments were recirculated with site bottom water, under *in situ* oxygen and temperature conditions overnight to allow the sediment and water to re-equilibrate. Denitrification was determined using the isotope pairing technique (Nielsen, 1992). The initial oxygen concentration was within $\pm 30 \mu\text{mol L}^{-1}$ of *in situ* at the start of the denitrification incubation. An initial 15 mL water sample was taken for NO_x analysis, and then 0.5 mL of $0.05 \text{ mol L}^{-1} \text{ }^{15}\text{N-NO}_3^-$ (98 %+, Cambridge Isotope Laboratories) was added to each core. The overlying water column was allowed to mix for ~1 minute after the addition of the tracer, and a 15 mL sample was then taken to determine the initial concentration of $^{15}\text{N-NO}_3^-$ within the overlying water of the core. The sample water removed from the core was replaced with 15 mL of bottom water and the core was sealed and isolated. A core was sacrificed at ~1, 3, 5, and 7 hours, depending on the rate at which oxygen was consumed. 1 mL of ZnCl_2 50 % w:v was added to the core after the measurement of DO and collection of a nutrient sample. The sediment core was slurried and allowed to settle before a N_2 gas sample was collected in a 12 mL exetainer (Labco) and preserved with 250 μL ZnCl_2 50 % w:v until analysis (*see* section 2.4.7).

The denitrification rate was calculated after the addition of $^{15}\text{N-NO}_3^-$ (D_{15}). The rate was determined from the linear relationship observed over time with respect to excess ^{15}N -labeled N_2 gas production (mean $^{29}\text{N}_2$ $R^2 = 0.75$, $n = 18$ and $^{30}\text{N}_2$ $R^2 = 0.74$, $n = 18$; Dalsgaard *et al.*, 2000; Nielsen, 1992). The *in situ* denitrification rate produced from $^{14}\text{N-NO}_3^-$ (D_{14}) was calculated based on the production of $^{14}\text{N}^{15}\text{N}$ and

$^{15}\text{N}^{15}\text{N}$. The contribution of nitrification driven denitrification (D_n) and water column driven denitrification (D_w) were calculated from the D_{14} rate (Dalsgaard *et al.*, 2000; Nielsen, 1992).

Anammox, the conversion of $^{15}\text{N-NO}_3^- + \text{NH}_4^+$ to N_2 gas, is a source of $^{29}\text{N}_2$ and could interfere with the calculation of nitrification-denitrification coupling. Rates of anammox were quantified by running anoxic slurries with $^{15}\text{N-NH}_4^+$ and $^{15}\text{N-NO}_3^-$ amendments in September 2009 at the three fixed core sites. Two amendments were used to identify the importance of anammox: (1) $^{15}\text{N-NH}_4^+$ and $^{14}\text{N-NO}_3^-$ were added to the slurry to achieve a final concentration of $100 \mu\text{mol L}^{-1}$ and $200 \mu\text{mol L}^{-1}$ respectively, (2) $^{15}\text{N-NO}_3^-$ to a final concentration of $100 \mu\text{mol L}^{-1}$.

The isotope pairing technique is based on a number of assumptions (Risgaard-Petersen *et al.*, 2003). The first assumption is that the addition of $^{15}\text{N-NO}_3^-$ does not affect the production of $^{14}\text{N-N}_2$. Two actions were taken to verify this assumption in the Yarra River estuary. First, anammox was measured to ensure denitrification was the only N_2 producing process. Second, a concentration series experiment was performed to confirm that $^{15}\text{N-NO}_3^-$ and $^{14}\text{N-NO}_3^-$ were uniformly mixed in the reduction zone and the concentration of $^{15}\text{N-NO}_3^-$ did not influence the amount of $^{14}\text{N-N}_2$ production. Sediment cores were collected from the Scotch College site and the denitrification incubation was performed at three different $^{15}\text{N-NO}_3^-$ concentrations of ~ 30 , 60 and $90 \mu\text{mol L}^{-1}$ (final concentration of $^{15}\text{N-NO}_3^-$ was $\sim 60 \mu\text{mol L}^{-1}$ throughout field surveys).

The second assumption of the isotope pairing technique is that $^{28}\text{N}_2$, $^{29}\text{N}_2$ and $^{30}\text{N}_2$ are binomially distributed. This is verified if the third assumption holds true which is $^{15}\text{N-NO}_3^-$ and $^{14}\text{N-NO}_3^-$ are uniformly mixed within the reduction zone. When there is non-uniform mixing of $^{14}\text{N-NO}_3^-$ and $^{15}\text{N-NO}_3^-$ a higher proportion of the homogenous isotope pairs $^{14}\text{N}^{14}\text{N}$ and $^{15}\text{N}^{15}\text{N}$ would be observed relative to the $^{14}\text{N}^{15}\text{N}$ pair (Nielsen 1992). In this study a high $^{15}\text{N-NO}_3^-$ concentration was used to increase the probability of $^{14}\text{N-NO}_3^-$ encountering $^{15}\text{N-NO}_3^-$ and producing $^{14}\text{N}^{15}\text{N}$, reducing the likelihood that $^{14}\text{N-N}_2$ was underestimated.

A sample for $^{15}\text{N-NH}_4^+$ was collected at the end of the denitrification incubation to determine the amount of DNRA occurring within the core (DNRA was not measured in September 2009). NH_4^+ was captured in an acid trap after being

extracted from a 1:1 slurry with 2 mol L⁻¹ KCl. DNRA rates for ¹⁵N were calculated from the linear production of ¹⁵N-NH₄⁺ over the incubation period (mean ¹⁵N-NH₄⁺ $R^2 = 0.65$, $n = 15$). To determine the rate of ¹⁴N-NH₄⁺ produced *in situ*, it is assumed that the ¹⁴N-NO₃⁻ and ¹⁵N-NO₃⁻ are uniformly mixed and the frequency in which they are reduced by DNRA bacteria is equivalent to denitrifying bacteria. Hence, DNRA₁₄ is determined using the original ¹⁵N-NH₄⁺ production and the frequency of NO₃⁻ consumption used in the calculation of denitrification (D₁₄; Eq. 2.2; Nielsen, 1992; Risgaard-Petersen and Rysgaard, 1995). Using the same principle as the denitrification method, the contribution of water column driven DNRA (DNRA_w) and nitrification driven DNRA (DNRA_n) can be calculated (Nielsen, 1992; Risgaard-Petersen and Rysgaard, 1995).

$$\text{DNRA}_{14} = \text{DNRA}_{15} \times f_{14}/f_{15} \quad \text{where } f_{14}/f_{15} = ({}^{15}\text{N}^{14}\text{N})/2({}^{15}\text{N}^{15}\text{N}) \quad (2.2)$$

2.4.6 Sediment profiles

To determine the DIC and NH₄⁺ concentration within the estuarine sediment, two sediment cores were collected from each site during the sampling in February 2011. The sediment was sliced at 1 cm intervals down to 6 cm depth and then 2 cm intervals thereafter down to 10 cm. To collect a porewater sample, half of the slice was immediately placed into 50 mL modified falcon tube (BD Falcon) and purged with argon gas before it was centrifuged at 4000 rpm for 10 minutes and the supernatant collected. A 12 mL sample of the supernatant was filtered (0.45 μm; 30 mm polypropylene housing; Bonnet) and frozen for NH₄⁺ analysis, and a 3 mL sample for DIC was filtered (0.2 μm; DISMIC 25 cs, Advantec) and preserved with 100 μL 6 % HgCl until analysis.

2.4.7 Analytical methods

NH₄⁺, NO_x and total dissolved nitrogen (TDN) for *in situ* and sediment flux samples were analysed using flow injection analysis (FIA; Lachat Quickchem 8000 Flow Injection Analyser with spectrophotometric detection). Samples for TDN were pre-treated using an alkaline persulfate digestion (APHA, 2005). The analysis of

nutrient samples via FIA followed the procedures in Standard Methods for Water and Wastewater (APHA, 2005) including standard and quality assurance checks. Dissolved organic nitrogen (DON) was calculated from the difference between TDN and total inorganic nitrogen species (NO_x and NH_4^+). Alkalinity for *in situ* and sediment flux samples were analysed via Gran titration using 100 μL aliquots of 0.01 mol L^{-1} HCl standardised with 1 mmol L^{-1} Na_2CO_3 (the precision of the test was < 1.5 % relative SD). DIC was calculated from measured pH and alkalinity using the carbonate equilibrium equations corrected for salinity and temperature (Millero, 2006).

N_2 gas samples for denitrification were analysed via gas chromatography coupled to isotope ratio mass spectrometry (GC-IRMS; Thermo Scientific GC with He carrier coupled to Delta V plus IRMS detector). DNRA was determined via the ammonium diffusion method (ADM), omitting the addition of Devarda's Alloy to convert NO_3^- to NH_4^+ . $^{15}\text{N-NH}_4^+$ was captured in an acid trap before analysis via the GC-IRMS fitted to an elemental analyser at 1050 $^\circ\text{C}$ (Sigman *et al.*, 1997). It was found that the ADM collected 98.6 ± 0.4 % of the NH_4^+ present in solution within the acid trap during the 10 day incubation period. DIC for the sediment profiles was analysed via gas diffusion flow injection analysis; the principles are outlined in Oshima *et al.* (2001), although we changed the reagents. We used a 0.1 mol L^{-1} H_2SO_4 carrier stream and bromothymol blue indicator concentration of 8×10^{-5} mol L^{-1} , in a 0.5 mol L^{-1} phosphate buffer adjusted to $\sim\text{pH}$ 7.

2.4.8 Constituent deviations

For *in situ* concentrations of NH_4^+ , NO_x and DON, constituent deviations from conservative behaviour were calculated based on the expected change in concentration due to the conservative mixing model versus the actual change in concentration (Eq. 2.3; Miyajima *et al.*, 2009). In highly episodic systems, considerable variation in the freshwater end member may be observed (Eyre, 2000), however, continuous measurements of nutrient and DIC concentrations over ~ 3 days in the Yarra River estuary showed no significant variation in the freshwater end member (Santos *et al.*, 2012). We therefore do not believe freshwater end member variation has a significant effect on the interpretation of our data.

$$\Delta\text{NH}_4^+ = [\text{NH}_4^+]_s - \frac{(S_s \times [\text{NH}_4^+]_m) + (S_m - S_s) \times [\text{NH}_4^+]_r}{S_m} \quad (2.3)$$

Where m denotes the marine end member, r the river end member, s the sampling point, S the salinity and Δ the difference between actual and expected concentrations (Eq. 2.3). A positive delta value corresponds to an increase in analyte concentration (production) compared to the conservative estimate, and a negative delta value denotes a decrease in the analyte (consumption).

2.4.9 Statistical analysis

Multiple linear regression analyses for denitrification, DNRA, the denitrification : DNRA ratio, and the predictor variables (O_2 and NO_3^-) were carried out using the statistics program R (version 2.11.1; R Core Team, 2012). To meet the requirements of the test, sample dates with missing data points had to be excluded. Regressions and comparison of means were carried out using a regression test and t-test of equal and unequal variance at the 95 % confidence interval depending on the variance result of the *F*-test. Microsoft Excel (2007) was used to perform these analyses.

2.5 Results

2.5.1 Verification of the isotope pairing technique assumptions

Denitrification was the only contributor to the production of $^{29}\text{N}_2$ in the Yarra River estuary. Anammox was $< 1\%$ of the total N_2 gas production and an insignificant contributor to NO_3^- removal. The rate of $^{14}\text{N-N}_2$ production was independent of the concentration of $^{15}\text{N-NO}_3^-$ ($^{14}\text{N-N}_2 = -0.06(^{15}\text{N-NO}_3^-) + 52.32$, $n = 3$, $p > 0.05$; Fig. 2.2A) confirming $^{15}\text{N-NO}_3^-$ and $^{14}\text{N-NO}_3^-$ were uniformly mixed in the reduction zone. In addition, there was no relationship between $^{15}\text{N-NO}_3^-$ and nitrification coupled denitrification and therefore we can assume there is uniform mixing of NO_3^- in the reduction zone (Fig. 2.2B; Nielsen 1992). In the concentration series experiment, nitrification-denitrification coupling was low because the salt wedge was hypoxic when the samples were collected, in agreement with our findings. The ^{15}N -labeled recovery for the isotope pairing technique including both denitrification and DNRA averaged $93 \pm 2\%$.

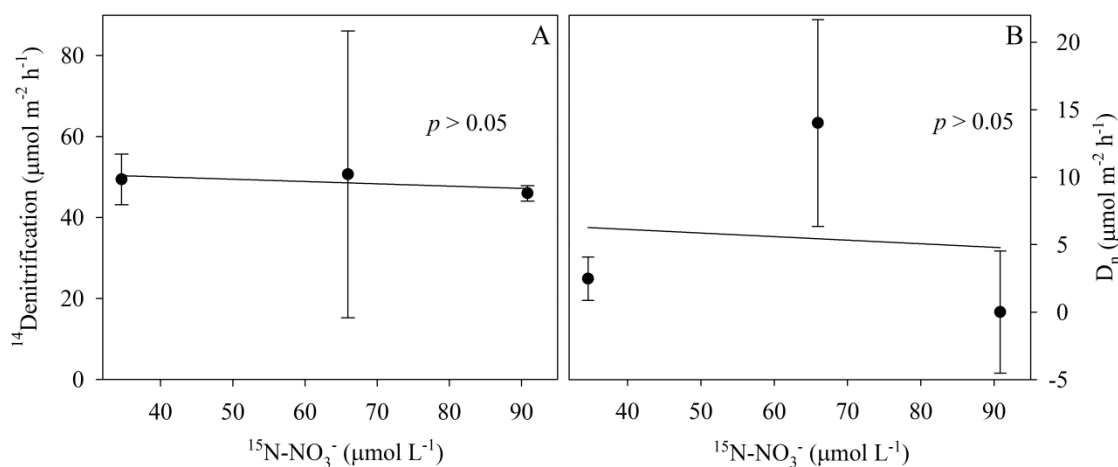


Figure 2.2 Assumptions of the isotope pairing technique were validated via (A) $^{14}\text{Denitrification}$ ($\pm \text{SE}$; $\mu\text{mol m}^{-2} \text{h}^{-1}$) with respect to $^{15}\text{N-NO}_3^-$ ($\mu\text{mol L}^{-1}$) and (B) Nitrification coupled denitrification (D_n ; $\pm \text{SE}$; $\mu\text{mol m}^{-2} \text{h}^{-1}$) with respect to $^{15}\text{N-NO}_3^-$ ($\mu\text{mol L}^{-1}$).

2.5.2 The behaviour of oxygen in the Yarra River estuary

Total inflow (ML day^{-1}) to the Yarra River estuary throughout 2008 was highly variable (Fig. 2.3). Episodic peaks in freshwater inflow correspond to drops in temperature and salinity and an increase in dissolved oxygen concentrations (Fig. 2.3). When the inflows were low, bottom water oxygen became depleted and remained low until the next large peak in flow.

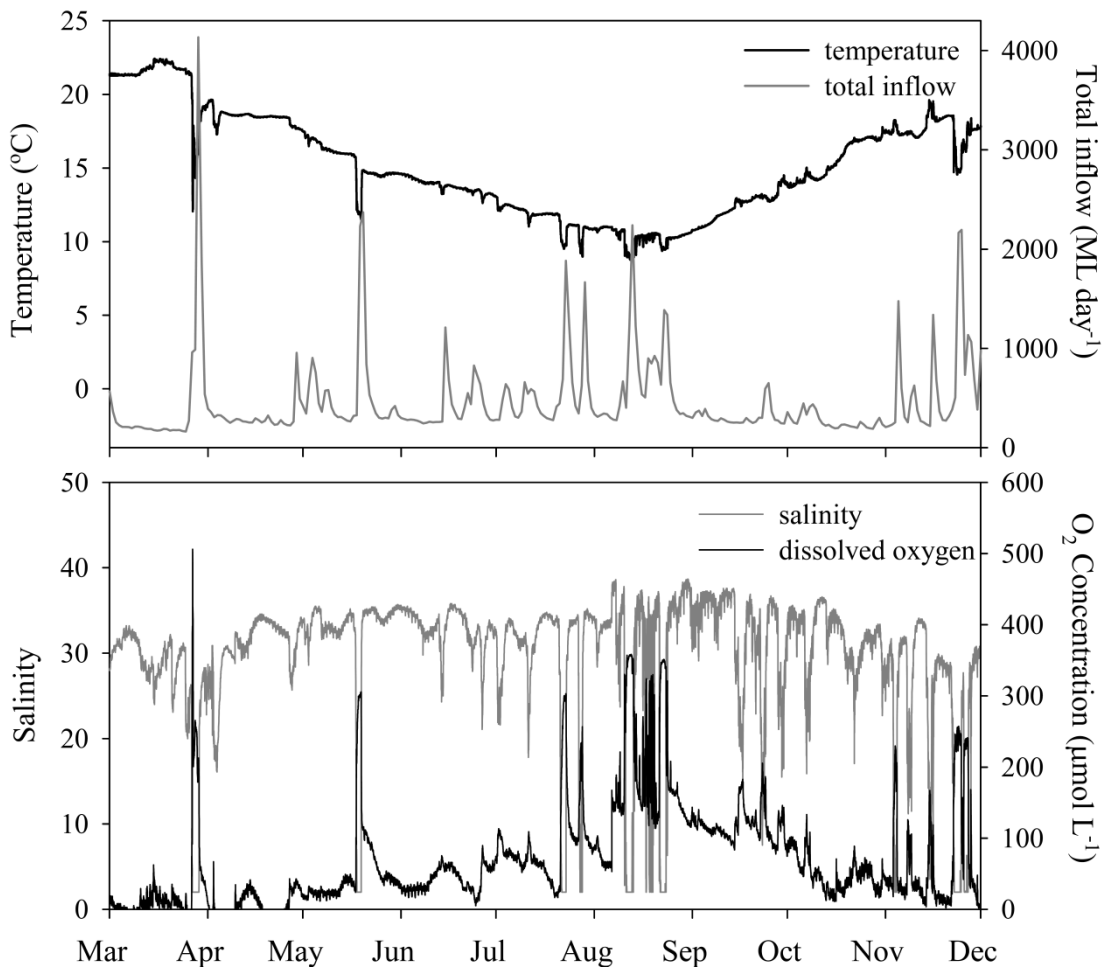
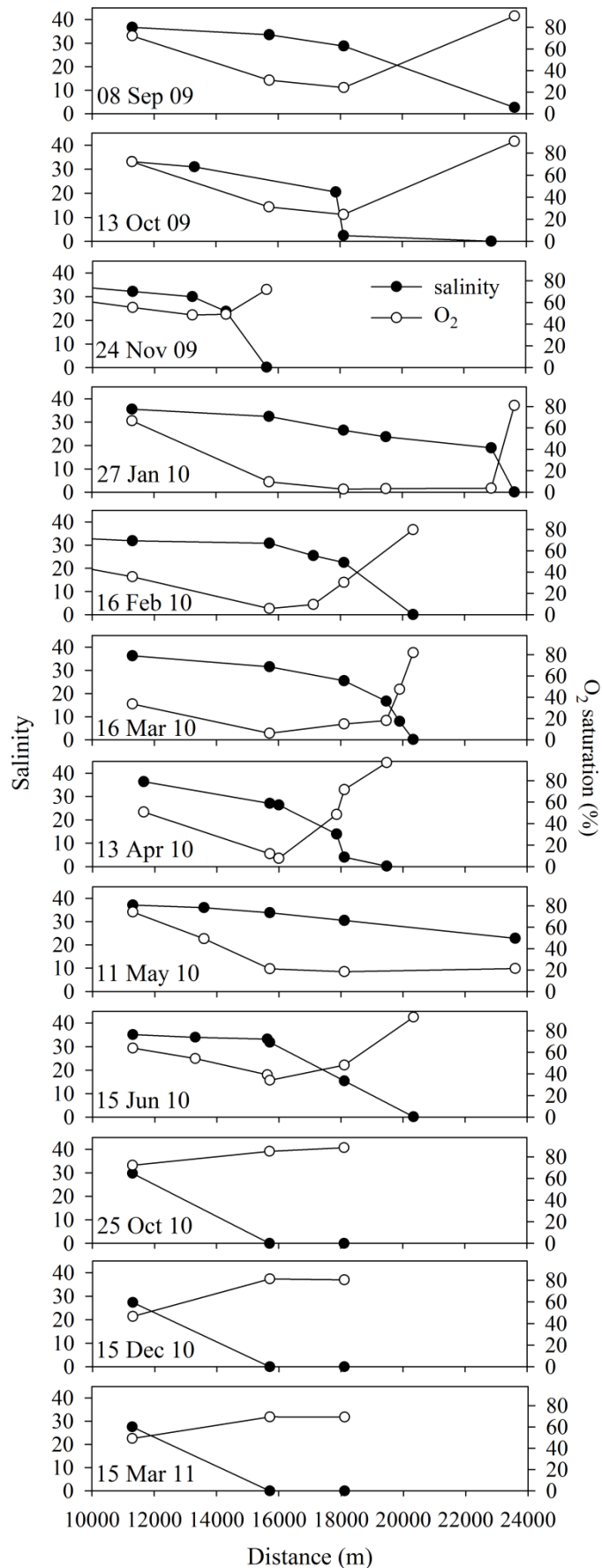


Figure 2.3 Temporal variation in total inflow (ML day^{-1}), salinity, temperature ($^{\circ}\text{C}$), and dissolved oxygen ($\mu\text{mol L}^{-1}$) in 2008. Data were collected from the bottom waters of the Scotch College site. Dissolved oxygen was corrected for salinity using Henry's Law.

Figure 2.4 Spatial variation in salinity and dissolved oxygen saturation (%) in the bottom waters of the Yarra River estuary for surveys from September 2009 to March 2011. Profiles from November 2010 and February 2011 are similar to December 2010 and March 2011, hence are not shown here. Distance was measured from the Bolte Bridge near the estuary mouth.



Hypoxia in the Yarra River estuary is driven by salinity stratification (Fig. 2.4). Percent oxygen saturation decreases with increasing bottom water salinity in the upper reaches of the estuary. At the front of the salt wedge, where salinity is greater than 25, the percent oxygen saturation was < 30 % on several occasions. Oxygen saturation increased toward the mouth of the estuary. Fig. 2.4 depicts the spatial variability of the salt wedge within the Yarra River estuary; it is highly dynamic and moved from 16 km (27 January 2010) to ~2 km (15 March 2011) upstream of the Bolte Bridge, during the study period. A negative linear relationship was found between *in situ* oxygen concentration and salinity: $O_2 (\mu\text{mol L}^{-1}) = -4.44 (\text{salinity}) + 245.19$ ($R^2 = 0.54$, $df = 551$, $p < 0.001$).

2.5.3 Light and sediment chlorophyll *a*

Measurements of nutrients and NO_3^- reduction pathways were based on the assumption that the sediments were aphotic owing to the high turbidity of the surface waters (24 - 192 NTU). At all three sites, benthic chlorophyll *a* could not be detected (detection limit $26 \mu\text{g m}^{-2}$). A strong exponential relationship was identified between euphotic depth and turbidity ($Z_{\text{eu}} = 2.16e^{-0.02(\text{turbidity})}$, $R^2 = 0.86$, $n = 15$, $p < 0.01$; Fig. 2.5). Throughout the surveyed period the turbidity in the surface water was > 24 NTU and the euphotic depth was < 1.3 m (Fig. 2.5). Sediment samples were collected from > 2 m depth on all occasions with the average fixed sediment sampling depth of 3.2 ± 0.1 m, suggesting the sediments were aphotic.

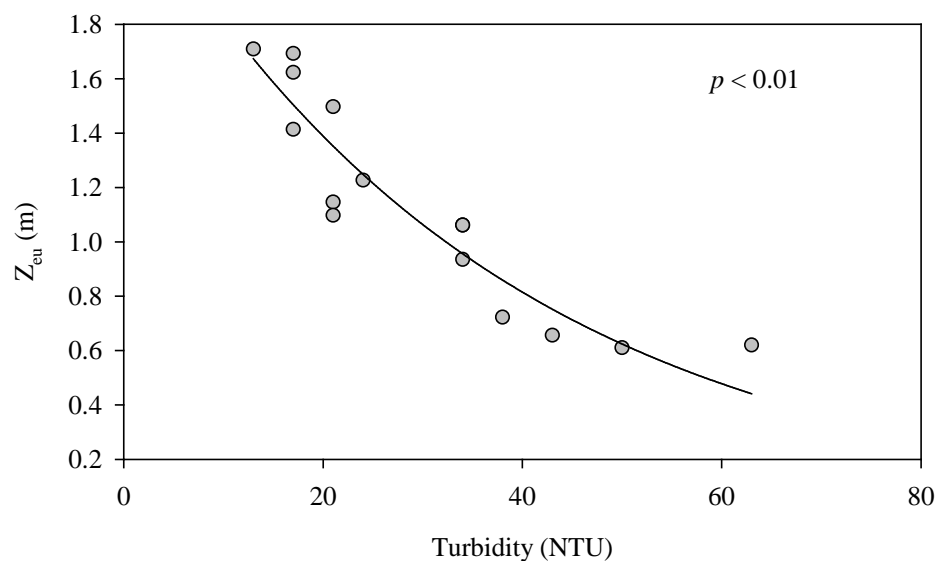


Figure 2.5 Euphotic depth (Z_{eu} ; m) with respect to turbidity (NTU) in the water column.

2.5.4 Sediment fluxes and nutrient behaviour

Ammonium in the bottom waters of the Yarra River estuary deviated from conservative mixing behaviour under low oxygen conditions ($< 100 \mu\text{mol-O}_2 \text{ L}^{-1}$) with a positive ΔNH_4^+ ($\mu\text{mol L}^{-1}$). Positive ΔNH_4^+ was also observed in the surface waters at an oxygen concentration between 200 - 300 $\mu\text{mol L}^{-1}$ (Fig. 2.6). At higher oxygen concentrations, NH_4^+ followed conservative mixing (Fig. 2.6). A positive linear relationship was found between NH_4^+ and salinity ($R^2 = 0.46$, $df = 138$, $p < 0.001$). A negative linear relationship was found between NO_3^- and salinity ($R^2 = 0.41$, $df = 138$, $p < 0.001$). In the bottom waters ΔNO_3^- was negative at low oxygen concentrations indicating consumption (Fig. 2.6). ΔDON positively deviated from conservative mixing in the bottom waters under low oxygen conditions ($< 100 \mu\text{mol L}^{-1}$) indicating production (Fig. 2.6).

The sediment-water oxygen fluxes were negative at all of the sites with the exception of Scotch College and Bridge Road in January 2010, where no flux was observed due to complete anoxia in the water column (Fig. 2.7). Production of DIC was apparent at all of the sites; large peaks were observed in January 2010 at the Scotch College and Bridge Road sites, respectively (Fig. 2.7). The flux of NH_4^+ was particularly high at the Bridge Road site during January 2010 (Fig. 2.7). NO_3^- flux was negative throughout most of the surveyed period, with the exception of a small positive flux in January 2010 at Morell Bridge that corresponds to a low denitrification rate and negligible DNRA (Fig. 2.7).

The mean ratio of $\Delta\text{DIC} : \Delta\text{NH}_4^+$ in the bottom waters of the Yarra River estuary was significantly lower under hypoxic (20 ± 3) than oxic conditions (85 ± 33 , $p < 0.05$), indicating that NH_4^+ is regenerated more efficiently under hypoxic conditions (Fig. 2.8). The mean $\text{DIC} : \text{NH}_4^+$ ratio ($\pm \text{SE}$) for the sediment fluxes show a similar relationship to that observed in the water column (the whole system estimates), and were significantly lower under hypoxic than oxic conditions (21 ± 3 and 52 ± 10 respectively, $p < 0.05$; Fig. 2.8B). Under hypoxic conditions the mean $\text{DIC} : \text{NH}_4^+$ ratio for the sediment and water were not significantly different ($p > 0.05$). Also, the mean $\text{DIC} : \text{NH}_4^+$ ratio under oxic conditions did not significantly differ for the water column and sediment measurements ($p > 0.05$). Negative DIC values were excluded from the data analysis.

The sediment profile of DIC and NH_4^+ at Morell Bridge in February 2011 showed very little change with depth (Fig. 2.9A). However, both NH_4^+ and DIC increased with depth at the Scotch College and Bridge Road core sites (Fig. 2.9B, C). There was a clear positive linear relationship between NH_4^+ and DIC in the sediment profiles from all three sites: $\text{NH}_4^+ = 7.7 (\text{DIC}) + 1372.5$ ($df = 50$, $R^2 = 0.98$, $p < 0.001$; Fig. 2.9D).

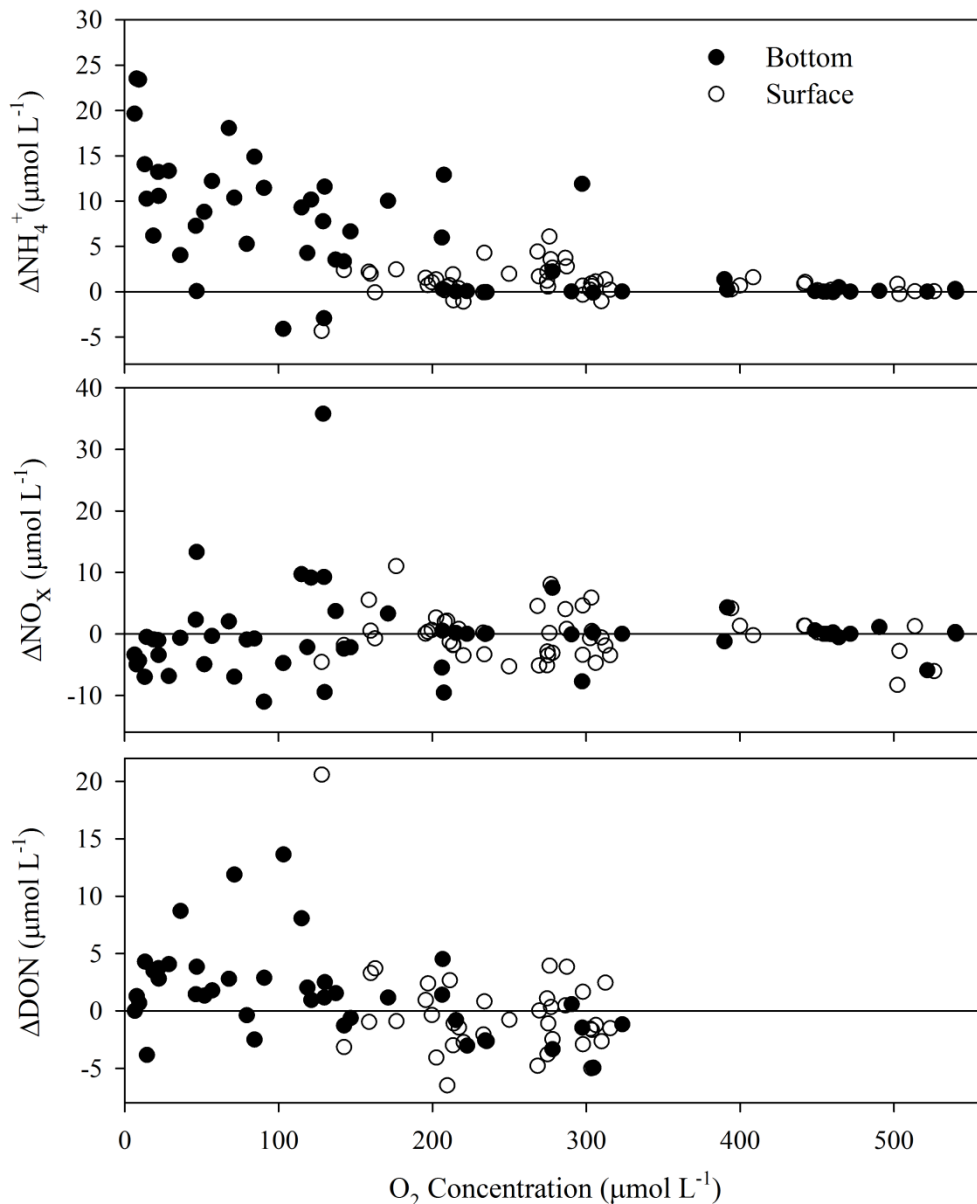


Figure 2.6 ΔNH_4^+ , ΔNO_x and ΔDON with respect to oxygen concentration ($\mu\text{mol L}^{-1}$). The line at delta 0 is the conservative mixing line, assuming linear mixing of analytes, as a result of dilution only between end-members.

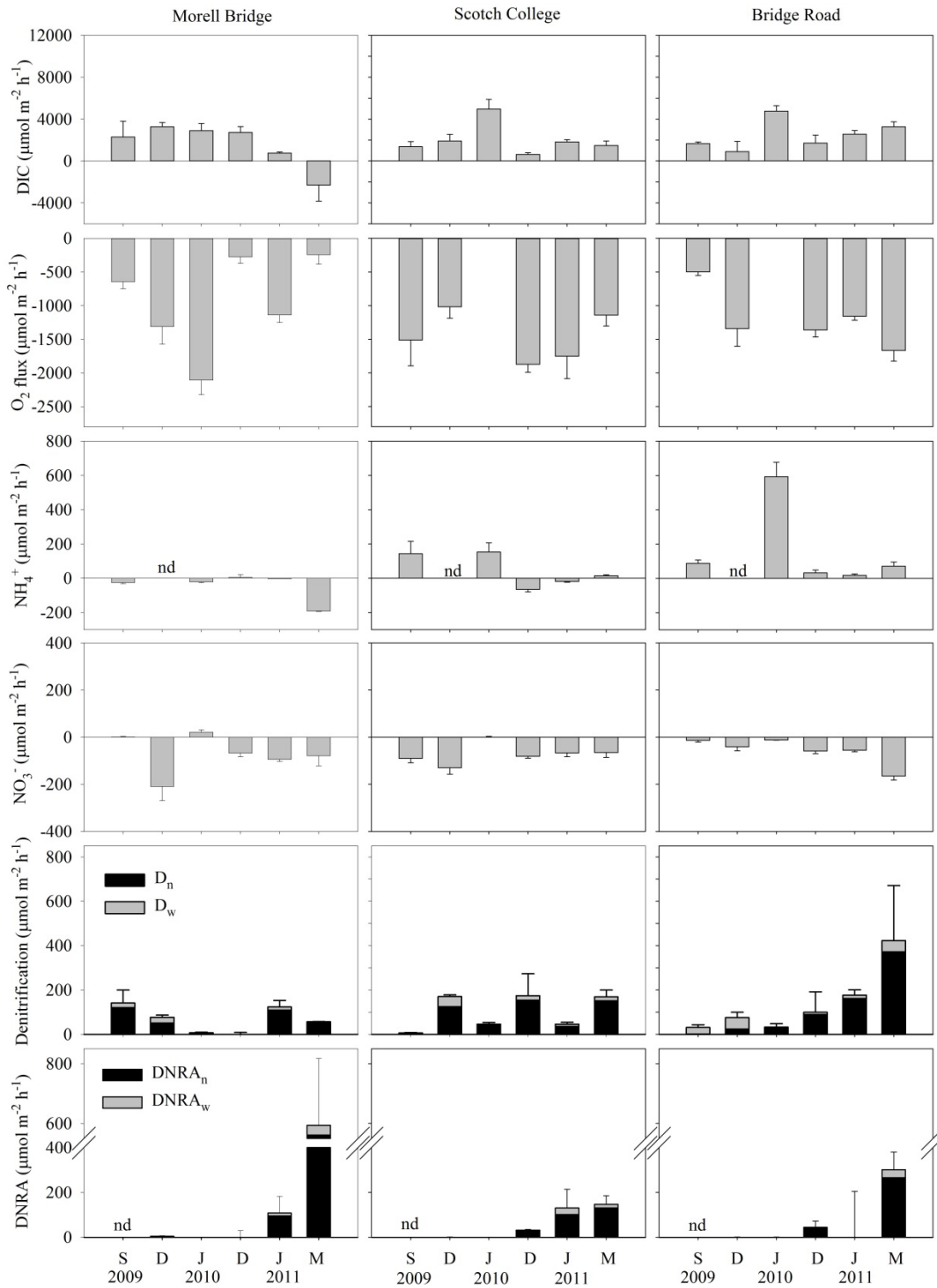


Figure 2.7² Sediment-water nutrient fluxes from September 2009 to March 2011. DIC, O₂, NH₄⁺ and NO_x flux (\pm SE; $\mu\text{mol m}^{-2} \text{h}^{-1}$). Denitrification and DNRA (\pm SE; $\mu\text{mol m}^{-2} \text{h}^{-1}$) subscript w represents water column driven NO₃⁻ reduction and subscript n NO₃⁻ sourced from nitrification. nd represents no data for the month.

² Appendix 1: Due to an underestimation of denitrification, data from February, April, May, June and November 2010 were omitted. Data for these months can be found in the attached Appendix.

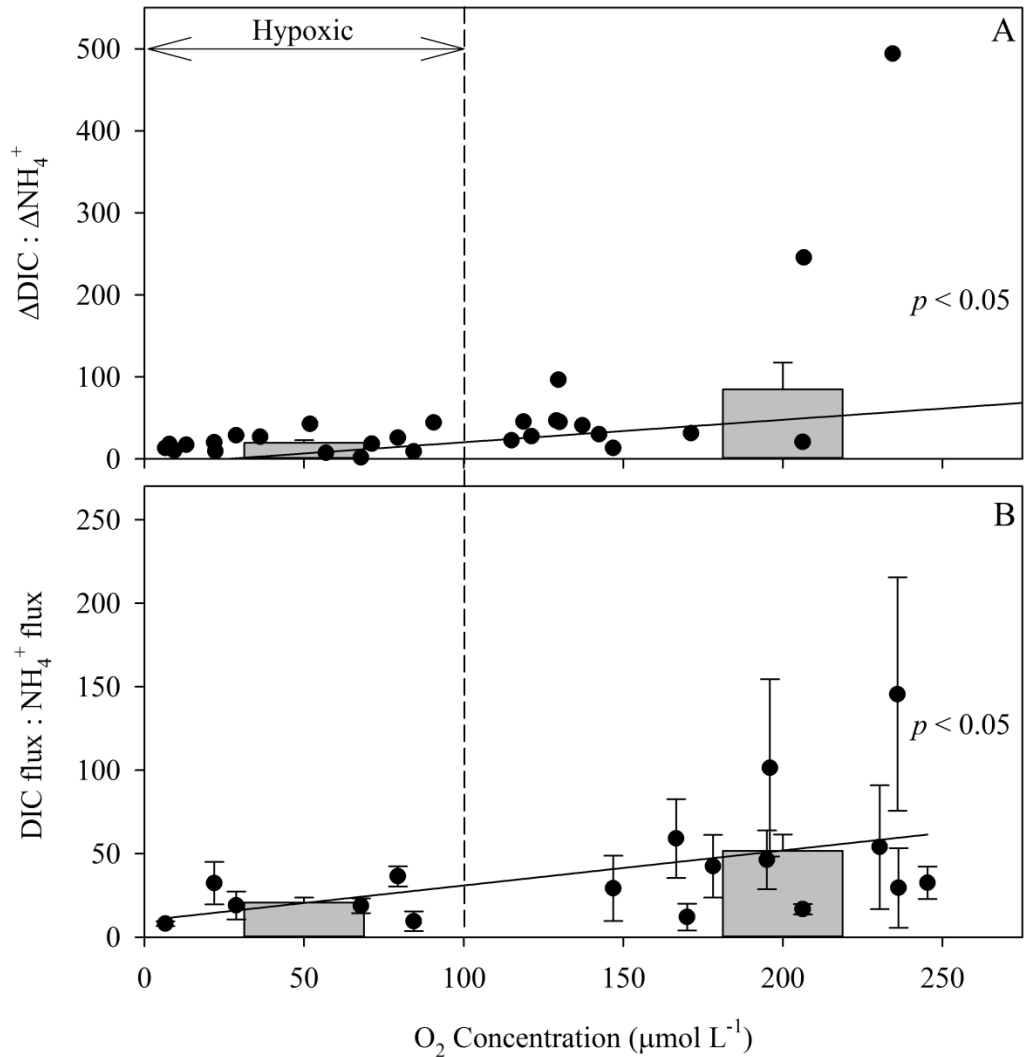


Figure 2.8 (A) Ratio of $\Delta\text{DIC}:\Delta\text{NH}_4^+$ with respect to dissolved oxygen concentration ($\mu\text{mol L}^{-1}$) in the bottom water of the Yarra River estuary, the bar graph represents mean $\Delta\text{DIC} : \Delta\text{NH}_4^+$ under hypoxic conditions ($< 100 \mu\text{mol-O}_2 \text{ L}^{-1}$) and oxic conditions ($> 100 \mu\text{mol-O}_2 \text{ L}^{-1}$); there was a significant difference between the means ($p < 0.05$); (B) Ratio of DIC flux : NH_4^+ flux \pm SE from the sediment. There was a significant difference between the mean DIC : NH_4^+ ratio under hypoxic and oxic conditions ($p < 0.05$).

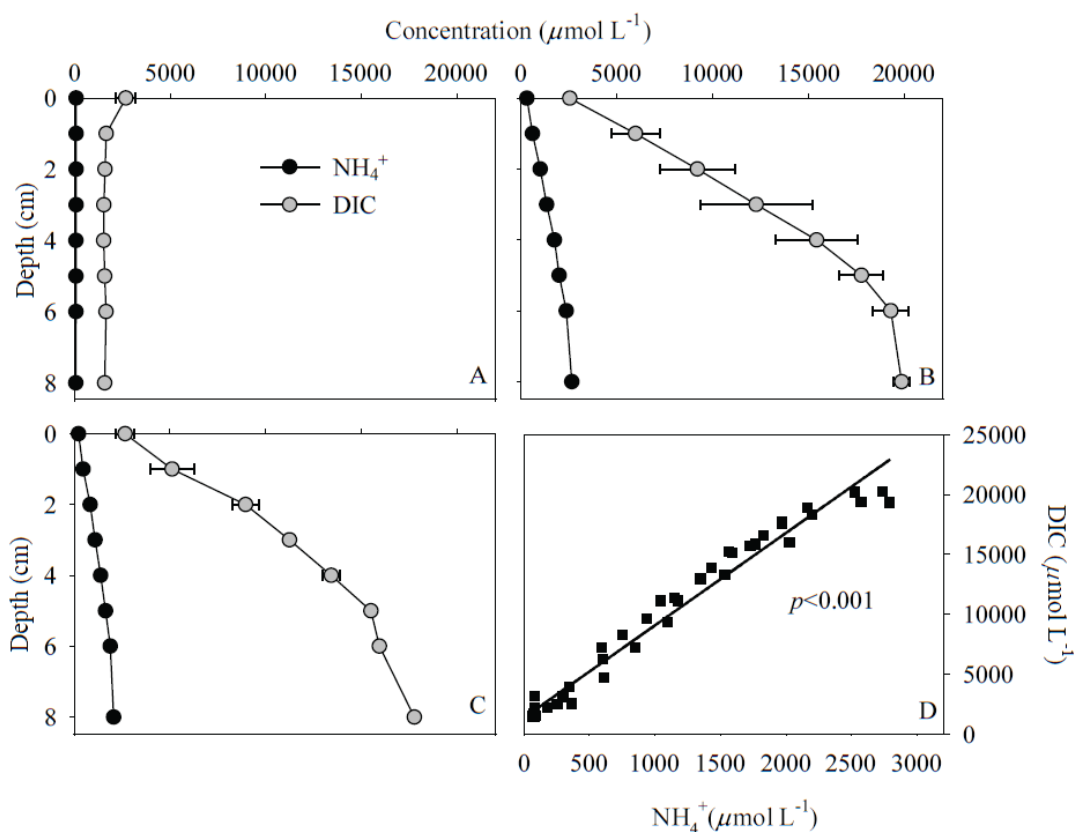


Figure 2.9 Mean NH_4^+ and DIC (\pm SE; $\mu\text{mol L}^{-1}$) with respect to sediment depth (cm) for sediment collected in February 2011 at (A) Morell Bridge, (B) Scotch College, and (C) Bridge Road; (D) DIC ($\mu\text{mol L}^{-1}$) with respect to NH_4^+ ($\mu\text{mol L}^{-1}$) for all profiles in February 2011; the regression was significant ($R^2 = 0.98$, $p < 0.001$)

2.5.5 Denitrification and DNRA

There was a trend for increasing denitrification rates moving upstream from Morell Bridge to Bridge Road, with the highest rates observed in March 2011 at Bridge Road corresponding to large fluxes of NO_3^- into the sediment (Fig. 2.7). DNRA followed the opposite trend, with the highest rate found at Morell Bridge (Fig. 2.7). At all sites DNRA was highest in January and March 2011, during a period of high freshwater inflows (Figs. 2.4, 2.7). During these months the front of the salt wedge was consistently observed at Morell Bridge and the water column was fresh and oxygenated at Scotch College and Bridge Road (Fig. 2.4).

There was a significant difference between mean denitrification : DNRA ratios under hypoxic and oxic conditions ($p < 0.05$; Fig. 2.10C). Under hypoxic conditions, denitrification contributed 99.1 ± 0.3 % of the total NO_3^- reduction (Fig. 2.10). When conditions were oxic, however, DNRA contributed a greater proportion

of the total NO_3^- reduction, averaging 39 ± 11 % of the NO_3^- reduction compared to < 1 % under hypoxic conditions. The denitrification : DNRA ratio was negatively related to oxygen concentration: Denitrification : DNRA = $-0.70(\text{O}_2) + 160.10$ ($df = 12$, $R^2 = 0.58$, $p < 0.01$). Multiple regression analysis of denitrification : DNRA against NO_x and oxygen resulted in a significant relationship: Denitrification : DNRA = $-0.63(\text{O}_2) - 0.83(\text{NO}_x) + 169.41$ ($df = 10$, $R^2 = 0.52$, $p < 0.05$). No relationship was observed between DNRA and salinity for both DNRA potential ($^{15}\text{N-NH}_4^+$ accumulation) and DNRA rate (Fig. 2.11A). Moreover, no significant relationship was observed between DNRA rates and salinity when O_2 concentrations $< 100 \mu\text{mol L}^{-1}$ were excluded to remove any interference by reducing conditions (Gardner *et al.*, 2006).

Total NO_3^- reduction increased with dissolved oxygen concentration, and a significant difference was found between the means under hypoxic (61 ± 5 (SE) $\mu\text{mol m}^{-2} \text{h}^{-1}$) and oxic ($250 \pm 30 \mu\text{mol m}^{-2} \text{h}^{-1}$) conditions ($n = 18$, $p < 0.05$). The mean DNRA rate, $124 \pm 31 \mu\text{mol m}^{-2} \text{h}^{-1}$, under oxic conditions was significantly higher than the mean DNRA rate $0.6 \pm 0.1 \mu\text{mol m}^{-2} \text{h}^{-1}$, under hypoxic conditions ($p < 0.05$; Fig. 2.10A). Comparison of denitrification rates under oxic and hypoxic conditions resulted in a marginally significant difference between the means ($p = 0.07$; Fig. 2.10B), however, the denitrification versus oxygen regression was not significant: Denitrification = $0.51(\text{O}_2) + 27.85$ ($df = 17$, $R^2 = 0.16$, $p = 0.10$) due to the high variability in the rates observed during oxic conditions. Nitrification-coupled denitrification significantly decreased with oxygen depletion: $D_n = 0.53(\text{O}_2) + 5.57$ ($df = 17$, $R^2 = 0.21$, $p = 0.05$). In addition, a significant difference was observed between mean nitrification-coupled denitrification during hypoxic and oxic conditions ($p < 0.05$) with nitrification-driven denitrification ~ 3 fold higher in the presence of oxygen. No significant difference was observed between water column driven denitrification under hypoxic and oxic conditions. Oxygen, and more importantly NO_x , were identified to be weak, but significant predictors of denitrification in multiple regression analysis: Denitrification = $-0.02(\text{O}_2) + 5.39(\text{NO}_x) - 8.80$ ($df = 10$, $R^2 = 0.52$, $p < 0.05$). No relationship was observed between DNRA potential ($^{15}\text{N-DNRA}$, $\mu\text{mol m}^{-2} \text{h}^{-1}$) and oxygen concentration (O_2 , $\mu\text{mol L}^{-1}$; Fig. 2.11B). No relationship was observed between DNRA rates ($^{14}\text{N-DNRA}$, $\mu\text{mol m}^{-2} \text{h}^{-1}$) and DIC flux ($\mu\text{mol m}^{-2} \text{h}^{-1}$; Fig. 2.11C).

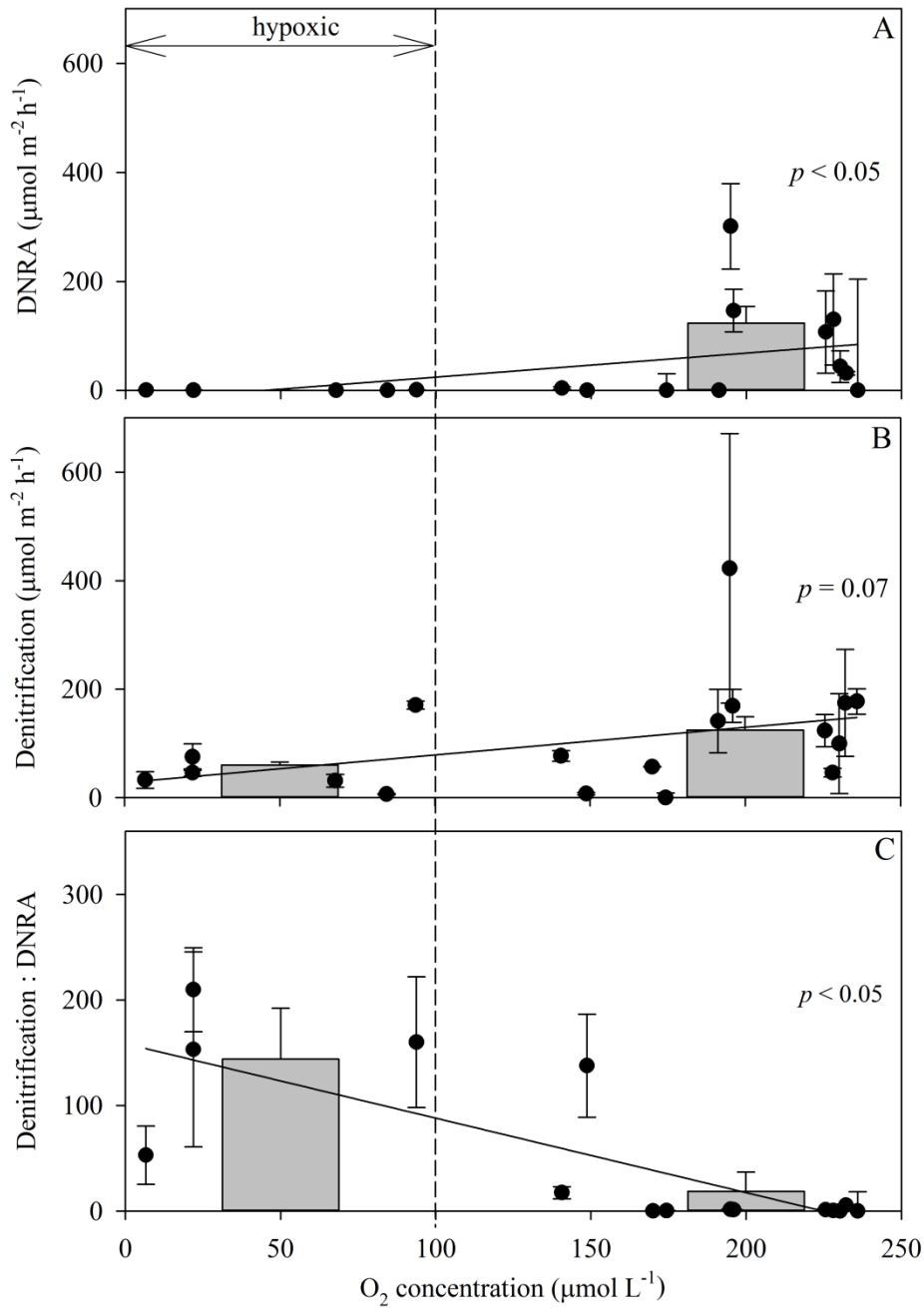


Figure 2.10 (A) DNRA (\pm SE; $\mu\text{mol m}^{-2} \text{h}^{-1}$) in response to dissolved oxygen concentration ($\mu\text{mol L}^{-1}$). The bar graphs represent the mean DNRA rates under hypoxic and oxic conditions; the means were significantly different ($p < 0.05$). (B) Denitrification (\pm SE; $\mu\text{mol m}^{-2} \text{h}^{-1}$) with respect to oxygen concentration. The bars represent mean denitrification under hypoxic and oxic conditions; means were marginally significant ($p = 0.07$). (C) Denitrification : DNRA \pm SE ratio in response to dissolved oxygen concentration ($\mu\text{mol L}^{-1}$). The bar graph represents the means of denitrification : DNRA ratio \pm SE under hypoxic conditions; the means were significantly different ($p < 0.05$).

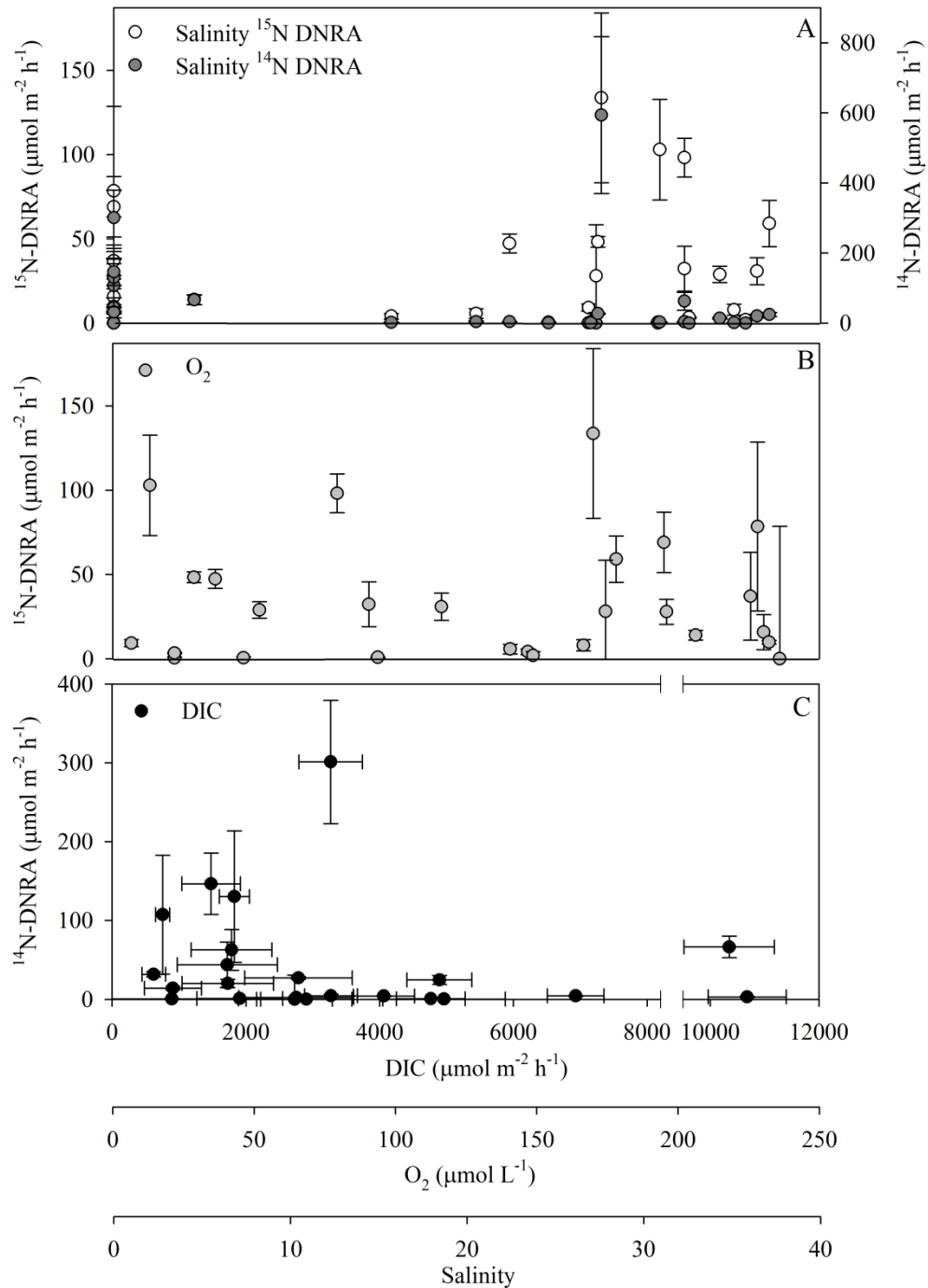


Figure 2.11 ³ (A) ^{15}N -DNRA potential (\pm SE; $\mu\text{mol m}^{-2} \text{h}^{-1}$) and DNRA rate (^{14}N -DNRA; \pm SE; $\mu\text{mol m}^{-2} \text{h}^{-1}$) with respect to salinity; and (B) ^{15}N -DNRA potential (\pm SE; $\mu\text{mol m}^{-2} \text{h}^{-1}$) with respect to bottom water oxygen concentration (O_2 , $\mu\text{mol L}^{-1}$). (C) DNRA rate (\pm SE; $\mu\text{mol m}^{-2} \text{h}^{-1}$) with respect to DIC flux (\pm SE; $\mu\text{mol m}^{-2} \text{h}^{-1}$) negative DIC values were excluded.

³DNRA rates measured during February, April, May and June 2011 are included (these months were not presented in Figure 2.7 due to an underestimation of denitrification only).

2.6 Discussion

2.6.1 Development of hypoxia in the Yarra River estuary

To draw together the interactions between the physical drivers (flow and stratification) and the nitrogen cycling processes, we have created a conceptual diagram which we refer to throughout the discussion (Fig. 2.12). Hypoxia in estuaries and coastal zones is increasing throughout the world (Diaz, 2001). In general, hypoxia is caused by a combination of stratification and an increase in carbon loading caused by high nutrient runoff (Kemp *et al.*, 2005). In contrast, hypoxia in the Yarra River estuary was caused by stratification induced by low freshwater inflows (Figs. 2.3, 2.12), which led to a high residence time of the bottom waters, an observation which has also been made in the Tone River estuary, Japan (Ishikawa *et al.*, 2004).

During the summer of 2009 - 2010, which had ~80 % of mean summer rainfall (www.bom.gov.au), the salt wedge persisted in the estuary, advancing up to ~16 km upstream of the Bolte Bridge, with oxygen saturation declining to < 3 % (Fig. 2.4). In contrast, during the 2010 - 2011 summer, the salt wedge did not advance beyond ~8 km upstream and oxygen saturation remained above 40 % (Fig. 2.4). High rainfall in the months following July 2010 through to March 2011 (~115 % of the average rainfall in 2010, www.bom.gov.au) resulted in high freshwater inflows into the Yarra River estuary forcing the salt wedge downstream toward Port Phillip Bay. Substantial peaks in freshwater inflow reduced the residence time of the salt wedge within the estuary preventing hypoxia from developing during this period (Fig. 2.12). This study, therefore, provides a unique insight into how nitrogen is recycled within an estuary under different flow regimes driven by climate variability (as opposed to seasonality).

2.6.2 DON production during hypoxia

In the Yarra River estuary, oxygen controls the behaviour of DON, the production of which was only observed during hypoxia in the bottom waters (Fig. 2.6). Burdige and Zheng (1998) observed a similar increase in DON during hypoxia at a salinity stratified site of Chesapeake Bay, USA. In that study, high organic matter inputs driving rapid mineralisation rates at the sediment surface contributed to

the elevated levels of DON (Fig. 2.12). The Chesapeake Bay study also observed preferential utilisation of nitrogen rich organic matter at low mineralisation rates. This lead to a decrease in DON during oxic conditions, while there was no selectivity for nitrogen rich organic matter at high mineralisation rates, leading to the accumulation of DON under hypoxic conditions (Burdige, 2001; Burdige and Zheng, 1998). Furthermore, in a study of the Aarhus Bight, Denmark, it was speculated the hypoxic release of DON was due to less efficient mineralisation of organic nitrogen during hypoxic conditions (Hansen and Blackburn, 1991). DON produced and accumulated during hypoxia in the salt wedge of the Yarra River estuary will be exported to Port Phillip Bay during the next high flow event and some of this DON may be bioavailable (Seitzinger and Sanders, 1997).

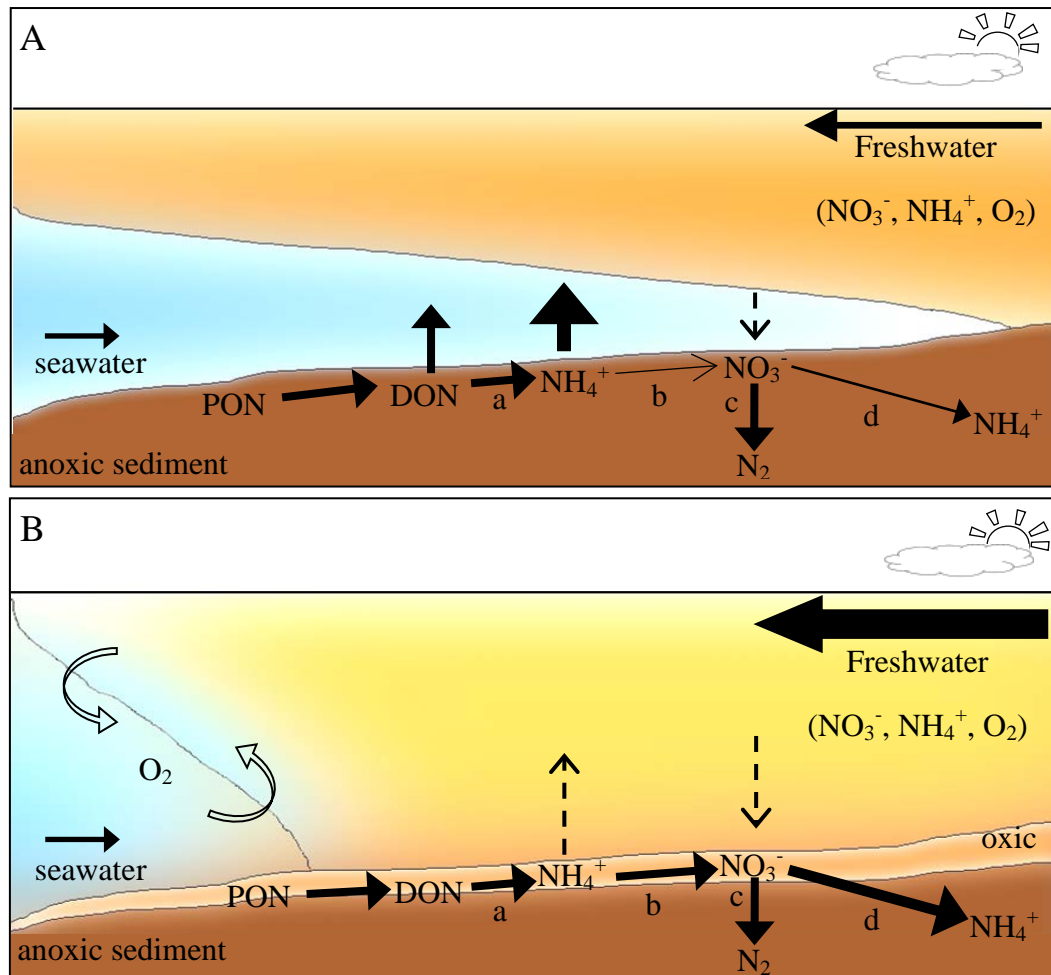


Figure 2.12 Conceptual diagram of the Yarra River estuary when conditions are: (A) a hypoxic stratified salt wedge, and (B) oxic where the salt and freshwater are mixed. The size of the arrow represents the relative contribution of each process; a) mineralisation, b) nitrification, c) denitrification and d) DNRA under hypoxic and oxic conditions.

2.6.3 Net efflux of NH_4^+ during hypoxia

The net production of NH_4^+ in the Yarra River estuary substantially deviated from conservative mixing when conditions were hypoxic in the bottom waters (Fig. 2.6). This has also been observed in a number of environments including lakes, lagoons and estuarine fjords (Christensen *et al.*, 2000; Rysgaard *et al.*, 1996; Rysgaard *et al.*, 1994). There are four mechanisms which could result in the increase in NH_4^+ during hypoxia:

- (1) Increased mineralisation
- (2) Cessation of nitrification
- (3) DNRA
- (4) Increased residence time

In the present study, the ΔNH_4^+ values provide insight into the behaviour of NH_4^+ at varied oxygen concentrations but they do not distinguish between NH_4^+ accumulated due to changes in the residence time of the hypoxic salt wedge or a shift in the production rate of NH_4^+ within the estuary. To remove the influence of residence time and mineralisation rate on NH_4^+ concentration we used DIC : NH_4^+ ratios which indicate how efficiently NH_4^+ is produced through mineralisation processes. Normally such an approach would not be very meaningful because of assimilation of both DIC and NH_4^+ by photoautotrophs. Exchange of DIC with the atmosphere also complicates such an analysis. In this case, however, we justify using this approach on the basis that the salt wedge of the estuary is aphotic owing to high turbidity in the surface waters. This was confirmed through chlorophyll *a* analysis as an indicator of microphytobenthos; no chlorophyll *a* was detected. Furthermore, the euphotic depth measured in the Yarra River estuary did not exceed 1.3 m, much less than the average sampling depth of 3.2 ± 0.1 m suggesting light did not penetrate to the sediment surface and as such, there are no active photoautotrophs in the salt wedge and assimilation of DIC is unlikely. The bottom waters are also isolated from the atmosphere meaning there will be minimal DIC exchange.

There was good agreement between the $\Delta\text{DIC} : \Delta\text{NH}_4^+$ ratios from the *in situ* measurements (whole system) and the DIC : NH_4^+ ratios of the fluxes measured in

the core incubations, indicating that the whole system concentrations reflected sediment biogeochemical processing. Under oxic conditions, the $\Delta\text{DIC} : \Delta\text{NH}_4^+$ ratio was 85 ± 33 , and the $\text{DIC} : \text{NH}_4^+$ flux ratio was 52 ± 10 (Fig. 2.8). Both of these values are much higher than the $\sim 8 : 1$ regeneration ratio observed in the anoxic sediment (Fig. 2.9). This is consistent with high rates of coupled nitrification and subsequent denitrification within the sediment, which were measured in the isotope pairing technique (Fig. 2.7). Under hypoxic conditions, this ratio decreased to 20 ± 3 and 21 ± 3 for the whole system measurements and cores, respectively (Fig. 2.8). The observed decrease in $\text{DIC} : \text{NH}_4^+$ is consistent with a reduction in the amount of NH_4^+ removed through coupled nitrification-denitrification (Fig. 2.12); under these conditions the hypoxic sediment supplied $\sim 40\%$ of the NH_4^+ released during hypoxia. When conditions were nearing anoxic ($\text{O}_2 < 10 \mu\text{mol L}^{-1}$) ~ 60 and 100% of the NH_4^+ present in the water column came from the anoxic sediment for the whole system measurements and cores, respectively. As such, hypoxia disconnected the link between nitrogen removal (via nitrification) and mineralisation, leading to a net efflux of NH_4^+ from the sediment (Fig. 2.12) which is also consistent with previous studies in Chesapeake Bay and the Etung de Prost Lagoon (Kemp *et al.*, 2005; Rysgaard *et al.*, 1996).

DNRA is unlikely to be responsible for the increased NH_4^+ seen during hypoxia. Rates of DNRA were measured in this study under both oxic and hypoxic conditions and DNRA was negligible under hypoxia (Figs. 2.7, 2.10). The mean DNRA rate under hypoxic conditions was $0.6 \pm 0.1 \mu\text{mol m}^{-2} \text{h}^{-1}$, which equates to $< 1\%$ of the mean total NO_3^- reduction. This is consistent with Nizzoli *et al.* (2010), who found that DNRA was of minimal importance in the hypolimnetic sediments of two lowland lakes in Italy. In that study, DNRA only contributed $1 - 6\%$ of the NH_4^+ produced; mineralisation and lack of nitrification were considered the causes of NH_4^+ regeneration during summer hypoxia.

2.6.4 Denitrification and DNRA in the Yarra River estuary

The factors controlling the relative importance of denitrification and DNRA are still poorly understood. In Chesapeake Bay, the effectiveness of denitrification as a sink decreased with persistent hypoxia due to the breakdown of nitrification (Kemp

et al., 2005). This is in agreement with our findings; denitrification was lower during hypoxia (marginally significant $p = 0.07$) and the contribution of nitrification coupled denitrification in the Yarra River estuary decreased during hypoxic conditions by ~3 fold (Figs. 2.10, 2.12). However, water column driven denitrification remained unchanged with oxygen concentration. In agreement with observations made by Rysgaard *et al.* (1994) in sediments from a freshwater lake in Denmark, the development of hypoxia in the Yarra River estuary reflects a reduction in denitrification and subsequent nitrogen removal due to the breakdown of nitrification-denitrification coupling.

In general, it is thought that DNRA is favoured over denitrification under reducing conditions (caused by low dissolved oxygen and/or high carbon loading) and a low availability of NO_3^- (Burgin and Hamilton, 2007). As a result, we expected DNRA to increase during hypoxia within the salt wedge of the Yarra River estuary due to increased rates of sulfate reduction and low NO_3^- concentrations. However, the highest rates of DNRA were observed in the summer and autumn of 2010 - 2011 when abnormally high rainfall resulted in the persistence of oxic conditions, particularly in March 2011 when DNRA was ~10 fold higher than denitrification (Fig. 2.7). The denitrification : DNRA ratio was significantly higher under hypoxic conditions and this observation is supported by laboratory studies on the Yarra River estuary sediments in November 2009 (Chp. 3 - Fig. 3.1). In agreement with our study, Tobias *et al.* (2001) also observed a similar decrease in the denitrification : DNRA ratio due to an influx of oxygen rich groundwater into Chesapeake Bay.

Tobias *et al.* (2001) hypothesised that the presence of DNRA during aerobic conditions was due to a seasonal shift in microbial populations. The existence of aerobic nitrate ammonifiers has been documented by Tiedje (1988), however, their ecological importance in the recycling of NH_4^+ is poorly understood. In the present study, there was no relationship between DNRA potential (DNRA driven by $^{15}\text{N-NO}_3^-$) and oxygen concentration (Fig. 2.11B). This suggests nitrate ammonifiers are present at all oxygen concentrations and another factor is causing the increased DNRA rates observed in the presence of oxygen. Multiple regression analysis identified NO_3^- as an important predictor of the denitrification : DNRA ratio. However, the relationship between DNRA and water column NO_3^- alone was weak, although it is difficult to evaluate available NO_3^- during oxic conditions due to the

production of NO_3^- within the sediment through nitrification. In this study, nitrification was an important source of NO_3^- for DNRA in the presence of oxygen (Figs. 2.7, 2.12). Therefore, it is possible the high rates of NO_3^- reduction during oxic conditions were stimulated by an excess of available NO_3^- , provided by both nitrification and freshwater inputs, alleviating competition between the two processes (Fig. 2.12B). These observations are consistent with Dong *et al.* (2011) where DNRA rates increased ~10 fold more than denitrification, and Erler *et al.* (2013) where DNRA rates increased 3 fold more than denitrification, after NO_3^- additions to sediment samples from tropical coastal systems. In addition, our observations are consistent with DNRA rates observed in forest soils of Puerto Rico, where aerobic conditions provided the highest rates of DNRA and the process was controlled by NO_3^- availability rather than oxygen concentration (Pett-Ridge *et al.*, 2006).

The other factor leading to reducing conditions is carbon loading, and this is often found to be a key control over DNRA. It is well known that sulfur oxidising bacteria are able to undertake DNRA, and these bacteria typically exist in environments with high organic carbon loading, leading to high rates of sulfide production (Hinck *et al.*, 2007; Sayama *et al.*, 2005; Zopfi *et al.*, 2001). Fermentative bacteria, which are also nitrate ammonifiers, are favoured under high carbon conditions (Burgin and Hamilton, 2007). In a shallow estuarine fjord in Denmark, the highest rates of DNRA were observed in the presence of high carbon loading and subsequent oxygen consumption below fish cages (Christensen *et al.*, 2000). In addition, Gardner and McCarthy (2009) observed the highest rates of DNRA where there was high sediment oxygen demand in Florida Bay. However, in both of these studies high DNRA rates could have been linked to sulfate reduction and the establishment of sulfur oxidisers stimulated by the high carbon inputs. In contrast to these studies, no relationship was observed between DIC production and DNRA rates (Fig. 2.11C), suggesting that carbon availability was not a predictor of DNRA in the Yarra River estuary. The fact that there was no link to reducing conditions within the Yarra River estuary may be due to the high supply of iron oxyhydroxides from the Yarra River (Blackwell *et al.*, 2010) that provide a buffer to the release of free sulfides via the precipitation of iron sulfide within the sediment.

Gardner *et al.* (2006) attributed an increase in DNRA with salinity to the increase in sulfate as a source for sulfate reducing bacteria to undertake DNRA. In the present study, no relationship was observed between salinity and DNRA, despite the *in situ* NH_4^+ concentration correlating with salinity (Fig. 2.11). In the Yarra River estuary, salinity is not independent of oxygen; high salinity correlates with low oxygen conditions and the potential for NH_4^+ production via mineralisation and cessation of nitrification rather than DNRA, as observed by Gardner *et al.* (2006).

Although this study contrasts with some previous work, many of these previous DNRA measurements were made on euphotic sediment where benthic microphytes may have assimilated the added $^{15}\text{N-NO}_3^-$ and reduced it to $^{15}\text{N-NH}_4^+$ for assimilation into biomass – assimilatory nitrate reduction to ammonium (ANRA). Some studies have attempted to overcome this problem by incubating sediments in the dark before tracer addition (Nizzoli *et al.*, 2010; Sorensen, 1978). However, benthic microphytes are ubiquitous in shallow water environments, and may assimilate nitrogen for many hours to days after darkening (Cook *et al.*, 2004b; Rysgaard *et al.*, 1993). Moreover, a number of studies have disregarded assimilation in the presence of high NH_4^+ concentrations. However, Rice and Tiedje (1989) showed that although high NH_4^+ concentrations suppressed NO_3^- assimilation, it was never completely inhibited. Silver *et al.* (2001) discussed the difficulty in measuring DNRA in the presence of assimilation where most of the NO_3^- reduction to NH_4^+ is undertaken by plants and benthic microalgae, rather than DNRA, but there have been no studies into the potential importance of this artefact. Given that sediment respiration rates in shallow waters are often controlled to a large extent by primary production (Cook *et al.*, 2004a; Maher and Eyre, 2011), great caution should be observed when interpreting strong positive correlations between sediment respiration and DNRA, for example Gardner and McCarthy (2009). The sediments from the Yarra River estuary were aphotic owing to the high turbidity in the surface waters as discussed previously. Therefore the DNRA estimates presented in this study are true estimates of DNRA in the absence of ANRA.

The range of DNRA rates observed in this study were higher than those observed in other temperate estuarine systems presented in the literature (Dong *et al.*, 2011). The Yarra River estuary, however, differs from typical temperate estuarine systems, for example those studied by Dong *et al.* (2006), because it is prone to

periods of hypoxia during low flow events and the system is subject to flushing during high flow events re-establishing oxic conditions, much like the tropical Cisadane estuary, Indonesia (Fig. 2.12; Dong *et al.*, 2011). In addition, DNRA in the Yarra River estuary differed greatly from observations made in Florida Bay and estuarine waters along the Texas coast, for example, where DNRA was enhanced by reducing conditions (Gardner and McCarthy, 2009; Gardner *et al.*, 2006). Observations in the Yarra River estuary contradict the general view of DNRA and its causative factors (reducing conditions, low NO_3^-), however this study was in good agreement with DNRA rates observed in tropical coastal systems by Dong *et al.* (2011) and Erler *et al.* (2013) where DNRA increased when NO_3^- limitation was removed. The importance of NO_3^- availability in determining DNRA rates remains poorly understood and is an important avenue for future research, particularly in the Yarra River estuary.

2.7 Concluding Remarks

The net production of NH_4^+ was enhanced by two different mechanisms within the Yarra River estuary during high and low flow events (Fig. 2.12). During low flow hypoxia, NH_4^+ recycling was enhanced through the inhibition of nitrification coupled denitrification, leading to less nitrogen removed as N_2 and the accumulation of NH_4^+ (Fig. 2.12A). High flow, oxic conditions and higher NO_3^- availability (both from the water column and nitrification) lead to higher rates of DNRA relative to denitrification (Fig. 2.12B). This highlights that DNRA may be an important process under oxic conditions in the water column, which to date, have not been regarded as conducive to this process. Understanding the controlling factors behind these two mechanisms is essential for deriving accurate budgets of nitrogen processing within the Yarra River estuary and is an important avenue for future research.

2.8 Acknowledgements

We are grateful to Scotch College and the Hawthorn Rowing Club for providing private boat ramp access. We would like to thank D. Kerr and A. Kessler for their assistance in the field. We thank Wayne S Gardner and an anonymous reviewer for their thoughtful and constructive review of the manuscript. We would like to acknowledge the support of the Australian Research Council (LP0991254), Melbourne Water Corporation and the Environment Protection Authority Victoria.

2.9 References

- An S. and Gardner W.S. (2002) Dissimilatory nitrate reduction to ammonium (DNRA) as a nitrogen link, versus denitrification as a sink in a shallow estuary (Laguna Madre/ Baffin Bay, Texas). *Marine Ecology Progress Series* **237**, 41-50.
- APHA (2005) *APHA-AWWA-WPCF, Standard Methods for the Examination of Water and Wastewater*. American Public Health Association, American Water Works Association and Water Environment Federation, Washington.
- Beckett R., Easton A.K., Hart B.T., and McKelvie I.D. (1982) Water movement and salinity in the Yarra and Maribyrnong Estuaries. *Australian Journal of Marine and Freshwater Research* **33**, 401-415.
- Bianchi T.S. (2007) *Biogeochemistry of Estuaries*. Oxford University Press, New York.
- Blackwell M.S.A., Yamulki S., and Bol R. (2010) Nitrous oxide production and denitrification rates in estuarine intertidal saltmarsh and managed realignment zones. *Estuarine, Coastal and Shelf Science* **87**, 591-600.
- Bonin P., Omnes P., and Chalamet A. (1998) Simultaneous occurrence of denitrification and nitrate ammonification in sediments of the French Mediterranean Coast. *Hydrobiologia* **389**, 169-182.
- Burdige D.J. (2001) Dissolved organic matter in Chesapeake Bay sediment pore waters. *Organic Geochemistry* **32**, 487-505.
- Burdige D.J. and Zheng S. (1998) The biogeochemical cycling of dissolved organic nitrogen in estuarine sediments. *Limnology and Oceanography* **43**, 1796-1813.
- Burgin A.J. and Hamilton S.K. (2007) Have we overemphasized the role of denitrification in aquatic ecosystems? A review of nitrate removal pathways. *Frontiers in Ecology and the Environment* **5**, 89-96.
- Childs C.R., Rabalais N.N., Turner R.E., and Proctor L.M. (2002) Sediment denitrification in the Gulf of Mexico zone of hypoxia. *Marine Ecology Progress Series* **240**, 285-290.

- Christensen P.B., Rysgaard S., Sloth N.P., Dalsgaard T., and Schwaerter S. (2000) Sediment mineralization, nutrient fluxes, denitrification and dissimilatory nitrate reduction to ammonium in an estuarine fjord and sea cage trout farms. *Aquatic Microbial Ecology* **21**, 73-84.
- Conley D.J., Carstensen J., Aertebjerg G., Christensen P.B., Dalsgaard T., Hansen J.L.S., and Josefson A.B. (2007) Long-term changes and impacts of hypoxia in Danish coastal waters. *Ecological Applications* **17**, S165-S184.
- Cook P.L.M., Butler E.C.V., and Eyre B.D. (2004a) Carbon and nitrogen cycling on intertidal mudflats of a temperate Australian estuary I. Benthic metabolism. *Marine Ecology Progress Series* **280**, 25-38.
- Cook P.L.M., Revill A.T., Butler E.C.V., and Eyre B.D. (2004b) Carbon and nitrogen cycling on intertidal mudflats of a temperate Australian estuary II. Nitrogen cycling. *Marine Ecology Progress Series* **280**, 39-54.
- CSIRO (1996) *Port Phillip Bay Environmental Study - The Findings 1992-1996*. CSIRO and Melbourne Water, Melbourne.
- Dalsgaard T., Nielsen L.P., Brotas V., Viaroli P., Underwood G.J.C., Nedwell D.B., Sundback K., Rysgaard S., Miles A., Bartoli M., Dong L.F., Thornton D.C.O., Ottosen L.D.M., Castaldelli G., and Risgaard-Petersen N. (2000) *Protocol Handbook for NICE - Nitrogen Cycling in Estuaries: a project under the EU research programme: Marine Science and Technology (MAST III)*. Ministry of Environment and Energy, National Environmental Research Institute, Department of Lake and Estuarine Ecology, Denmark.
- Diaz R.J. (2001) Overview of hypoxia around the world. *Journal of Environmental Quality* **30**, 275-281.
- Dong L.F., Nedwell D.B., and Stott A. (2006) Sources of nitrogen used for denitrification and nitrous oxide formation in sediments of the hypernutrified Colne, the nutrified Humber, and the oligotrophic Conway estuaries, United Kingdom. *Limnology and Oceanography* **51**, 545-557.
- Dong L.F., Sobery M.N., Smith C.J., Rusmana I., Phillips W., Stott A., Osborn A.M., and Nedwell D.B. (2011) Dissimilatory reduction of nitrate to ammonium, not denitrification dominates benthic nitrate reduction in tropical estuaries. *Limnology and Oceanography* **56**, 279-291.

- Erler D.V., Trott L.A., Alongi D.M., and Eyre B.D. (2013) Denitrification, anammox and dissimilatory nitrate reduction to ammonia in the sediments of the southern Great Barrier Reef lagoon. *Marine Ecology Progress Series* **478**, 57-70.
- Eyre B.D. (2000) Regional evaluation of nutrient transformation and phytoplankton growth in nine river-dominated sub-tropical east Australian estuaries. *Marine Ecology Progress Series* **205**, 61-83.
- Eyre B.D. and Ferguson A.J.P. (2009) Denitrification efficiency for defining critical loads of carbon in shallow coastal ecosystems. *Hydrobiologia* **629**, 137-146.
- Gardner W.S. and McCarthy M.J. (2009) Nitrogen dynamics at the sediment-water interface in shallow, sub-tropical Florida Bay: why denitrification efficiency may decrease with increased eutrophication. *Biogeochemistry* **95**, 185-198.
- Gardner W.S., McCarthy M.J., An S., Sobolev D., Sell K.S., and Brock D. (2006) Nitrogen fixation and dissimilatory nitrate reduction to ammonium (DNRA) support nitrogen dynamics in Texas estuaries. *Limnology and Oceanography* **51**, 558-568.
- Hansen L.S. and Blackburn T.H. (1991) Aerobic and anaerobic mineralization of organic material in marine sediment microcosms. *Marine Ecology Progress Series* **75**, 283-291.
- Hinck S., Neu T.R., Lavik G., Mussmann M., De Beer D., and Jonkers H.M. (2007) Physiological adaptation of a nitrate-storing *Beggiatoa* sp. to diel cycling in a phototrophic hypersaline mat. *Applied and Environmental Microbiology* **73**, 7013-7022.
- Howarth R.W. and Marino R. (2006) Nitrogen as the limiting nutrient for eutrophication in coastal marine ecosystems: evolving views over three decades. *Limnology and Oceanography* **51**, 364-376.
- Ishikawa T., ASCE M., Suzuki T., and Qian X. (2004) Hydraulic study of the onset of hypoxia in the Tone River estuary. *Journal of Environmental Engineering* **130**, 551-561.
- Jorgensen K.S. (1989) Annual pattern of denitrification and nitrate ammonification in estuarine sediment. *Applied and Environmental Microbiology* **55**, 1841-1847.

- Kemp W.M., Boynton W.R., Adolf J.E., Boesch D.F., Boicourt W.C., Brush G., Cornwell J.C., Fisher T.R., Glibert P.M., Hagy J.D., Harding L.W., Houde E.D., Kimmel D.G., Miller W.D., Newell R.I.E., Roman M.R., Smith E.M., and Stevenson J.C. (2005) Eutrophication of Chesapeake Bay: historical trends and ecological interactions. *Marine Ecology Progress Series* **303**, 1-29.
- Kirk J.T.O. (1994) *Light and photosynthesis in aquatic ecosystems* Cambridge University Press, Cambridge.
- Lorenzen C.J. (1967) Determination of chlorophyll and pheo-pigments: spectrophotometric equations. *Limnology and Oceanography* **12**, 343-346.
- Maher D. and Eyre B.D. (2011) Benthic carbon metabolism in southeast Australian estuaries: habitat importance, driving forces, and application of artificial neural network models. *Marine Ecology Progress Series* **439**, 97-115.
- Millero F.J. (2006) *Chemical Oceanography*. CRC Press Taylor and Francis Group, Boca Raton.
- Miyajima T., Tsuboi Y., Tanaka Y., and Koike I. (2009) Export of inorganic carbon from two Southeast Asian mangrove forests to adjacent estuaries as estimated by the stable isotope composition of dissolved inorganic carbon. *Journal of Geophysical Research* **114**.
- Nielsen L.P. (1992) Denitrification in sediment determined from nitrogen isotope pairing. *FEMS Microbiology Ecology* **86**, 357-362.
- Nizzoli D., Carraro E., Nigro V., and Viaroli P. (2010) Effect of organic enrichment and thermal regime on denitrification and dissimilatory nitrate reduction to ammonium (DNRA) in hypolimnetic sediments of two lowland lakes. *Water Research* **44**, 2715-2724.
- Oshima M., Wei Y., Yamamoto M., Tanaka H., Takayanagi T., and Motomizu S. (2001) Highly sensitive determination method for total carbonate in water samples by flow injection analysis coupled with gas-diffusion separation. *Analytical Sciences* **17**, 1285-1290.
- Paerl H.W., Pinckney J.L., Fear J.M., and Peieris B.L. (1998) Ecosystem responses to internal watershed organic matter loading: consequences for hypoxia in the eutrophying Neuse River Estuary, North Carolina, USA. *Marine Ecology Progress Series* **166**, 17-25.

- Pett-Ridge J., Silver W.L., and Firestone M.K. (2006) Redox fluctuations frame microbial community impacts on N-cycling rates in a humid tropical forest soil. *Biogeochemistry* **81**, 95-110.
- R Core Team (2012) *R: A language and environment for statistical computing*. R Foundation for Statistical Computing www.R-project.org/, Vienna.
- Rice C.W. and Tiedje J.M. (1989) Regulation of nitrate assimilation by ammonium in soils and in isolated soil microorganisms. *Soil Biology and Biogeochemistry* **21**, 597-602.
- Risgaard-Petersen N., Nielsen L.P., Rysgaard S., Dalsgaard T., and Meyer R.L. (2003) Application of the isotope pairing technique in sediments where anammox and denitrification coexist. *Limnology and Oceanography: Methods* **1**, 63-73.
- Risgaard-Petersen N. and Rysgaard S. (1995) Nitrate reduction in sediments and waterlogged soil measured by ¹⁵N techniques, in: Alef, K., Nannipieri, P. (Eds.), *Methods in Applied Soil Microbiology and Biochemistry*. Academic Press, London, pp. 287-295.
- Ritter C. and Montagna P.A. (1999) Seasonal hypoxia and models of benthic response in a Texas Bay. *Estuaries* **22**, 7-20.
- Rysgaard S., Risgaard-Petersen N., Nielsen L.P., and Revsbech N.P. (1993) Nitrification and denitrification in lake and estuarine sediments measured by the ¹⁵N dilution technique and isotope pairing. *Applied and Environmental Microbiology* **59**, 2093-2098.
- Rysgaard S., Risgaard-Petersen N., and Sloth N.P. (1996) Nitrification, denitrification, and nitrate ammonification in sediments of two coastal lagoons in Southern France. *Hydrobiologia* **329**, 133-141.
- Rysgaard S., Risgaard-Petersen N., Sloth N.P., Jensen K., and Nielsen L.P. (1994) Oxygen regulation of nitrification and denitrification in sediments. *Limnology and Oceanography* **39**, 1643-1652.
- Santos I.R., Cook P., Rogers L., de Weys J., and Eyre B.D. (2012) The “salt wedge pump”: Convection-driven porewater exchange as a driver of carbon and nitrogen cycling in an estuary. *Limnology and Oceanography* **57**, 1415-1426.

- Sayama M., Risgaard-Petersen N., Nielsen L.P., Fossing H., and Christensen P.B. (2005) Impact of bacterial NO₃⁻ transport on sediment biogeochemistry. *Applied and Environmental Microbiology* **71**, 7575-7577.
- Seitzinger S.P. and Sanders R.W. (1997) Contribution of dissolved organic nitrogen from rivers to estuarine eutrophication. *Marine Ecology Progress Series* **159**, 1-12.
- Sigman D.M., Altabet M.A., Michener R., McCorkle D.C., Fry B., and Holmes R.M. (1997) Natural abundance-level measurement of the nitrogen isotopic composition of oceanic nitrate: an adaptation of the ammonia diffusion method. *Marine Chemistry* **57**, 227-242.
- Silver W.L., Herman D.J., and Firestone M.K. (2001) Dissimilatory nitrate reduction to ammonium in upland tropical forest soils. *Ecology* **82**, 2410-2416.
- Soetaert K., Middelburg J.J., Herman P.M.J., and Buis K. (2000) On the coupling of benthic and pelagic biogeochemical models. *Earth-Science Reviews* **51**, 173-201.
- Sorensen J. (1978) Capacity for denitrification and reduction of nitrate to ammonia in a coastal marine sediment. *Applied and Environmental Microbiology* **35**, 301-305.
- Tiedje J.M. (1988) Ecology of denitrification and dissimilatory nitrate reduction to ammonium, in: Zehnder, A.J.B. (Ed.), *Biology of Anaerobic Microorganisms*. Wiley, New York, pp. 179-244.
- Tobias C.R., Anderson I.C., Canuel E.A., and Macko S.A. (2001) Nitrogen cycling through a fringing marsh-aquifer ecotone. *Marine Ecology Progress Series* **210**, 25-39.
- Yin S.X., Chen D., Chen L.M., and Edis R. (2002) Dissimilatory nitrate reduction to ammonium and responsible microorganisms in two Chinese and Australian paddy soils. *Soil Biology and Biogeochemistry* **34**, 1131-1137.
- Zopfi J., Kjaer T., Nielsen L.P., and Jorgensen B.B. (2001) Ecology of *Thioploca* spp.: nitrate and sulfur storage in relation to chemical microgradients and influence of *Thioploca* spp. on the sedimentary nitrogen cycle. *Applied and Environmental Microbiology* **67**, 5530-5537.

3. Denitrification and DNRA in sediment profiles combining the isotope pairing technique and diffusive equilibrium in thin layer gels



Part of this chapter has been submitted for publication in Geochimica et Cosmochimica Acta: Roberts, K.L, Kessler, A.J, Grace, M.R and Cook, P.L.M (2013) 'Increased rates of DNRA under aerobic conditions in a periodically anoxic estuary are linked to the availability of iron'

3.1 Abstract

The Yarra river estuary is a salt wedge estuary prone to periods of hypoxia ($< 100 \mu\text{mol-O}_2 \text{ L}^{-1}$) in the bottom waters caused by low freshwater inflow. To further examine the findings in Chapter Two, NO_3^- reduction pathways were examined under changing oxygen conditions using bulk measurements and sediment profiles in intact cores. Denitrification was the main NO_3^- reduction pathway under all oxygen conditions in the Yarra River estuary. DNRA was $< 1 \%$ of total NO_3^- reduction under anoxic conditions and increased up to $\sim 18 \%$ in the presence of oxygen in the water column, in agreement with previous observations in the Yarra River estuary. The mean denitrification : DNRA ratio under anoxic conditions was 126 ± 17 and decreased to 5.3 ± 0.5 upon re-aeration of the water column. Sediment profiles of denitrification and DNRA confirmed the findings of the observational study and the long-term oxygen experiments. In both the September 2012 and January-February 2013 sediment profiles, DNRA was only observed in the presence of oxygen. S^{2-} was not a strong predictor of DNRA, however, the January-February profiles showed DNRA coincides with the presence of Fe^{2+} in the sediment and DNRA may be linked to Fe^{2+} availability.

The effectiveness of the two denitrification profile methods - the combined N_2O microelectrode-acetylene inhibition technique and the combined ^{15}N isotope pairing technique in diffusive equilibrium in thin layer (DET) gels - was dependent on oxygen concentration. The acetylene inhibition method inhibits nitrification and therefore only measures denitrification driven by NO_3^- supplied from the water column. Under anoxic conditions the N_2O and the $^{15}\text{N-N}_2$ method were comparable because denitrification is driven by water column NO_3^- . However, under oxic conditions the $^{15}\text{N-N}_2$ method was more representative of denitrification because it accounts for both nitrification and water column driven denitrification under these conditions, while the N_2O method most likely underestimated denitrification. In addition, the new $^{15}\text{N-N}_2$ method allows for the simultaneous measurement of denitrification and DNRA in the same core and DET gel. To improve resolution of the peak in the DET gel method the deployment time should be reduced and a peeper-like gel mould used to avoid lateral diffusion within the gel and relaxation of the peak. The new $^{15}\text{N-N}_2$ method is a valuable tool in determining the behaviour of NO_3^- reduction pathways simultaneously along with possible electron donors.

3.2 Introduction

In recent decades nitrogen cycling has received a great deal of attention in coastal waters because of its role in the increased incidences of eutrophication and hypoxia ($< 100 \mu\text{mol-O}_2 \text{ L}^{-1}$; Diaz and Rosenberg, 2008). To determine the fate of nitrogen within coastal waters, it is imperative to understand the controls on nitrogen cycling under these changing oxygen conditions. Estuarine systems are often prone to high inputs of bio-available nitrogen in the form of nitrate (NO_3^-). Two competing anaerobic processes can determine the fate of NO_3^- within an aquatic system; denitrification and dissimilatory nitrate reduction to ammonium (DNRA; Bianchi, 2007). Denitrification converts NO_3^- to di-nitrogen (N_2) gas which can diffuse from the system effectively removing the nitrogen in contrast to DNRA which converts NO_3^- to NH_4^+ retaining bio-available nitrogen within the system⁴. The balance between these two processes in an estuarine environment can determine whether nitrogen is removed or recycled, respectively, before it is transported into coastal waters.

Several hypotheses have been proposed to explain the partitioning between denitrification and DNRA¹. DNRA is considered to be favoured when conditions are reducing in addition to the presence of;

- ⇒ high organic carbon (Christensen *et al.*, 2000; Fazzolari *et al.*, 1998) and low NO_3^- (Jorgensen, 1989; King and Nedwell, 1985),
- ⇒ high temperatures ($> 10 \text{ }^\circ\text{C}$; Dong *et al.*, 2011; Ogilvie *et al.*, 1997),
- ⇒ sulfur oxidising bacteria (An and Gardner, 2002; Sayama *et al.*, 2005),
- ⇒ iron oxidising bacteria (Edwards *et al.*, 2007; Weber *et al.*, 2006).

At present, rates of denitrification and DNRA have been studied via three approaches;

- 1) bacterial culture studies (Sayama *et al.*, 2005; Weber *et al.*, 2006),
- 2) slurry experiments with additions of $^{15}\text{N-NO}_3^-$ and electron donors (Brunet and Garcia-Gil, 1996; King and Nedwell, 1985) and,

⁴ See general introduction for detailed description of denitrification and DNRA and Chapter Four for detailed information on the possible predictors of denitrification and DNRA.

- 3) bulk measurements using the ^{15}N isotope pairing technique (Nielsen, 1992) and slurrying the sediment after the incubation (Christensen *et al.*, 2000; Dong *et al.*, 2011; Rysgaard *et al.*, 1996).

While bacterial studies are useful to determine preferred energy pathways of denitrification and DNRA under controlled conditions, *in situ* bacterial communities are more complex and are subject to variable environmental conditions. As such, it is inaccurate to scale up the behaviour of denitrification and DNRA to complex ecosystems from bacterial studies alone. Alternatively, slurries are used to elucidate causative factors on NO_3^- reduction pathways, however by slurrying the sample, *in situ* gradients are destroyed and NO_3^- reducing communities are mixed often leading to an overestimation of NO_3^- reduction (Behrendt *et al.*, 2013; Revsbech *et al.*, 2006). Bulk measurements of denitrification and DNRA, although useful in determining general ecosystem trends, provide little information about the spatial distribution of these processes within the sediment and possible electron donor relationships. In sediments from Janssand, Germany, Behrendt *et al.* (2013) observed a shift in the relative contribution of denitrification and DNRA dependent on the method used; from a denitrification dominated system (87 % total NO_3^- reduction) for bulk measurements to a DNRA dominated system (82 %) in slurries.

At present there are two methods of determining the spatial distribution of NO_3^- reduction pathways and electron donors in intact sediment cores. In both methods $^{15}\text{N-NO}_3^-$ is added to the overlying water column before:

- 1) the core is sectioned (> 0.5 cm resolution) and each sediment slice slurried to determine the concentration of $^{15}\text{N-N}_2$ and $^{15}\text{N-NH}_4^+$ in the sediment slice (Preisler *et al.*, 2007)
- 2) a diffusive equilibrium thin layer (DET) gel is inserted into the sediment and later sliced (> 1 mm resolution) to determine the concentration of $^{15}\text{N-NH}_4^+$ (Stief *et al.*, 2010). Whilst in a separate core denitrification is measured using the acetylene inhibition technique and the accumulation of N_2O is measured using a microelectrode (100 μm resolution) (Sorensen, 1978; Stief *et al.*, 2010).

The simultaneous measurement of denitrification and DNRA in the first method is useful because heterogeneity in between sediment samples is avoided,

however the resolution is low and the sediment must be sliced before analysis. The second method provides higher resolution DNRA and denitrification data however these two parameters are measured in separate cores and therefore the method suffers from heterogeneity between samples. In addition, the use of the acetylene inhibition technique inhibits nitrification and therefore leads to the underestimation of total denitrification (Binnerup *et al.*, 1992). In a new method proposed by Kessler *et al.* (Under Review), $^{15}\text{N-N}_2$ is measured in DET gels. The present study provides the first example of the simultaneous high resolution profile measurement of denitrification and DNRA in intact sediment.

In the previous chapter, DNRA rates, measured in the Yarra River estuary, were comparable to denitrification rates under oxic conditions and insignificant under hypoxic conditions; contradicting the current paradigm (Chp. 2, Fig. 2.10). Here I made bulk measurements and intact sediment profiles using the new high resolution ^{15}N -DET gel method to determine the behaviour of denitrification and DNRA under changing oxygen conditions. The specific research questions addressed in this chapter were:

- 1) Can the change in the denitrification : DNRA ratio previously observed in the Yarra estuary be replicated experimentally?
- 2) Is there a change in the spatial distribution of denitrification and DNRA within the sediment? And if so, does this coincide with the presence or absence of available reductants such as S^{2-} or Fe^{2+} ?
- 3) Which method - the combined N_2O microelectrode-acetylene inhibition method or the combined ^{15}N isotope pairing technique in DET gels - is more representative of denitrification in high resolution sediment profiles?

3.3 Methods

3.3.1 Site Description

Nitrate reduction pathways were measured in the Yarra River estuary, Melbourne, Australia in November 2009, September 2012 and January-February 2013. In November 2009 sediment samples were collected near Morell Bridge (55°32'27.25''E 58°11'38.5''N), on all other sampling occasions sediment samples were collected from ~4.5 km upstream at Scotch College (55°32'63.48''E 58°10'85.4''N) to determine the behaviour of denitrification and DNRA within the Yarra River estuary. The estuary exhibits a typical salt wedge structure and is prone to extended periods of hypoxia during low rainfall. The salt wedge region of the estuary is aphotic in the bottom waters owing to the high turbidity of the surface waters (*see* Chp. 2 - 2.5.3).

3.3.2 Sampling

Sediment cores were collected in 27.5 × 6.6 cm polycarbonate cylinders and stoppered. Saline bottom water was collected using a bilge pump or a 5 L Niskin bottle. Sediment cores were transferred to a temperature-controlled water bath. Each core was mixed using a magnetic stirrer (~40 rpm) suspended ~2 cm above the sediment surface to prevent disturbance of the sediment.

3.3.3 Intact core incubations

Sediment and water samples were collected on the 24th November 2009 at Morell Bridge. The ¹⁵N isotope pairing technique (IPT; Dalsgaard *et al.*, 2000; Nielsen, 1992) was used to determine rates of denitrification and DNRA in two treatments (oxic and hypoxic) over a period of 21 days; rates were measured in the water column on day 1, 7, 11, 13, 18 and 21. Water was circulated through the cores using a peristaltic pump; for each treatment the reservoir was bubbled with air for oxic and argon for hypoxic conditions to maintain the desired oxygen concentration over the 21 day period. Four cores were kept oxic (200 - 300 μmol-O₂ L⁻¹) for the 21 day incubation period as the control treatment, and eight cores were hypoxic (< 100 μmol-O₂ L⁻¹) for the first 11 days. On day 11, the incubation of four of the eight

hypoxic cores was terminated to determine the concentration of $^{15}\text{N-NH}_4^+$ accumulated within the sediment. The remaining four hypoxic cores were made oxic by aerating the reservoir. Denitrification and DNRA were measured using the methods in Dalsgaard *et al.* (2000), however, to continue the experiment over the 21 day incubation period, the core was kept intact and a sample collected from the water column only. Water removed was replaced with saline water and accounted for in calculations.

At the start of the incubation, the dissolved oxygen (DO) and pH were measured in each core using a HQ-40d Hach multimeter (Germany). A NO_x ($\text{NO}_3^- + \text{NO}_2^-$) sample was filtered (0.45 μm ; 30 mm polypropylene housing, Bonnet) and stored until analysis. An aliquot of 0.4 mL of 0.05 mol L^{-1} $^{15}\text{N-NO}_3^-$ was added to each core and mixed thoroughly without disturbing the surface of the sediment. A 12 mL NO_x sample was collected after stirring to determine the final concentration of $^{15}\text{N-NO}_3^-$ in the sediment core; the displaced water was replaced and the core sealed. The cores were incubated for ~7 hours. At the end of the incubation period the DO and pH were measured and a 12 mL sample was filtered for the analysis of NO_x . A 12.5 mL unfiltered sample was collected for N_2 in a gas tight exetainer and preserved with 100 μL ZnCl_2 (50 % w:v). A 200 mL unfiltered sample was also collected for analysis of $^{15}\text{N-NH}_4^+$ via the ammonium diffusion method (ADM; *see* section 3.3.5). After the incubation period, the core was slowly refilled with saline water from the reservoir to avoid disturbance of the sediment surface. The cores were circulated to allow for re-equilibration before NO_3^- reduction pathways were measured again. To determine the background concentration and account for the carry-over of $^{15}\text{N-NO}_3^-$ for subsequent measurements on day 7, 11, 13, 18 and 21, a sample for $^{15}\text{N-N}_2$ and $^{15}\text{N-NH}_4^+$ was collected from the reservoir at the start of the incubation.

At the end of the experiment, the water was removed from the sediment surface and the core extruded. The surface 100 mL of sediment was homogenised and a 20 mL subsample extracted with 1:1 (v:v) 2 mol L^{-1} KCl shaken at 120 rpm for an hour and then centrifuged. The supernatant was measured for $^{15}\text{N-NH}_4^+$ via the ADM (*see* section 3.3.5). Denitrification (D_{15}) and DNRA (DNRA_{15}) were calculated from the accumulation of $^{15}\text{N-N}_2$ and $^{15}\text{N-NH}_4^+$, respectively, over time (*see* section 3.3.5, Table 3.1; Dalsgaard *et al.*, 2000; Nielsen, 1992).

3.3.4 Micro-profiles of nitrate reduction pathways

Sediment cores were collected in September 2012 and January and February 2013 (*see* section 3.3.2). In September, three treatments were tested: i) long-term anoxic, ii) sub-oxic and iii) short term oxic and in January-February 2013 three treatments were examined: i) short-term oxic, ii) long-term oxic and iii) long-term anoxic. Short-term refers to a pre-incubation period of 2-5 days after collection and long-term 2-3 weeks after collection. Six cores were collected for each treatment, three for H₂S and O₂ measurements (denitrification in September) and three for NO₃⁻ reduction pathways, nutrients and total Fe measurements. Oxic conditions were maintained during pre-incubation by circulating aerated site water above the sediment; during incubations the core was gently bubbled with air. Sub-oxic cores were initially purged with argon for ~10 mins and then kept sealed until the O₂ dropped to ~20 % air saturation. Anoxic cores were circulated with argon-purged site water and then sealed during incubations. Denitrification (N₂O or ¹⁵N-N₂) and DNRA (¹⁵N-NH₄⁺) were profiled alongside O₂, total Fe, NO₃⁻, total NH₄⁺ (¹⁴N-NH₄⁺ and ¹⁵N-NH₄⁺) and total S²⁻ in triplicate cores for each treatment. In September, denitrification profiles were measured using the acetylene inhibition technique and in January-February the ¹⁵N isotope pairing technique in diffusive equilibrium in thin layer (DET) gels was used to determine ¹⁵N-N₂ profiles after calibration.

Profiles of O₂ were measured in triplicate for each core using a fibre-optic sensor and a computer controlled micromanipulator (Pyroscience OXR230 connected to a Firesting O₂ meter and MUX2 profiler). The O₂ sensor was calibrated with 0 and 100 % O₂ saturated water of site salinity (Table 3.1).

Total S²⁻ was determined from the measurement of H₂S and pH. H₂S was measured in triplicate using an amperometric microsensor (Unisense H₂S-100 connected to a Unisense microsensor amplifier). H₂S data was logged in SensorTrace Basic V3.1.1 alongside O₂ profiles. The H₂S microsensor was calibrated in accordance with the Unisense procedure; calibration standards were prepared under anoxic conditions in pH 4 buffer over the linear sensor range of 0 to 300 μmol L⁻¹ (Table 3.1). Profiles of pH (Unisense pH-100, calibrated pH 4, 7 and 10, Table 3.1) were measured under oxic and anoxic conditions in September 2013 however the microsensor broke during use. As such, we have based the calculation of total S²⁻ on

the assumption the pH profiles were similar in both September 2012 and January-February 2013 for the oxic and anoxic treatment.

In September, denitrification was determined via the acetylene inhibition technique. The production of N₂O was measured using a microsensor (Unisense N₂O-100 connected to a Unisense microsensor amplifier calibrated following the Unisense calibration guidelines, Table 3.1) in a separate core to the DET gels (Sorensen 1978, Stief et al 2010). At the commencement of the experiments, ~10 % of the water column was replaced with acetylene saturated site water, then dosed with 1.5 mL 0.05 mol L⁻¹ NO₃⁻. The core was sealed and stirred in the temperature-controlled water bath for ~16 hours, allowing the acetylene to diffuse into the sediment. Profiles of N₂O were logged in SensorTrace V3.1.1 and aligned with O₂ measurements to determine sediment depth. The denitrification : DNRA ratio is not presented for September due to the underestimation of denitrification using the acetylene inhibition technique (*see* section 3.5.4).

Nitrate reduction pathways were measured using DET gels combined with the ¹⁵N isotope pairing technique. DNRA was measured as described in Stief *et al.* (2010) and denitrification (January-February) measured as described in Kessler *et al.* (Under Review). The acrylic gel probes were constructed as described previously in Krom *et al.* (1994) with the dimensions 8.5 (h) x 6 (w) x 0.8 (d) cm and a window where the gel is in contact with the sediment of 4.6 (w) x 5.0 (h) cm. Gels were cast as described in Stief *et al.* (2010); 80 mL acrylamide (15 % w:v) was mixed with 40 mL N,N- methylenebisacrylamide (2 % w:v) and slowly stirred. 1.5 mL dipotassium peroxodisulfate (0.11 mol L⁻¹) was added to initiate the polymerisation reaction and 120 µL N,N,N',N'- tetramethylethylenediamine was used as the catalyst. The gel was cast between two glass plates (pre-heated to ~40 °C) with 1 mm spacers and then clamped into position. The mould was heated to ~40 °C for ~20 minutes until polymerisation was complete. After the gel was cast it was hydrated in NaCl solution at the same salinity as the site water for 24 hours. The gel was ~2 mm thick after hydration. The gel was then cut to size, placed inside the gel probe and covered with 0.2 µm pore size polyethersulfone filter membrane (Pall, Australia) to prevent bacterial and physical degradation of the gel (Fig. 3.1A). The constructed gel probe was then stored at 4 °C in NaCl solution (site salinity) until used in experiments.

The overlying water column of the sediment core was dosed with 1.5 mL $0.05 \text{ mol L}^{-1} \text{ }^{15}\text{N-NO}_3^-$ ~24 hours before the deployment of the gel. The probe storage solution was purged for ~6 hours with N_2 before deployment to remove oxygen from the gel surface and then the gels were inserted vertically into the sediment (Fig. 3.1B). Oxidic conditions were maintained within the sealed core by gently bubbling with air and anoxic cores were kept sealed.

In September, one gel probe was inserted into each core and three replicate cores were examined; two cores for measurement of DNRA and one core for nutrients (NO_3^- and total NH_4^+). In January-February, two gel probes were inserted back to back in each core, one for the measurement of NO_3^- reduction pathways and the other for total NH_4^+ , NO_x and total Fe. The gels were allowed to equilibrate for ~30 hours before the gels were removed rinsed and sliced into 2 mm slices with depth (Fig. 3.1C). The gel was cut on an acid-washed glass plate using a homemade stainless steel cutting device which was acid-washed between samples. Gel slices for nutrients and total Fe were placed into 10 mL of ultrapure water and frozen until analysis (*see* section 3.3.5). Denitrification and DNRA were determined from the accumulation of $^{15}\text{N-N}_2$ and $^{15}\text{N-NH}_4^+$ within the gel, respectively. After slicing, each gel slice was immediately placed into a pre-filled 3 mL exetainer containing ultrapure water and 100 μL ZnCl_2 (50 % w:v). The process was filmed to calculate the exposure time of the gel to air and these times were used in the correction of N_2 concentration after calibration of the method (*see* section 3.3.5). A 1.5 mL He headspace was introduced into the 3mL exetainer for the analysis of $^{29}\text{N}_2$ and $^{30}\text{N}_2$ gas (Table 3.1). The 1.5 mL water sample removed was placed in a separate exetainer and purged with He, then $^{15}\text{N-NH}_4^+$ was collected from the sample using the hypobromite method (*see* section 3.3.5, Table 3.1). To account for any differences in the width of the gel slices, four gels were hydrated in ultrapure water and sliced, the slices were weighed and the average volume of the slice used in the calculation of concentration. The variation in between replicate slices was < 5 %.



Figure 3.1 (A) The gel sampler preparation before re-hydration, (B) the gel sampler inserted into the sediment and (C) the gel sampler removed and gel cut from the exposed window then sliced using the homemade stainless steel cutting device.

3.3.5 Analytical methods

Nutrient samples (NO_x and NH_4^+) were analysed via flow injection analysis (FIA, Table 3.1; Lachat Quickchem 8000 Flow injection Analyser, spectrophotometric detector). Standards, spikes and standard reference materials (SRM) were analysed following the procedures in Standard Methods for Water and Wastewater (2005) (Table 3.1) and were all within acceptable limits.

In January-February the iron from the DET gels was determined via the ferrozine method (Stookey, 1970; Voillier *et al.*, 2000). Standards were prepared in the range 0 - 1 mg L⁻¹ Fe and triplicate absorbance readings taken at 632 nm using a UV-Visible Spectrophotometer (GBC UV Visible Spectrophotometer - 918). All reagents were prepared as described in Voillier *et al.* (2000) (Table 3.1). Total Fe was determined by the addition of 0.5 mL ferrozine and 1 mL hydroxylamine hydrochloride and allowed to react ~20 minutes before the addition of 0.25 mL of ammonium acetate buffer. After the reagents were added, the samples were left for at least 1 hour for colour development before analysis.

Denitrification for the intact core experiment and the January- February DET gels was determined from the accumulation of ²⁹N₂ and ³⁰N₂ over time. ¹⁵N-N₂ from

the intact core experiments was determined after the introduction of a 4 mL He headspace into the 12.5 mL exetainer. For the gels, a 0.5 mL He headspace was introduced into the 3 mL exetainer and the sample was shaken vigorously before a further 1 mL He headspace was added and the sample shaken. The headspace was added stepwise to release the maximum amount of N₂ into the headspace to ensure the concentration of ¹⁵N-N₂ was detectable. Samples of ¹⁵N-N₂ for the gels were spiked with 50 µL of air to increase the background concentration of ¹⁴N in the sample and then analysed via a gas chromatograph coupled to a mass spectrometer (Sercon GC with He carrier coupled to 20-22 continuous flow IRMS or Shimadzu GCMS-QP5050; Table 3.1).

To account for diffusive loss of N₂ in the gel samples, a set of N₂ calibration standards were prepared. The gels were prepared as described previously, but were then hydrated and stored in ultrapure water. Five nitrite standards were prepared in gas tight glass jars to give final concentrations of ~5, 10, 25, 50 and 100 µmol L⁻¹ ¹⁵N-NO₂⁻. To convert NO₂⁻ to N₂, sulfamic acid prepared in 5 % HCl was added to the standards to a final concentration of 16.5 mmol L⁻¹ and a final pH of 1.5 - 2 (Kessler *et al.*, Under Review). Standards were then sealed and shaken overnight. The pH of the standard was neutralised using 2 mol L⁻¹ NaOH to stop the conversion of NO₂⁻ to N₂ and the gel probe was inserted. The standards were sealed for > 24 hours and a N₂ gas sample was collected and preserved with 100 µL ZnCl₂ (50 % w:v) to determine the initial concentration of ¹⁵N-N₂ (t = 0). The gels were then removed, sliced and analysed as described previously. The process was filmed to calculate the exposure time of the gels to air. To account for the loss of N₂ over time, a multi-variable regression was used to fit the concentration observed in the gels as a function of initial concentration and exposure time. The amount of ¹⁵N-N₂ detected after exposure (*c_t*) was related to the initial concentration of ¹⁵N-N₂ (*c_i*) and the time the gel was exposed to air (*t*) (Eq. 3.1).

$$c_t = (Ac_i + B) \ln(t + 1) + (Cc_i + D) \quad (3.1)$$

The fitted constants A = -0.0713, B = -0.5939, C = 0.5459 and D = 3.247 were used to determine the initial concentration from Equation 3.1. The R² of the calibration was 0.97 and the uncertainty was greatest at high ¹⁵N-N₂ concentrations,

however experimental data was not in this upper range (Fig. 3.6). The correction was applied to the samples to determine actual concentrations in the gel strips.

The $^{15}\text{N-NH}_4^+$ was collected using two different techniques. In November 2009, the ADM was used and $^{15}\text{N-NH}_4^+$ collected in the acid trap was measured via GC-IRMS coupled to an elemental analyser at 1050 °C (Sigman *et al.*, 1997). In 2012 and 2013 $^{15}\text{N-NH}_4^+$ was measured using the hypobromite method (Rysgaard and Risgaard-Petersen, 1997); samples were purged with He to remove background N_2 then 60 μL of 16 mol L^{-1} NaOH was added to the 3 mL exetainer containing the sample, shaken, then 60 μL of hypobromite added. The samples were shaken for 24 hours before analysis to ensure all the NH_4^+ was converted to N_2 then analysed via a gas chromatograph coupled to an isotope ratio mass spectrometer (Sercon GC with a He carrier coupled to a 20 - 22 continuous flow IRMS; Table 3.1). Both the ADM and hypobromite methods achieved $\geq 90\%$ recovery of $^{15}\text{N-NH}_4^+$.

Table 3.1 Outline of methods used in bulk measurements and sediment profiles including sample pre-treatment, standards and analysis techniques.

	Method	Analyte Measured	Calibration Method	Analysis Method	Checks and reference materials
Denitrification/ DNRA	IPT	$^{15}\text{N-N}_2$, $^{15}\text{N-NH}_4^+$ ($\mu\text{mol L}^{-1}$)	<i>Denitrification:</i> Air 20, 50, 100, 200 μL <i>DNRA:</i> see 'DNRA DET gel'	IRMS (ADM)	<u>Gas:</u> Air reference <u>Solid:</u> USGS40, USGS41
Denitrification (September)	Microelectrode	N_2O ($\mu\text{mol L}^{-1}$)	<i>Standards:</i> 10, 50,150 $\mu\text{mol-N}_2\text{O L}^{-1}$ in water site salinity	-	-
Denitrification (Jan-Feb)	DET	$^{15}\text{N-N}_2$ ($\mu\text{mol L}^{-1}$)	<i>Standards:</i> 5, 10, 25, 50 and 100 $\mu\text{mol L}^{-1}$ $^{15}\text{N-NO}_2^-$ acidic standards, neutralised after 24h	IRMS	Air reference, blank
DNRA	DET	$^{15}\text{N-NH}_4^+$ ($\mu\text{mol L}^{-1}$)	1 and 10 $\mu\text{g } ^{15}\text{N-NH}_4^+$ in 100 $\mu\text{g } ^{14}\text{N-NH}_4^+$ 1 and 10 $\mu\text{g } ^{15}\text{N-NO}_3^-$ in 100 $\mu\text{g } ^{14}\text{N-NH}_4^+$	IRMS (hypobromite)	Air reference, blank
$\text{NO}_3^-/\text{NH}_4^+_{\text{tot}}$	DET	NO_3^- or NH_4^+ ($\mu\text{mol L}^{-1}$)	<i>Standards:</i> 0, 0.005, 0.01, 0.02, 0.05, 0.1, 0.2, 0.5, 0.75 and 1 mg-N L^{-1} in ultrapure water	FIA	Standard check, blank, SRM, NO_2^- standard
O_2	Microsensor (Optode)	O_2 (% Saturation)	0 % and 100 % saturated water site salinity	-	-
$\text{S}^{2-}_{\text{tot}}$	Microelectrode	H_2S ($\mu\text{mol L}^{-1}$)	<i>Anoxic standards:</i> standards 10, 50, 150 and 300 $\mu\text{mol-S}^{2-} \text{L}^{-1}$ in pH 4 buffer	-	-
pH	Microelectrode	pH	Standards: pH 4, 7 and 10	-	-
Fe_{total}	DET	Fe_{total} ($\mu\text{mol L}^{-1}$)	<i>Standards:</i> 0, 0.025, 0.01, 0.05, 0.1, 0.25, 0.5, 1 and 2 mg-N L^{-1} in ultrapure water and reagents	UV-Visible Spectrometry	Standard check, blank, SRM

3.3.6 Modelling Fe and S profiles

A reactive transport model was run to simulate the changes to iron and sulfur species profiles under switching oxic-anoxic conditions. The model uses the pH/iron/sulfur formulation (Table 3.2) written in the open-source programming language *R* as previously described in Faber *et al.* (2012), but utilising only the inundated boundary conditions from that study.

Briefly, this model employs the mass balance equations 3.2 and 3.3

$$\text{Solutes: } \varphi \frac{\partial C_i^{PW}}{\partial t} = \frac{\partial}{\partial x} \left[\varphi D_i \frac{\partial C_i^{PW}}{\partial x} \right] + \sum_k v_{i,k} R_k \quad (3.2)$$

$$\text{Solids: } (1 - \varphi) \frac{\partial C_i^S}{\partial t} = \sum_k v_{i,k} R_k \quad (3.3)$$

where C_i^{PW} and C_i^S are solute and solid concentrations. Diffusion coefficients D_i are calculated using the *R* package Tools for Aquatic Sciences (marelac; Soetaert *et al.*, 2010) and corrected for tortuosity (Boudreau, 1996). Porosity φ was set to 0.4 and treated as constant with depth. The term $v_{i,k} R_k$ describes the product of the stoichiometric coefficient and the reaction rate in the reactions modelled, which are listed in Tables 3.2. The kinetic rate expressions for the reactions included in the model are listed in Table 2 of Faber *et al.* (2012). Table 3.3 describes the boundary conditions and parameter values used for this study. Bioturbation was modelled as described by Fossing *et al.* (2004) with a bio-diffusion coefficient of $10 \text{ cm}^2 \text{ y}^{-1}$ at the surface exponentially decreasing to zero at infinite depth. Bioirrigation was not modelled.

The model was first brought to steady state with an oxic water column boundary condition ($\text{O}_2 = 300 \text{ } \mu\text{mol L}^{-1}$), then the water column was made anoxic ($\text{O}_2 = 0 \text{ } \mu\text{mol L}^{-1}$) for 60 days. Profiles of S^{2-} , FeOOH , Fe^{2+} and FeS were extracted from the model before and after the oxic period. The simulation was run twice, with the pH in the overlying water fixed at 7 and 8.5, and no difference between the overall behaviour in the sediment was observed. The pH 8.5 simulation data are shown.

Table 3.2 Kinetic reactions included in the model from Faber *et al.* (2012).

R1	$\{\text{CH}_2^{\text{O}}\}_{\text{f}} + \text{O}_2 \rightarrow \text{CO}_2 + \text{H}_2\text{O}$
R2	$\{\text{CH}_2^{\text{O}}\}_{\text{f}} + 4\text{FeOOH} + 8\text{H}^+ \rightarrow 4\text{Fe}^{2+} + \text{CO}_2 + 7\text{H}_2\text{O}$
R3	$\{\text{CH}_2^{\text{O}}\}_{\text{f}} + \frac{1}{2}\text{SO}_4^{2-} + \frac{1}{2}\text{H}^+ \rightarrow \text{CO}_2 + \frac{1}{2}\text{HS}^- + \text{H}_2\text{O}$
R4	$\{\text{CH}_2^{\text{O}}\}_{\text{s}} + \text{O}_2 \rightarrow \text{CO}_2 + \text{H}_2\text{O}$
R5	$\{\text{CH}_2^{\text{O}}\}_{\text{s}} + 4\text{FeOOH} + 8\text{H}^+ \rightarrow 4\text{Fe}^{2+} + \text{CO}_2 + 7\text{H}_2\text{O}$
R6	$\{\text{CH}_2^{\text{O}}\}_{\text{s}} + \frac{1}{2}\text{SO}_4^{2-} + \frac{1}{2}\text{H}^+ \rightarrow \text{CO}_2 + \frac{1}{2}\text{HS}^- + \text{H}_2\text{O}$
R7	$\text{HS}^- + 2\text{O}_2 \rightarrow \text{SO}_4^{2-} + \text{H}^+$
R8	$\text{Fe}^{2+} + \frac{1}{4}\text{O}_2 + \frac{3}{2}\text{H}_2\text{O} \rightarrow \text{FeOOH} + 2\text{H}^+$
R9	$8\text{FeOOH} + \text{HS}^- + 15\text{H}^+ \rightarrow 8\text{Fe}^{2+} + \text{SO}_4^{2-} + 12\text{H}_2\text{O}$
R10	$\text{Fe}^{2+} + \text{HS}^- \rightarrow \text{FeS} + \text{H}^+$
R11	$\text{FeS} + \frac{9}{4}\text{O}_2 + \frac{3}{2}\text{H}_2\text{O} \rightarrow \text{FeOOH} + \text{SO}_4^{2-} + 2\text{H}^+$
R12	$\text{FeS} + \frac{1}{4}\text{SO}_4^{2-} + \frac{3}{4}\text{HS}^- + \frac{5}{4}\text{H}^+ \rightarrow \text{FeS}_2 + \text{H}_2\text{O}$
R13	$\text{FeS}_2 + \frac{15}{4}\text{O}_2 + \frac{5}{2}\text{H}_2\text{O} \rightarrow \text{FeOOH} + 2\text{SO}_4^{2-} + 4\text{H}^+$

Table 3.3 Parameters used to model Fe and S under varying oxygen conditions.

Parameter	Value	Units
K.fast (highly labile organic matter)	10	y ⁻¹
K.slow (less labile organic matter)	0.1	y ⁻¹
K_O ₂ (Monod constant for O ₂ consumption)	0.005	mmol cm ⁻³
K_FeOOH (Monod constant for FeOOH reduction)	200*ρ _{sed}	mmol cm ⁻³
K_SO ₄ ²⁻ (Monod constant for SO ₄ ²⁻ reduction)	1.6	mmol cm ⁻³
k_H ₂ S.Ox (Rate constant for H ₂ S oxidation)	160	mmol ⁻¹ cm ³ y ⁻¹
k_Fe.Ox (Rate constant for Fe oxidation)	20 000	mmol ⁻¹ cm ³ y ⁻¹
k_FeS.Ox (Rate constant for FeS oxidation)	160	mmol ⁻¹ cm ³ y ⁻¹
k_FeS ₂ .Ox (Rate constant for FeS ₂ oxidation)	160	mmol ⁻¹ cm ³ y ⁻¹
k_Fe.H ₂ S (Rate constant FeOOH/H ₂ S redox reaction)	26	mmol ⁻¹ cm ³ y ⁻¹
k_FeS.form (Rate constant for FeS formation)	1 000 000	mmol ⁻¹ cm ³ y ⁻¹
k_FeS ₂ .form (Rate constant for FeS ₂ formation)	1	mmol ⁻¹ cm ³ y ⁻¹
ρ _{sed} (density of solid sediment)	2.6	g cm ⁻³
SedFlux (sedimentation flux)	2	g cm ⁻² y ⁻¹
F.CH ₂ O (depositional flux of organic C)	48	mmol m ⁻² d ⁻¹
F.FeOOH (sedimentation flux of FeOOH)	0.01*SedFlux	g cm ⁻² y ⁻¹

3.4 Results

3.4.1 Intact core experiments

During the control oxic treatment, mean DNRA was $28 \pm 2 \mu\text{mol m}^{-2} \text{h}^{-1}$ and denitrification initially $210 \pm 60 \mu\text{mol m}^{-2} \text{h}^{-1}$, decreasing to a mean of $83 \pm 17 \mu\text{mol m}^{-2} \text{h}^{-1}$ after day 11 with a mean denitrification : DNRA ratio of 3.4 ± 0.7 after day 11 (Fig. 3.2). During the anoxic treatment, however, the mean denitrification : DNRA ratio was 126 ± 17 , which dropped significantly upon re-aeration to 5.3 ± 0.5 . The ratio increased significantly throughout the anoxic incubation (Denitrification : DNRA = $8.3(\text{day}) + 73.1$, $R^2 = 0.999$, $n = 3$, $p < 0.01$) owing to a decrease in DNRA activity and subsequent increase in denitrification in comparison to the control treatment (Fig. 3.2C). Mean denitrification under anoxic conditions ($740 \pm 40 \mu\text{mol m}^{-2} \text{h}^{-1}$) decreased significantly when conditions were made oxic ($155 \pm 12 \mu\text{mol m}^{-2} \text{h}^{-1}$, $df = 3$, $p < 0.05$; Fig. 3.2A). Mean DNRA under anoxic conditions ($6.7 \pm 1.0 \mu\text{mol m}^{-2} \text{h}^{-1}$) increased significantly (~5 fold), when the water column was oxygenated ($33.1 \pm 1.2 \mu\text{mol m}^{-2} \text{h}^{-1}$, $df = 3$, $p < 0.05$; Fig. 3.2C).

3.4.2 Micro-profiles in intact cores - September 2012

Oxygen concentration decreased with sediment depth, penetrating ~0.5 cm into the sediment in the oxic treatment (Fig. 3.3I). This behaviour is observed to a lesser extent in the sub-oxic core where oxygen penetrated ~0.2 cm into the sediment (Fig. 3.3F). There was no oxygen penetration in the anoxic treatment (Fig. 3.3C). The profile of NO_3^- in all treatments (anoxic, sub-oxic and oxic) from September 2012 decreased from the sediment surface (Fig. 3.3B, E, H). Small peaks were observed between 1.5 - 2.0 cm depth for the sub-oxic and anoxic treatments (Fig. 3.3E, H). NH_4^+ ($\mu\text{mol L}^{-1}$) increased moving from depth toward the sediment surface for the anoxic treatment (Fig 3.3B). In contrast, under sub-oxic and oxic conditions, the NH_4^+ profile remained unchanged with depth (Fig. 3.3E, H). Total sulfide was observed at high concentrations in both the anoxic and sub-oxic cores. A large peak was observed at 1.5 cm in the anoxic treatment and a much broader peak observed in the sub-oxic treatment (Fig. 3.3C, F respectively). In contrast, there was $< 100 \mu\text{mol L}^{-1}$ total S^{2-} in the oxic core (Fig. 3.3I).

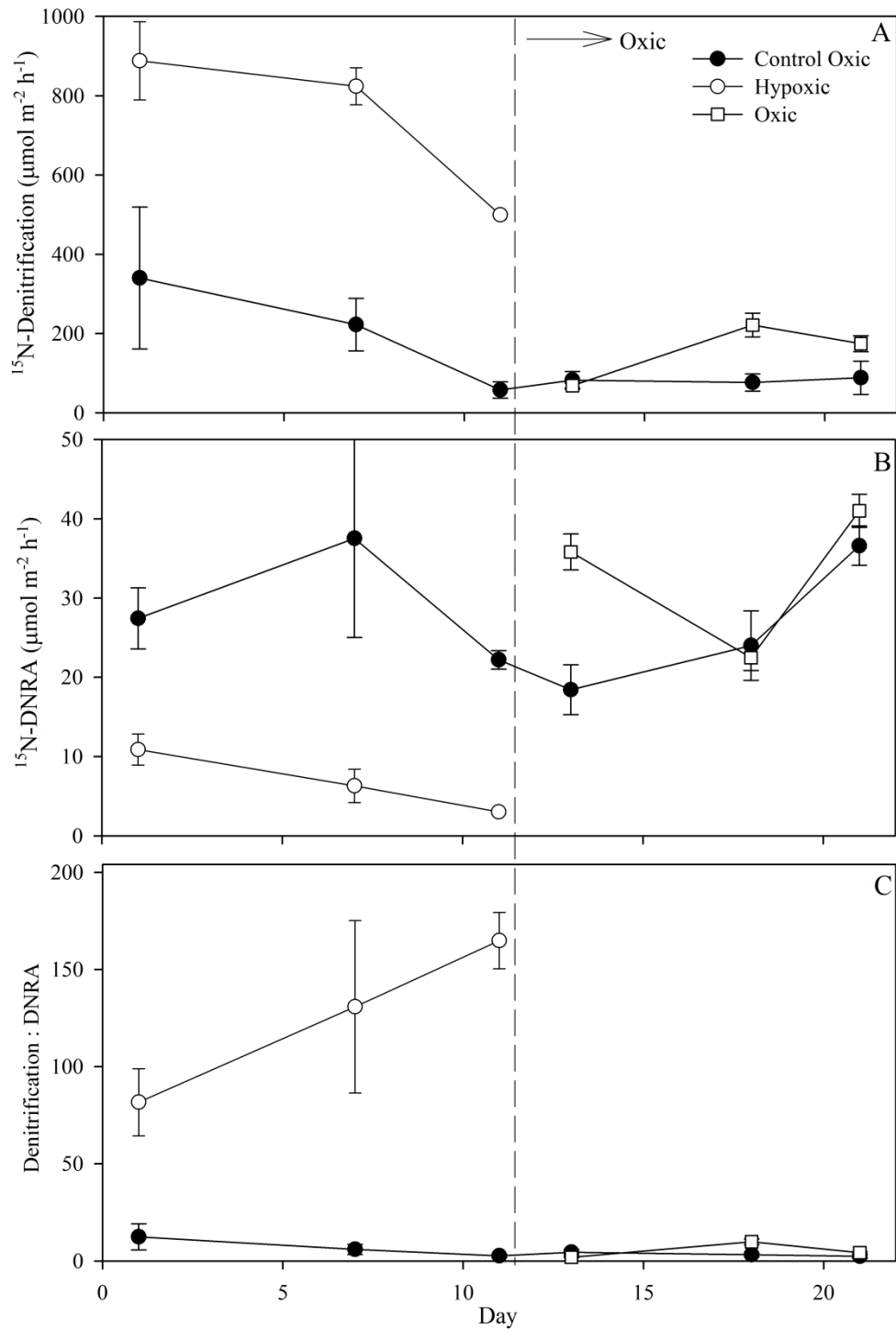


Figure 3.2 The control treatment (●) was oxic for the 21 day period. The treated cores are represented by open shapes for the first 11 days hypoxic (○) and subsequent oxic duration (□). (A) Denitrification ($\mu\text{mol m}^{-2} \text{h}^{-1}$), (B) DNRA ($\mu\text{mol m}^{-2} \text{h}^{-1}$) and (C) Denitrification: DNRA ratio over the incubation period, 21 days.

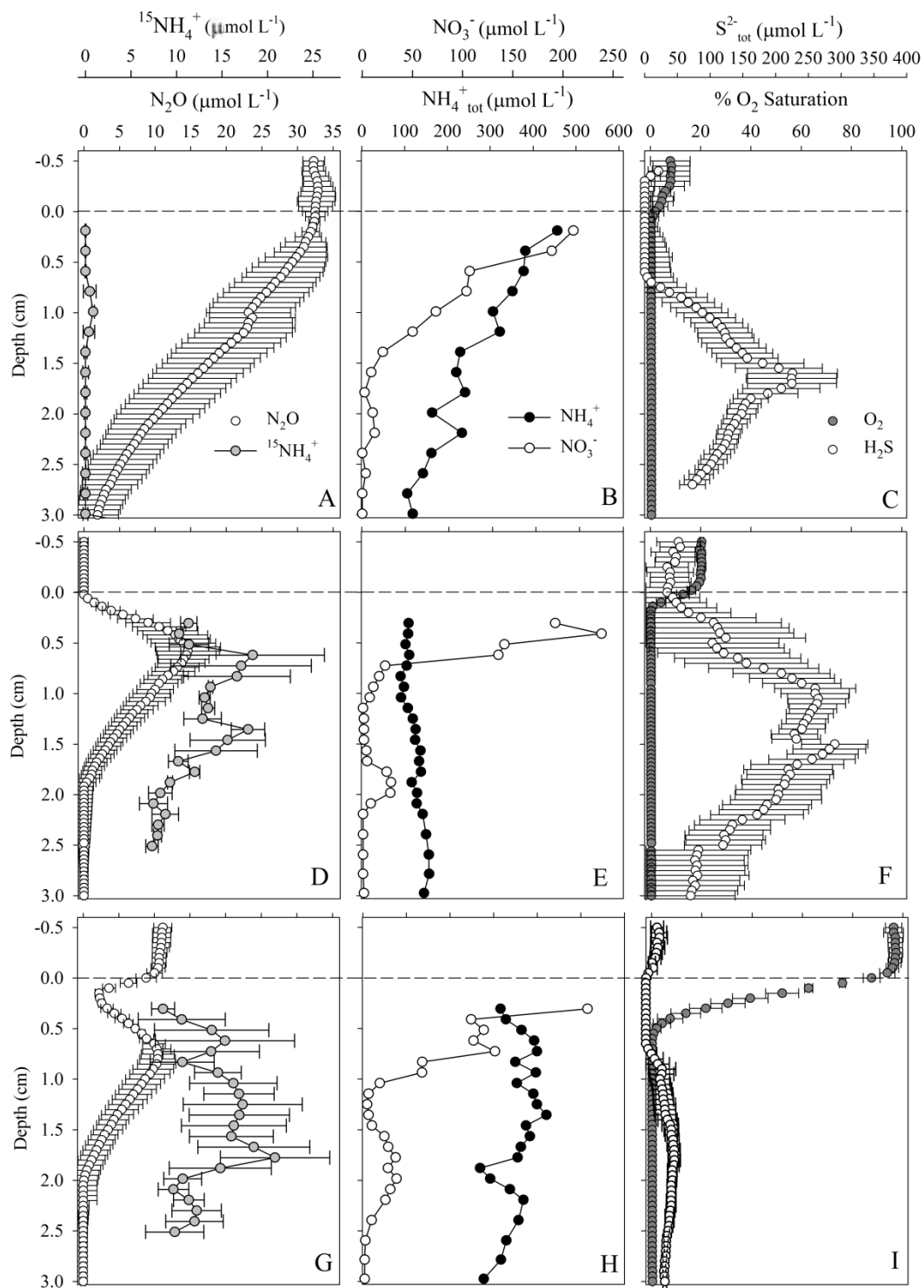


Figure 3.3 September 2012 micro-profiles denitrification (N_2O , $\mu\text{mol L}^{-1}$), DNRA ($^{15}\text{N-NH}_4^+$; $\mu\text{mol L}^{-1}$), NO_3^- ($\mu\text{mol L}^{-1}$), $\text{NH}_4^+_{\text{tot}}$ ($\mu\text{mol L}^{-1}$), total S^{2-} ($\mu\text{mol L}^{-1}$) and O_2 (% saturation) with respect to depth (cm) for anoxic (A-C), sub-oxic (D-F) and oxic (G-I) conditions. All plots show error bars \pm SE.

N_2O concentration, indicative of denitrification, was highest in the anoxic treatment increasing steadily toward the sediment surface to a maximum of $\sim 33 \mu\text{mol L}^{-1}$ (Fig. 3.3A). In the sub-oxic and oxic treatments denitrification peaked below the oxic surface layer of the sediment with the peak observed at 0.75 cm and 0.5 cm for the oxic and sub-oxic treatments respectively (Fig. 3.3D, G). DNRA, inferred from the $^{15}\text{N-NH}_4^+$ concentration, was negligible under anoxic conditions, producing $< 1 \mu\text{mol L}^{-1} \text{ }^{15}\text{N-NH}_4^+$ (Fig. 3.3A). The sub-oxic and oxic treatments however observed peaks in DNRA below the denitrification zone at ~ 1.5 cm in both treatments (Fig. 3.3D, G).

3.4.3 Micro-profiles in intact cores – January-February 2013

For the anoxic treatment, the $^{15}\text{N-N}_2$ concentration profile, indicative of denitrification, displayed a maximum concentration ($190 \pm 20 \mu\text{mol L}^{-1}$) at the sediment-water interface and decreased with sediment depth (Fig. 3.4A). Denitrification in the short-term and long-term oxic treatments, however, increased with depth, reaching a peak (highest $^{15}\text{N-N}_2$) at ~ 1.0 cm depth below the oxic surface layer of the sediment (Fig. 3.4E, I). For the anoxic treatment, DNRA, inferred from the $^{15}\text{N-NH}_4^+$ profile, was uniform with sediment depth, with $^{15}\text{N-NH}_4^+$ averaging $3.4 \pm 0.1 \mu\text{mol L}^{-1}$ (Fig. 3.4A). In contrast, under short-term oxic conditions, DNRA reached a maximum at 1.0 cm depth with $^{15}\text{N-NH}_4^+$ of $14.8 \pm 1.9 \mu\text{mol L}^{-1}$ (Fig. 3.4E). The short-term oxic profile was mirrored in the long-term oxic treatment with DNRA reaching a maximum at 1.2 cm depth, with $^{15}\text{N-NH}_4^+$ of $7.0 \pm 2.0 \mu\text{mol L}^{-1}$ (Fig. 3.4I). The DNRA profile for both the short and long-term oxic treatments followed a similar trend to the denitrification profile, however it was an order of magnitude lower (Fig 3.4). The denitrification : DNRA ratio was much higher in the anoxic treatment corresponding to high denitrification and low DNRA; the maximum denitrification : DNRA was observed at the sediment surface (53 ± 7 , Fig. 3.4B). The denitrification : DNRA ratio in the short-term oxic treatment was independent of sediment depth, averaging 5.0 ± 0.2 , which was significantly different from the mean under anoxic conditions (33 ± 2 , $p < 0.001$; Fig. 3.4F). Similarly, the denitrification : DNRA ratio for the long-term oxic treatment averaged 14.4 ± 0.6 in the sediment (Fig. 3.4J) and was also significantly different from the mean under anoxic conditions (33 ± 2 , $p < 0.001$).

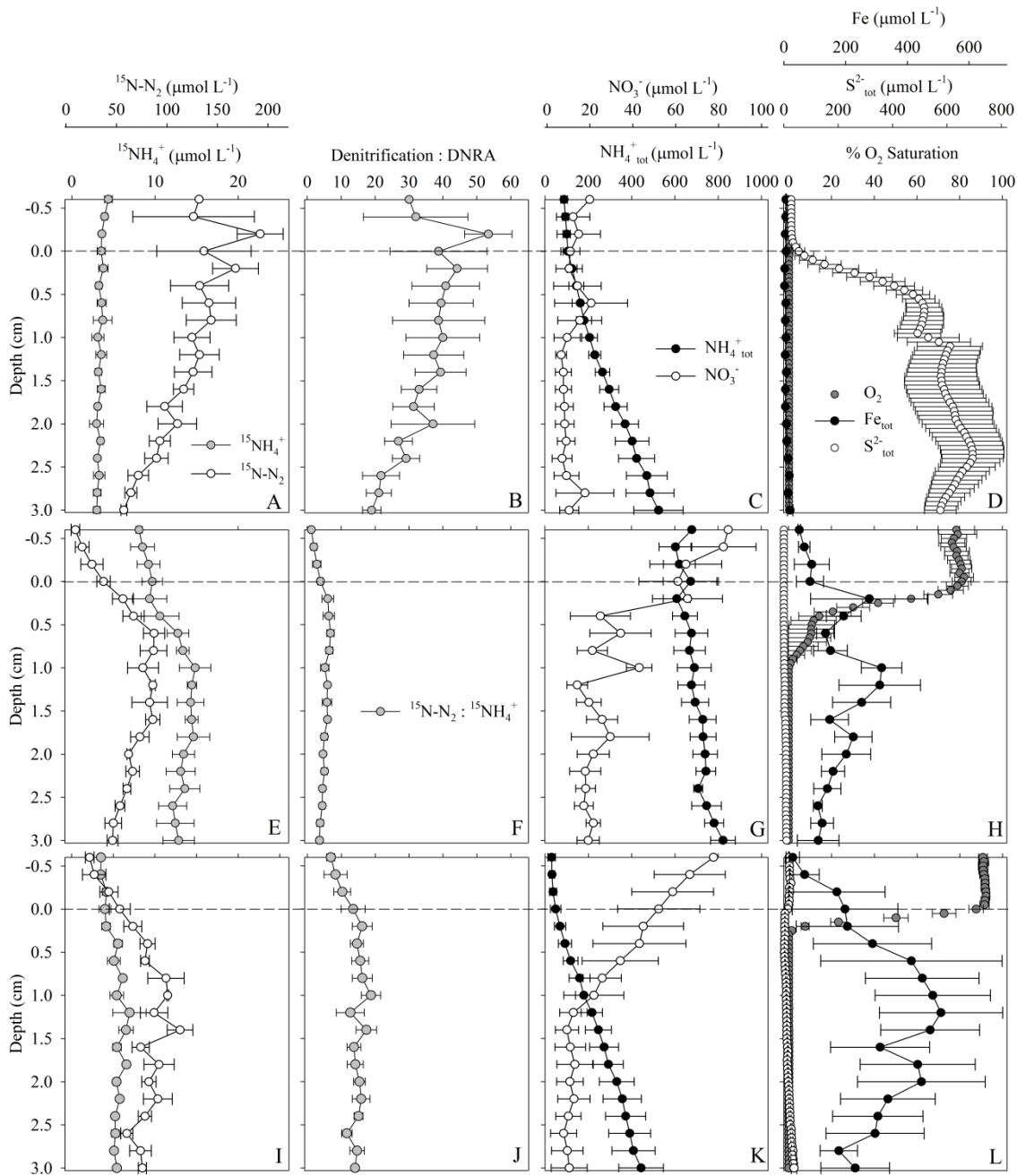


Figure 3.4 January-February 2013 micro-profiles of $^{15}\text{N-NH}_4^+$ ($\mu\text{mol L}^{-1}$; indicating DNRA); $^{15}\text{N-N}_2$ ($\mu\text{mol L}^{-1}$, indicating denitrification); $^{15}\text{N-N}_2 : ^{15}\text{N-NH}_4^+$ (indicating denitrification : DNRA ratio), NO_3^- ($\mu\text{mol L}^{-1}$), $\text{NH}_4^+_{\text{tot}}$ ($\mu\text{mol L}^{-1}$), Fe_{tot} ($\mu\text{mol L}^{-1}$), $\text{S}^{2-}_{\text{tot}}$ ($\mu\text{mol L}^{-1}$) and oxygen (% O_2 saturation). All plots show error bars \pm SE with $n = 3$. (A-D) represents long-term anoxic conditions, (E-H) short-term oxic conditions and (I-L) oxic conditions.

NO_3^- concentration decreased with sediment depth in both oxic treatments, however it was completely depleted at the surface in the anoxic treatment. NH_4^+ increased with sediment depth in all treatments reaching a maximum of $\sim 820 \mu\text{mol L}^{-1}$ at 3.0 cm depth under short-term oxic conditions (Fig. 3.4G). Free S^{2-} was observed under anoxic conditions and increased with depth reaching a maximum of $\sim 695 \mu\text{mol L}^{-1}$ at ~ 2.5 cm; S^{2-} was not observed at high concentrations in the water column (Fig. 3.4D). In both the short-term and long-term oxic treatments, total S^{2-} was $< 40 \mu\text{mol L}^{-1}$ (Fig. 3.4H, L). Total Fe averaged $8.2 \pm 0.9 \mu\text{mol L}^{-1}$ in the anoxic treatment (Fig. 3.4D). In contrast, the total Fe concentration in the short and long-term oxic treatments reached maxima of $320 \pm 70 \mu\text{mol L}^{-1}$ at 1.0 cm and $500 \pm 200 \mu\text{mol L}^{-1}$ at 1.2 cm, respectively (Fig. 3.4H, L).

The oxygen concentration was < 1 % saturation in the anoxic treatment in both the water column and the sediment (Fig. 3.4D). The concentration of oxygen in the water column of the short-term oxic treatment was 87 % saturation, and oxygen penetrated ~ 0.5 cm into the sediment before conditions become anoxic (Fig. 3.4H). The oxygen in the long-term oxic treatment reached 92 % saturation in the water column and penetrated ~ 0.3 cm into the sediment (Fig. 3.4L).

The $^{15}\text{N-N}_2$ ($\mu\text{mol L}^{-1}$) standards decreased exponentially with respect to the exposure time of the gel to air (Fig. 3.5A). The concentration of $^{15}\text{N-N}_2$ decreased rapidly in the first 30 seconds and was 14.0 ± 0.5 % of the initial $^{15}\text{N-N}_2$ concentration after 5 minutes of air exposure. The calculated concentration of $^{15}\text{N-N}_2$ was representative of the actual $^{15}\text{N-N}_2$ concentration as shown by a positive linear relationship (Calculated $^{15}\text{N-N}_2 = 1.0 (\text{Actual } ^{15}\text{N-N}_2) + 0.002$, $R^2 = 0.97$, $p < 0.001$). The most uncertainty was observed in the $55 \mu\text{mol-}^{15}\text{N-N}_2 \text{ L}^{-1}$ standard. In all of the profiles, the initial $^{15}\text{N-N}_2$ gel concentration did not exceed $50 \mu\text{mol } ^{15}\text{N-N}_2 \text{ L}^{-1}$, in addition, 94 % of all gel slices were $< 30 \mu\text{mol } ^{15}\text{N-N}_2 \text{ L}^{-1}$.

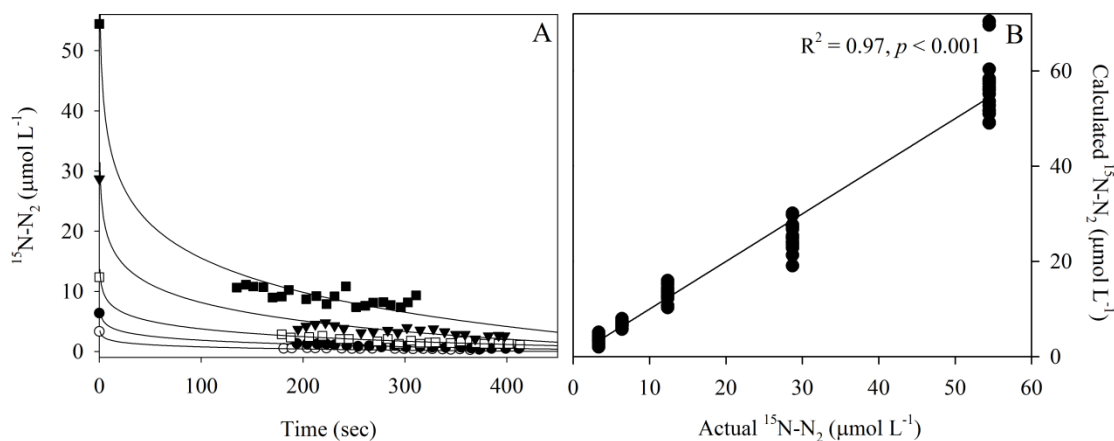


Figure 3.5 Calibration of $^{15}\text{N-N}_2$ in DET gels after exposure to air, (A) calibration standards of starting $^{15}\text{N-N}_2$ concentration 3.3 (\circ), 6.4 (\bullet), 12.3 (\square), 28.7 (\blacktriangledown) and 54.5 (\blacksquare) $\mu\text{mol L}^{-1}$ and the decrease in $^{15}\text{N-N}_2$ with exposure to air over ~ 420 seconds. (B) Actual $^{15}\text{N-N}_2$ ($t = 0$) and calculated $^{15}\text{N-N}_2$ from the regression equation. The line represents the relationship between the actual and calculated concentrations of $^{15}\text{N-N}_2$.

3.4.4 Comparison of N_2O and $^{15}\text{N-N}_2$ method

Both $^{15}\text{N-N}_2$ ($\mu\text{mol L}^{-1}$) and N_2O ($\mu\text{mol L}^{-1}$) in the short term oxic treatment peaked below the oxic surface layer (Fig. 3.6A, B). The presence of $^{15}\text{N-N}_2$ is observed down to 3 cm and a broad denitrification band was observed (Fig. 3.6A). The N_2O method, however, indicated the denitrification zone was narrow and denitrification (N_2O) ceased below 2.0 cm (Fig. 3.6B). A peak in N_2O was also observed in the water column reaching concentrations higher than that observed in the sediment (Fig. 3.6B). A similar trend was observed in the long-term oxic treatment with a broad peak for $^{15}\text{N-N}_2$ and a sharp peak for N_2O at ~ 0.75 cm (Fig. 3.6C, D). When conditions were anoxic, the profile of $^{15}\text{N-N}_2$ and N_2O were similar with depth peaking at the sediment surface and decreasing with depth (Fig. 3.6E, F). Under anoxic conditions the $^{15}\text{N-N}_2$ concentration was an order of magnitude higher than N_2O produced under anoxic conditions (Fig. 3.6E, F).

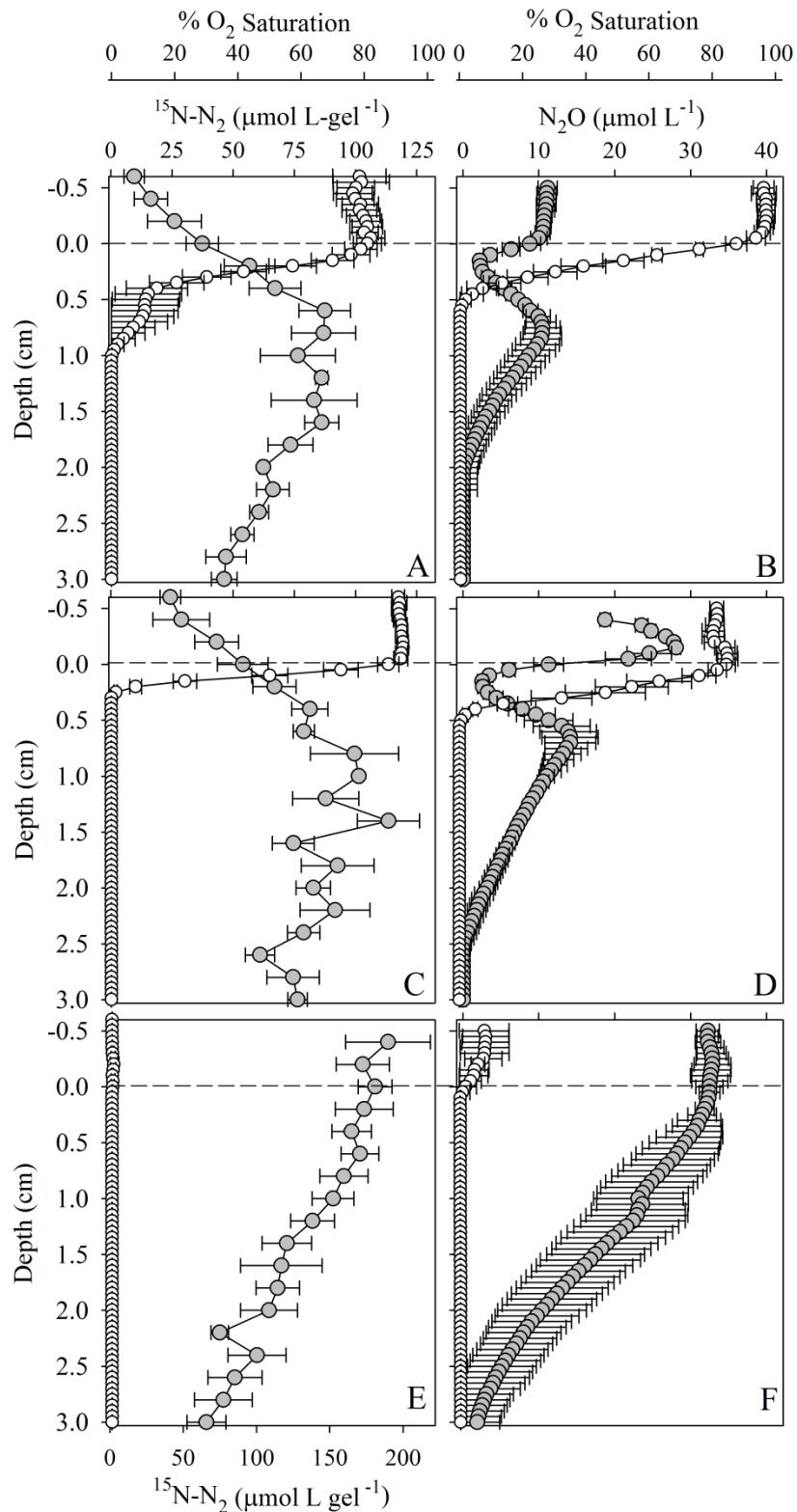


Figure 3.6 Comparison of the $^{15}\text{N-N}_2$ ($\mu\text{mol L}^{-1}$) and N_2O ($\mu\text{mol L}^{-1}$) method under short term oxic (A, B), long-term oxic (C,D) and anoxic (E,F) conditions. (A, C, E) $^{15}\text{N-N}_2$ (grey dots), (B, D, F) N_2O (grey dots) and (A-F) O_2 (% saturation) (\circ) with respect to depth (cm). '0.0 cm' and the dashed line represent the sediment surface and '-0.5 cm' the water column.

3.4.5 Modelling Fe and S

The modelled concentrations of Fe and S were similar to the measured profiles. When conditions were oxic in the water column, the modelled S^{2-} concentration was $< 2 \mu\text{mol L}^{-1}$ down to 2.0 cm depth reaching a maximum of $45 \mu\text{mol L}^{-1}$ at 3.0 cm. Modelled Fe^{2+} reached a maximum of $\sim 570 \mu\text{mol L}^{-1}$ at 1.0 cm depth and FeOOH formation was highest at the sediment surface (Fig. 3.7). After 60 days of anoxia, the modelled S^{2-} concentration increased to a maximum of $\sim 550 \mu\text{mol L}^{-1}$; under these conditions Fe^{2+} was removed from the sediment corresponding to an increase in FeS formation ($\sim 1.6 \text{ mol L}^{-1}$; Fig. 3.7).

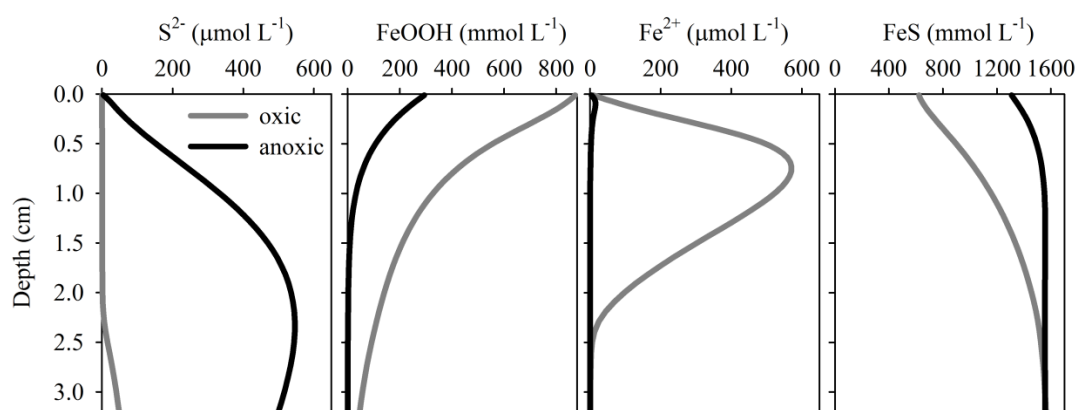


Figure 3.7 Modelled profiles of S^{2-} ($\mu\text{mol L}^{-1}$), FeOOH (mmol L^{-1}), Fe^{2+} ($\mu\text{mol L}^{-1}$) and FeS (mmol L^{-1}) with respect to depth. The grey line represents steady state oxic water column conditions and the black steady state anoxic conditions.

3.5 Discussion

3.5.1 Long-term oxygen treatment in intact cores

The results presented here support field observations in the Yarra River estuary which showed that denitrification was the main NO_3^- reduction pathway under hypoxic conditions (Fig. 2.10 and 3.2). In the observational study of the Yarra River estuary, DNRA became more prevalent, increasing from $< 1\%$ of total NO_3^- reduction under anaerobic conditions to $\sim 50\%$ under aerobic conditions, despite denitrification rates also increasing in the presence of oxygen (Fig. 2.10). Long-term core experiments in the present study show the same behaviour under extended aerobic conditions (Fig. 3.2). Under prolonged hypoxic conditions the denitrification : DNRA ratio increased, driven by high denitrification rates combined with low DNRA rates resulting in DNRA comprising $< 1\%$ of total NO_3^- reduction. Re-oxygenation decreased the denitrification : DNRA ratio and DNRA represented $\sim 18\%$ of total NO_3^- reduction. High rates of DNRA after re-oxygenation of the water column contradict the current paradigm; previously the highest rates of DNRA have been observed in environments with low NO_3^- concentrations, where conditions are strongly reducing driven by either carbon decomposition or sulfate reduction (An and Gardner, 2002; Childs *et al.*, 2002; Christensen *et al.*, 2000).

3.5.2 Sediment profiles of denitrification and DNRA

Intact sediment profiles of denitrification and DNRA further support the field observations in the Yarra River estuary (Fig 2.10) and the long-term oxygen experiments in this study (Fig 3.2). DNRA was only observed under oxic and sub-oxic conditions; in the absence of oxygen, DNRA ceased (Fig 3.3, 3.4).

Several hypotheses explain the partitioning between denitrification and DNRA on the basis of direct competition for NO_3^- , however, an alternate hypothesis is that the processes are spatially separated within the sediment. In Eckenförde Bay, Germany, a peak in DNRA activity was observed at ~ 2 cm depth below denitrification activity at the surface of the sediment (Preisler *et al.*, 2007). This separation was explained by the presence of motile sulfur oxidising bacteria (*Beggiatoa* sp.) capable of moving NO_3^- into the S^{2-} zone to carry out DNRA.

Moreover, the separation of denitrification and DNRA activity has been observed in freshwater river sediments in the Weser River near Bremen, Germany, where DNRA occurred deeper in the sediment, explained by the low ratio of electron acceptor to donor in the DNRA layer (Stief *et al.*, 2010). In the present study, the DNRA activity in the September profiles, appeared to occur deeper in the sediment than denitrification, using the same method as Stief *et al.* (2010), however no separation of denitrification and DNRA activity was observed in January-February (Fig 3.3., 3.4). Stief *et al.* (2010) noted the use of the acetylene inhibition method should only be used with sediments overlain with NO_3^- rich water, due to the inhibition of nitrification-denitrification. It is unlikely that the coexistence of denitrification and DNRA in the Yarra River estuary is the result of spatial separation of these processes within the sediment, because in January-February, total denitrification was measured using the $^{15}\text{N-N}_2$ gel method and both denitrification and DNRA activity overlapped in the sediment (Fig. 3.4). A small amount of spatial separation was observed in September, however this was more likely due to a systematic error in the measurement, because denitrification is underestimated by the acetylene inhibition technique (*see* section 3.5.4).

Under anoxic conditions, denitrification in the September and January-February profiles were comparable, and denitrification was the dominant process driven by water column NO_3^- (Fig. 3.3, 3.4). In the presence of oxygen, denitrification was observed below the oxic surface layer of the sediment in September and January-February, however, in January-February a broader denitrification peak was observed deeper in the sediment (*see* discussion on peak flattening in section 3.5.3 and N_2O method limitations in section 3.5.4). Several studies have observed inhibition of both nitrification and denitrification by S^{2-} (Joye and Hollibaugh, 1995; Sorensen *et al.*, 1980), however, in the Yarra River estuary, nitrogen loss via denitrification was not influenced by the presence or absence of S^{2-} . Similar observations were made by Stief *et al.* (2010) and Behrendt *et al.* (2013).

For the purpose of this discussion I have assumed Fe^{2+} was the major component of total iron in the gels, owing to the $0.2\ \mu\text{m}$ membrane covering the gel surface excluding insoluble Fe^{3+} (Davison *et al.*, 1994). In both the September and January-February profiles, DNRA was only observed in the presence of oxygen (Fig 3.3, 3.4). In January-February the mean denitrification : DNRA ratios were 5.0 ± 0.2

and 14.4 ± 0.6 under short- and long-term oxic conditions, respectively, and both aerobic treatments were significantly lower than the mean denitrification : DNRA ratio under anoxic conditions (33.1 ± 2.1). The decrease in the denitrification : DNRA ratio under aerobic conditions arose as a consequence of an increase in DNRA (Fig. 3.4). These sediment profiles show DNRA coincides with the presence of high concentrations of Fe^{2+} in the sediment (Fig. 3.4). Hou *et al.* (2012) reported similar findings in Copano Bay, Texas, where iron oxide concentrations were significantly correlated with NH_4^+ production. Under long-term anoxic conditions, the formation of free sulfides increased to $\sim 695 \mu\text{mol L}^{-1}$ and Fe^{2+} decreased to $< 20 \mu\text{mol L}^{-1}$ (Fig. 3.4). High S^{2-} concentrations were characteristic of anoxic conditions and although several studies have identified the role of S^{2-} in determining DNRA rates, in this study high DNRA rates were not correlated with the presence of S^{2-} (Figs. 3.3 and 3.4; An and Gardner, 2002; Brunet and Garcia-Gil, 1996).

Total S^{2-} was modelled under two pH conditions, 7 and 8.5, to investigate the sensitivity of FeS formation to pH, given the uncertainty in the applicability of the pH profiles measured in September 2012 to subsequent experiments in January-February 2013. The modelled behaviour of total S^{2-} under oxic and anoxic conditions did not change significantly from pH 7.0 to 8.5; as a result, only pH 8.5 profiles are presented (Fig. 3.7). The modelled total S^{2-} profiles are comparable with the measured profiles in the Yarra River estuary (Fig. 3.3, 3.4) under both oxic and anoxic conditions (Fig. 3.3, 3.4, 3.7). In addition to total S^{2-} , the behaviour of iron was modelled and matched the observations made in the January-February profiles; this showed a decrease in S^{2-} and an increase in Fe^{2+} under oxic conditions. The modelled behaviour of sulfur and iron under changing oxygen conditions provides a plausible explanation for the absence of DNRA under anoxic conditions, which is attributed to the formation of FeS precipitates under anoxic conditions and removal of available Fe^{2+} from the sediment (Fig. 3.8). A conceptual model presented in Figure 3.8 depicts the behaviour of S^{2-} and Fe^{2+} under oxic and anoxic conditions and the possible link between DNRA and Fe^{2+} availability in the sediment.

Enzymatic NO_3^- -dependent Fe^{2+} oxidation is well documented, with the main product being N_2 gas, produced via denitrification (Benz *et al.*, 1998; Nealson and Saffarini, 1994; Straub *et al.*, 1996) or the more recently described process anammox (Oshiki *et al.*, 2013). Several studies have linked abiotic NO_3^- -dependent Fe^{2+}

oxidation to the production of NH_4^+ (Hansen *et al.*, 2001; Hansen *et al.*, 1996). However, to my knowledge, Weber *et al.* (2006) was the first study to link enzymatic NO_3^- -dependent Fe^{2+} oxidation to the formation of NH_4^+ in a bacterial study. The importance of Fe^{2+} availability in determining DNRA rates in the Yarra River estuary requires further investigation and will be addressed in Chapter Four.

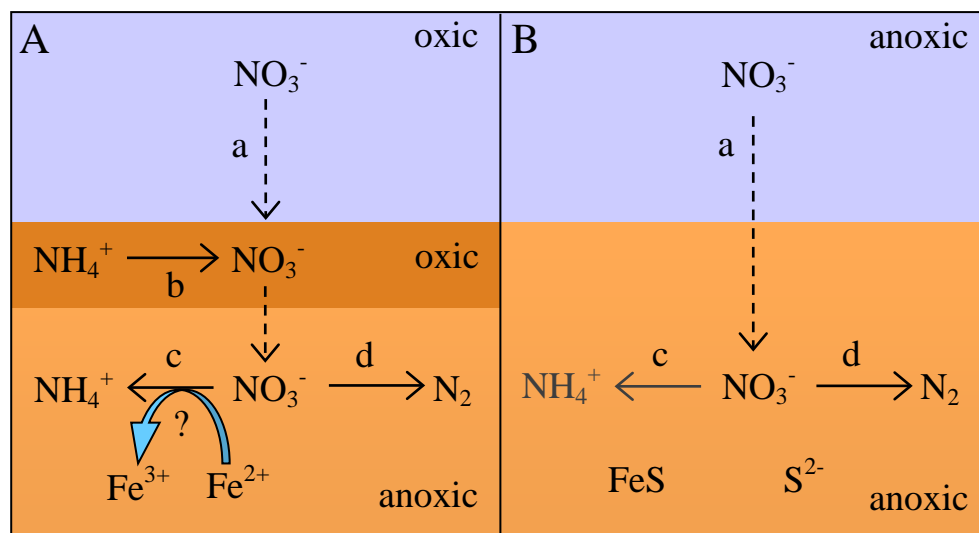


Figure 3.8 Conceptual model of denitrification and DNRA in the Yarra River estuary under (A) oxic and (B) anoxic conditions. a) diffusion, b) nitrification, c) DNRA, d) denitrification.

3.5.3 Comments on the combined $^{15}\text{N-N}_2$ and $^{15}\text{N-NH}_4^+$ DET gels

Stief *et al.* (2010) compared zones of denitrification and DNRA activity, using the coupled N_2O microelectrode-acetylene inhibition technique for denitrification and the ^{15}N isotope pairing technique in DET gels for DNRA, measured in separate cores. The uncertainty associated with the use of different measurement techniques is avoided using the $^{15}\text{N-N}_2$ (Kessler *et al.*, Under Review) and $^{15}\text{N-NH}_4^+$ (Stief *et al.*, 2010) combined DET gel method, which allows for direct comparison of nutrients within a single gel and core. Diffusion coefficients for a number of nutrients usually differ by $< 15\%$ ($D_{\text{mol}} = 1.72, 1.77$ and $1.96 \times 10^{-9} \text{ m}^2 \text{ s}^{-1}$ for NO_3^- , NH_4^+ and N_2 respectively at 20°C (Boudreau, 1996) and this uncertainty in D_{mol} would be small compared to the heterogeneity of nutrient concentrations in between replicate cores. Hence, the direct comparison of $^{15}\text{N-N}_2$ and $^{15}\text{N-NH}_4^+$ measured in a DET gel, although associated with a small margin of error, is a more

appropriate method than the comparison of denitrification and DNRA activity using different techniques as discussed further in 3.5.4.

The combined ^{15}N isotope pairing technique in DET gels relies on diffusion of the ^{15}N product ($^{15}\text{N}\text{-N}_2$ or $^{15}\text{N}\text{-NH}_4^+$) from the pore water into the gel. A peak in the concentration profile will only be observed if there is a constant pore water source of the ^{15}N product during the gel deployment. During deployment, ‘flattening’ in the concentration peak will be observed due to the high porosity of the gel compared to the sediment leading to faster lateral diffusion within the gel (Fig. 3.9A).

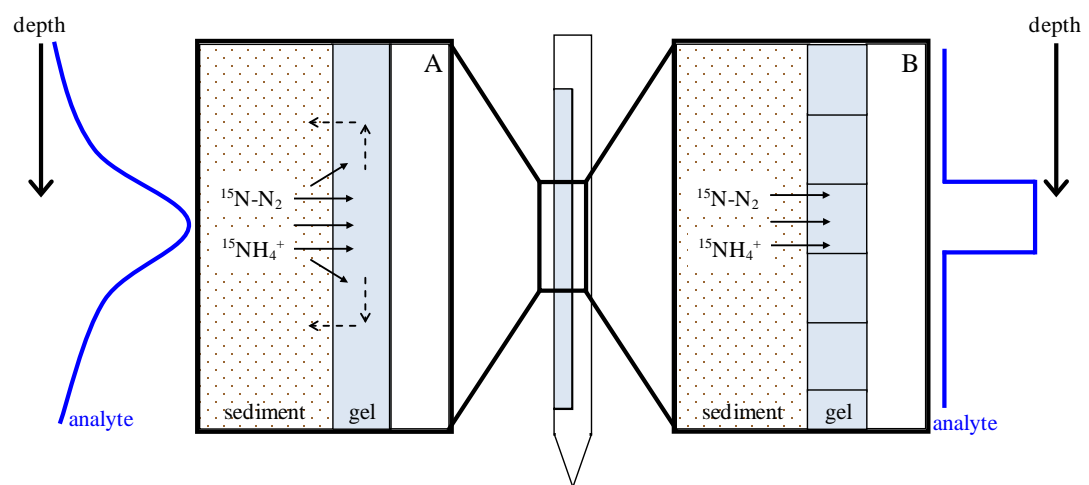


Figure 3.9 Lateral diffusion of an analyte into a gel from the sediment. The blue line represents predicted peak in the analyte concentration within the gel (adapted from Harper *et al.* (1997)) (A) Lateral diffusion in a single gel sheet and (B) lateral diffusion into a gel separated into discrete slices before deployment.

The flattening of the analyte peak over time, predicted from a computational model presented in Harper *et al.* (1997) is shown in Figure 3.10. The figure depicts the modelled concentration of an analyte in a DET gel reliant on diffusion of the analyte into the gel from the pore water (Fig. 3.10). In that study increasing the length of deployment increased the flattening of the observed peak. However, the simulations suggested that if the pore water profile is steady, then the observed peak will be aligned at the same depth (in phase) as the actual peak (Fig. 3.10). In the simulation, the concentration of the analyte in the gel reached a maximum of < 50 % of the pore water concentration after 20 minutes and reduced to ~20 % after 6 hours for a steady state diffusion-driven profile (Fig. 3.10; Harper *et al.*, 1997). The model

suggested after 10 hours the concentration profile in the gel would be close to homogenous, dependent on the diffusion coefficient of the analyte, and after the traditional 24 hour deployment any gradients in the concentration profile will have completely disappeared (Harper *et al.*, 1997). According to the model presented in Harper *et al.* (1997) (Fig. 3.10) the 30 hour deployment of the gel, in the present study, would have resulted in flattening of the analyte peak. Although flattening (smoothed peak) in the profile is observed a clear peak can be determined, indicating that there was a constant source of the ^{15}N product within the pore water and the rate of $^{15}\text{N-N}_2$ and $^{15}\text{N-NH}_4^+$ production was greater than diffusion out of the gel (Fig. 3.4 A, E, I).

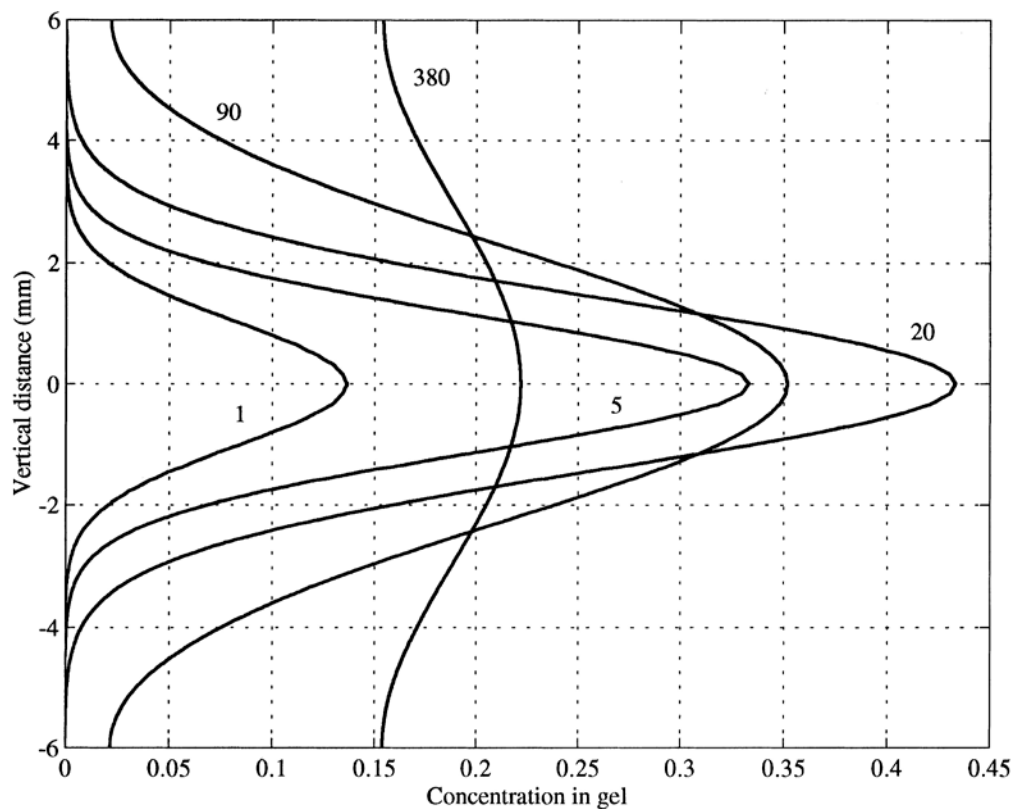


Figure 3.10 Figure 5 from Harper *et al.* (1997). Concentration changes over time in a DET gel for the diffusive case. Time given in minutes. The concentration of the gel is the fraction of the total concentration.

I have two recommendations to reduce lateral diffusion and peak flattening within the DET gel and produce an analyte peak more representative of *in situ* conditions (Fig. 3.9B):

- 1) *Reduce the length of gel deployment* – In this study the incubation time after $^{15}\text{N-NO}_3^-$ addition was 24 hours to allow for diffusion of $^{15}\text{N-NO}_3^-$ into the sediment then the gel was deployed for an additional ~30 hours. The extended gel deployment was to account for;
 - a. equilibration of the gel with the pore water and,
 - b. sediment re-equilibration after the disturbance caused by the gel deployment.

Stief *et al.* (2010) calculated the equilibration time of a 2 mm thick DET gel with sediment pore water would be < 3 hours and justified the extended gel deployment to allow for pore water gradients to re-establish after the sediment disturbance. Reducing the time to < 12 hours should allow the sediment to re-equilibrate after the disturbance and ensure there is a consistent $^{15}\text{N-N}_2$ or $^{15}\text{N-NH}_4^+$ source within the pore water to produce a large peak and counteract peak flattening.

- 2) *Peeper-like gel sampler design* – In this study the single gel was sliced after deployment and the profile created (Fig 3.11A-B), to avoid lateral diffusion within the gel, a mould containing discrete 2 mm slices in the gel sampler could be prepared and the gel cast within the sampler (Fig 3.11 C-D). Moulding the gel into discrete layers will decrease the length of lateral diffusion within the gel, minimise peak flattening and allow for the measurement of steep concentration gradients. A similar approach has been used in 2D gels where the gel was prepared in a 1.0 x 1.0 cm well array (Kessler *et al.*, Under Review).

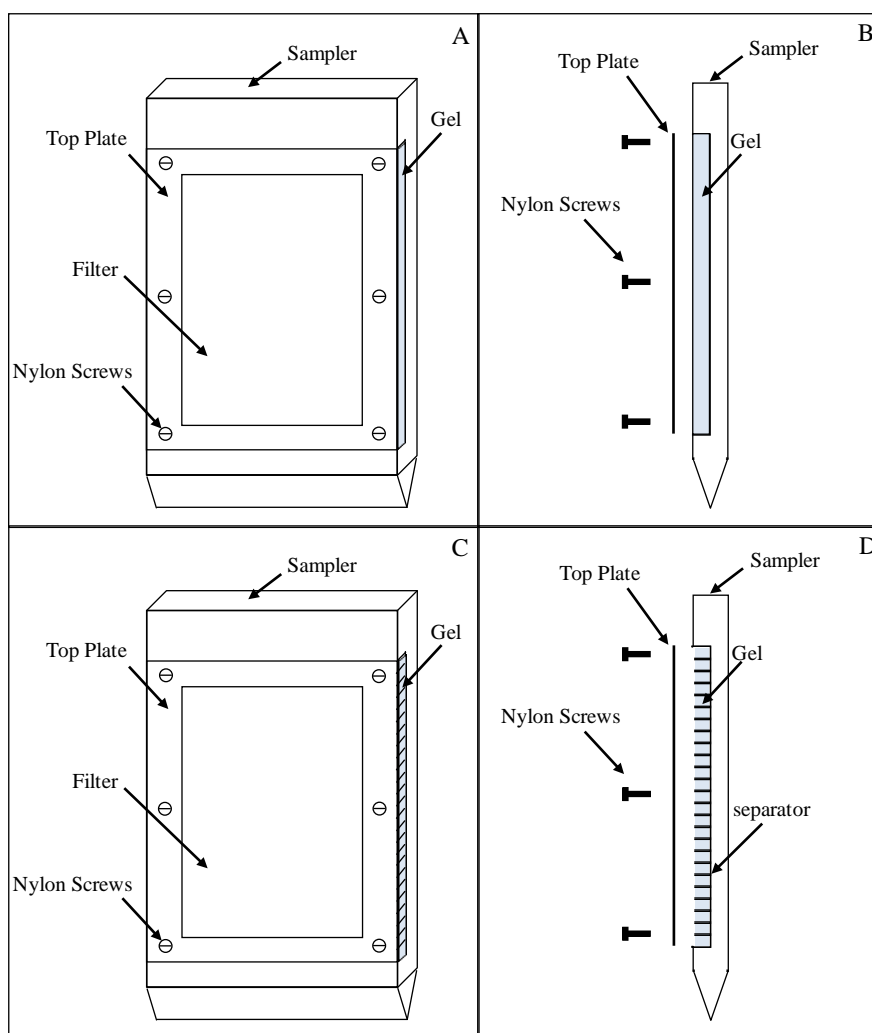


Figure 3.11 (A-B) Gel sampler design used in the present study and (C-D) modified sampler design to include discrete slices and reduce peak flattening.

3.5.4 Comparison of the N_2O and $^{15}N-N_2$ denitrification methods

The measurement of N_2O using the acetylene inhibition technique can lead to an underestimation of denitrification (Binnerup *et al.*, 1992). The addition of acetylene, even at concentrations as low as 0.1 % (v:v), inhibits nitrification (Walter *et al.*, 1979). In the presence of oxygen and where nitrification-denitrification coupling is important, nitrification may be a significant source of NO_3^- for denitrification. Because the acetylene inhibition technique inhibits nitrification, only NO_3^- sourced from the water column is denitrified leading to an underestimation of denitrification (Binnerup *et al.*, 1992). The $^{15}N-N_2$ technique is a more representative

measure of total denitrification because both nitrification coupled denitrification and water column driven denitrification are included in the one measurement.

Stief *et al.* (2010) measured high resolution profiles of denitrification and DNRA in freshwater and marine sediments using the N_2O microelectrode-acetylene inhibition technique to measure denitrification and the coupled ^{15}N isotope pairing technique in DET gels to measure DNRA. This method was also used in the present study in September 2012. However, denitrification and DNRA were measured in separate cores and, therefore, direct comparison of these two processes is subject to errors caused by heterogeneity in between samples. The simultaneous measurement of denitrification and DNRA using the ^{15}N isotope pairing technique in DET gels avoids the problem of sample heterogeneity because $^{15}\text{N}\text{-N}_2$ and $^{15}\text{N}\text{-NH}_4^+$ are measured in the same sediment sample and gel slice, allowing for comparison of these two processes with sediment depth.

Figure 3.5 shows a comparison of the sediment profiles from September 2012 (N_2O acetylene inhibition method) and January 2013 (^{15}N isotope pairing technique in DET gels). Under anoxic conditions the N_2O microelectrode method is representative of total denitrification (Fig. 3.5E, F). Under anoxic conditions nitrification is inhibited and therefore the supply of NO_3^- for denitrification is sourced from the water column. Long-term and short term oxic conditions, however, indicate denitrification is underestimated (Fig. 3.5A-D). The peak in denitrification using the N_2O method is observed below the oxic surface layer and tapers rapidly with sediment depth, whereas the $^{15}\text{N}\text{-N}_2$ peak suggests denitrification occurs at greater depths. Although in this study the profiles suffer from peak relaxation as discussed in 3.5.3, assuming the observed $^{15}\text{N}\text{-N}_2$ peak is in phase with the actual $^{15}\text{N}\text{-N}_2$ peak, denitrification occurs deeper in the sediment and over a wider depth range. When comparing the possible zonation of denitrification and DNRA, the underestimation of denitrification by the N_2O method could lead to inaccurate conclusions drawn from these profiles. For example, the September profiles would suggest that denitrification and DNRA occur within separate zones; denitrification below the oxic surface layer and DNRA below the denitrification zone (Fig 3.3). The January-February profiles clearly indicate there is no zonation of denitrification or DNRA within the sediment profile (Fig 3.4).

The N₂O microelectrode-acetylene inhibition technique is useful under anoxic conditions. However, the underestimation of denitrification in the presence of oxygen is problematic. Although the ¹⁵N-N₂ gel method has some weaknesses, when taking into account the recommendations discussed in 3.5.3, the ¹⁵N-N₂ gel method coupled with the ¹⁵N-NH₄⁺ method proposed by Stief *et al.* (2010) is a useful tool in determining the behaviour of denitrification and DNRA in sediment profiles along with available reductants.

3.6 Concluding Remarks

In summary, the findings here support the *in situ* measurements of denitrification and DNRA in the Yarra River estuary, where DNRA became more important in the presence of oxygen in the water column (Fig 2.10). A significant decrease in the denitrification : DNRA ratio was observed when the water column oxygen conditions were switched from hypoxic to oxic (Fig 3.2). In addition the denitrification : DNRA ratio decreased in the presence of oxygen due to an increase in DNRA. No correlation was observed between DNRA rates and total S^{2-} . January-February profiles indicate DNRA only occurred in the presence of Fe^{2+} under oxic conditions. In the Yarra River estuary, the partitioning between denitrification and DNRA appears to be linked to the availability of Fe^{2+} in the sediment.

The $^{15}N-N_2$ gel method is more representative of total denitrification in sediment profiles when compared to the N_2O acetylene inhibition technique, particularly in the presence of oxygen. Taking into consideration the two recommendations (reduced gel deployment time and peeper-like assembly) the combined $^{15}N-N_2$ and $^{15}N-NH_4^+$ gel method is a powerful tool to determine simultaneously the responses of denitrification and DNRA in intact cores to available reductants such as Fe^{2+} and S^{2-} .

3.7 Acknowledgements

I am grateful to Scotch College for providing private boat ramp access. I would like to thank A. Kessler, K. Browne, E. Richmond, T. Scicluna, and M. Bourke for assistance in the field and laboratory. K. Browne and V. Evrard undertook the isotope ratio mass spectrometry analyses. I would like to thank R. Roberts and H. Sarkissian for their help with the design and assembly of the gel cutting device. I would like to acknowledge A. Kessler for his assistance with modelling Fe and S. I appreciate the helpful advice of B. Thamdrup, R.N. Glud and E. Robertson. I would like to acknowledge the support of the Australian Research Council (LP0991254), Melbourne Water Corporation and the Environment Protection Authority Victoria.

3.8 References

- An S. and Gardner W.S. (2002) Dissimilatory nitrate reduction to ammonium (DNRA) as a nitrogen link, versus denitrification as a sink in a shallow estuary (Laguna Madre/ Baffin Bay, Texas). *Marine Ecology Progress Series* **237**, 41-50.
- APHA (2005) *APHA-AWWA-WPCF, Standard Methods for the Examination of Water and Wastewater*. American Public Health Association, American Water Works Association and Water Environment Federation, Washington.
- Behrendt A., De Beer D., and Stief P. (2013) Vertical activity distribution of dissimilatory nitrate reduction in coastal marine sediments. *Biogeosciences Discussions* **10**, 8065-8101.
- Benz M., Brune A., and Schink B. (1998) Anaerobic and aerobic oxidation of ferrous iron at neutral pH by chemoheterotrophic nitrate reducing bacteria. *Archives of Microbiology* **169**, 159-165.
- Bianchi T.S. (2007) *Biogeochemistry of Estuaries*. Oxford University Press, New York.
- Binnerup S.J., Jensen K., Revsbech N.P., Jensen H., and Sorensen J. (1992) Denitrification, dissimilatory reduction of nitrate to ammonium and nitrification in a bioturbated estuarine sediment as measured with ¹⁵N and microsensor techniques. *Applied and Environmental Microbiology* **58**, 303-313.
- Boudreau B.P. (1996) *Diagenetic models and their implementation: modelling transport and reactions in aquatic sediments*. Springer, New York.
- Brunet R.C. and Garcia-Gil L.J. (1996) Sulfide-induced dissimilatory nitrate reduction to ammonia in anaerobic freshwater sediments. *FEMS Microbiology Ecology* **21**, 131-138.
- Childs C.R., Rabalais N.N., Turner R.E., and Proctor L.M. (2002) Sediment denitrification in the Gulf of Mexico zone of hypoxia. *Marine Ecology Progress Series* **240**, 285-290.
- Christensen P.B., Rysgaard S., Sloth N.P., Dalsgaard T., and Schwaerter S. (2000) Sediment mineralization, nutrient fluxes, denitrification and dissimilatory nitrate reduction to ammonium in an estuarine fjord and sea cage trout farms. *Aquatic Microbial Ecology* **21**, 73-84.
- Dalsgaard T., Nielsen L.P., Brotas V., Viaroli P., Underwood G.J.C., Nedwell D.B., Sundback K., Rysgaard S., Miles A., Bartoli M., Dong L.F., Thornton D.C.O.,

- Ottosen L.D.M., Castaldelli G., and Risgaard-Petersen N. (2000) *Protocol Handbook for NICE - Nitrogen Cycling in Estuaries: a project under the EU research programme: Marine Science and Technology (MAST III)*. Ministry of Environment and Energy, National Environmental Research Institute, Department of Lake and Estuarine Ecology, Denmark.
- Davison W., Zhang H., and Grime G.W. (1994) Performance characteristics of gel probes used for measuring the chemistry of pore waters. *Environmental Science and Technology* **28**, 1623-1632.
- Diaz R.J. and Rosenberg R. (2008) Spreading dead zones and consequences for marine ecosystems. *Science* **321**, 926-929.
- Dong L.F., Sobery M.N., Smith C.J., Rusmana I., Phillips W., Stott A., Osborn A.M., and Nedwell D.B. (2011) Dissimilatory reduction of nitrate to ammonium, not denitrification dominates benthic nitrate reduction in tropical estuaries. *Limnology and Oceanography* **56**, 279-291.
- Edwards L., Kusel K., Drake H., and Kostka J.E. (2007) Electron flow in acidic subsurface sediments co-contaminated with nitrate and uranium. *Geochimica et Cosmochimica Acta* **71**, 643-654.
- Faber P.A., Kessler A.J., Bull J.K., McKelvie I.D., Meysman F.J.R., and Cook P.L.M. (2012) The role of alkalinity generation in controlling the fluxes of CO₂ during exposure and inundation on tidal flats. *Biogeosciences Discussions* **9**, 5445-5469.
- Fazzolari E., Nicolardot B., and Germon J.C. (1998) Simultaneous effects of increasing levels of glucose and oxygen partial pressures on denitrification and dissimilatory nitrate reduction to ammonium in repacked soil cores. *European Journal of Soil Biology* **34**, 47-52.
- Fossing H., Berg P., Thamdrup B., Rysgaard S., Sorensen H.M., and Nielsen K. (2004) A model set-up for an oxygen and nutrient flux model for Aarhus Bay (Denmark) - NERI Technical Report No. 483. National Environmental Research Institute - Ministry of the Environment, Denmark.
- Hansen H.C.B., Guldborg S., Erbs M., and Koch C.B. (2001) Kinetics of nitrate reduction by green rusts - effects of interlayer anion and Fe(II):Fe(III) ratio. *Applied Clay Science* **18**, 81-91.
- Hansen H.C.B., Koch C.B., Nancke-Krogh H., Borggaard O.K., and Sorensen J. (1996) Abiotic nitrate reduction to ammonium: key role of green rust. *Environmental Science and Technology* **30**, 2053-2056.

- Harper M.P., Davison W., and Tych W. (1997) Temporal, spatial, and resolution constraints for *in situ* sampling devices using diffusional equilibration: dialysis and DET. *Environmental Science and Technology* **31**, 3110-3119.
- Hou L., Liu M., Carini S.A., and Gardner W.S. (2012) Transformation and fate of nitrate near the sediment-water interface of Copano Bay. *Continental Shelf Research* **35**, 86-94.
- Jorgensen K.S. (1989) Annual pattern of denitrification and nitrate ammonification in estuarine sediment. *Applied and Environmental Microbiology* **55**, 1841-1847.
- Joye S.B. and Hollibaugh J.T. (1995) Influence of sulfide inhibition of nitrification on nitrogen regeneration in sediments. *Science* **270**, 623-625.
- Kessler A.J., Glud R.N., Cardenas M.B., and Cook P.L.M. (Under Review) Transport zonation limits coupled nitrification-denitrification in permeable sediments. *Environmental Science and Technology* **Under Review**.
- King D. and Nedwell D.B. (1985) The influence of nitrate concentration upon the end-products of nitrate dissimilation by bacteria in anaerobic salt marsh sediment. *FEMS Microbiology Ecology* **31**, 23-28.
- Krom M.D., Davison P., Zhang H., and Davison W. (1994) High-resolution pore-water sampling with a gel sampler. *Limnology and Oceanography* **39**, 1967-1972.
- Nealson K.H. and Saffarini D. (1994) Iron and Manganese in anaerobic respiration: environmental significance, physiology, and regulation. *Annual review of Microbiology* **48**, 311-343.
- Nielsen L.P. (1992) Denitrification in sediment determined from nitrogen isotope pairing. *FEMS Microbiology Ecology* **86**, 357-362.
- Ogilvie B.G., Rutter M., and Nedwell D.B. (1997) Selection by temperature of nitrate-reducing bacteria from estuarine sediments: species composition and competition for nitrate. *FEMS Microbiology Ecology* **23**, 11-22.
- Oshiki M., Ishii S., Yoshida K., Fujii N., Ishiguro M., Satoh H., and Okabe S. (2013) Nitrate-dependent ferrous iron oxidation by anaerobic ammonium oxidation (anammox) bacteria. *Applied and Environmental Microbiology* **79**, 4087-4093.
- Preisler A., de Beer D., Lichtschlag A., Lavik G., Boetius A., and Jorgensen B.B. (2007) Biological and chemical sulfide oxidation in a *Beggiatoa* inhabited marine sediment. *The ISME Journal* **1**, 341-353.

- Revsbech N.P., Risgaard-Petersen N., Schramm A., and Nielsen L.P. (2006) Nitrogen transformations in stratified aquatic microbial ecosystems. *Antonie van Leeuwenhoek* **90**, 361-375.
- Rysgaard S. and Risgaard-Petersen N. (1997) A sensitive method for determining nitrogen-15 isotope in urea. *Marine Biology* **128**, 191-195.
- Rysgaard S., Risgaard-Petersen N., and Sloth N.P. (1996) Nitrification, denitrification, and nitrate ammonification in sediments of two coastal lagoons in Southern France. *Hydrobiologia* **329**, 133-141.
- Sayama M., Risgaard-Petersen N., Nielsen L.P., Fossing H., and Christensen P.B. (2005) Impact of bacterial NO_3^- transport on sediment biogeochemistry. *Applied and Environmental Microbiology* **71**, 7575-7577.
- Sigman D.M., Altabt M.A., Michener R., McCorkle D.C., Fry B., and Holmes R.M. (1997) Natural abundance-level measurement of the nitrogen isotopic composition of oceanic nitrate: an adaptation of the ammonia diffusion method. *Marine Chemistry* **57**, 227-242.
- Soetaert K., Petzoldt T., and Meysman F. (2010) marelac: Tools for Aquatic Sciences, R Package version 2.1, <http://cran.stat.auckland.ac.nz/web/packages>.
- Sorensen J. (1978) Capacity for denitrification and reduction of nitrate to ammonia in a coastal marine sediment. *Applied and Environmental Microbiology* **35**, 301-305.
- Sorensen J., Tiedje J.M., and Firestone R.B. (1980) Inhibition by sulfide of nitric and nitrous oxide reduction by denitrifying *Pseudomonas fluorescens*. *Applied and Environmental Microbiology* **39**, 105-108.
- Stief P., Behrendt A., Lavik G., and De Beer D. (2010) Combined gel probe and isotope labeling technique for measuring dissimilatory nitrate reduction to ammonium in sediments at millimeter-level resolution. *Applied and Environmental Microbiology* **76**, 6239-6247.
- Stookey L.L. (1970) Ferrozine - A new spectrophotometric reagent for iron. *Analytical Chemistry* **42**, 779-781.
- Straub K.L., Benz M., Shinck B., and Widdel F. (1996) Anaerobic, nitrate-dependent microbial oxidation by ferrous iron. *Applied and Environmental Microbiology* **62**, 1458-1460.

- Voillier E., Inglett P.W., Hunter K., Roychoudhury A.N., and Van Cappellen P. (2000) The ferrozine method revisited: Fe(II)/Fe(III) determination in natural waters. *Applied Geochemistry* **15**, 785-790.
- Walter H.M., Keeney D.R., and Fillery I.R. (1979) Inhibition of nitrification by acetylene. *Soil Science Society of America Journal* **43**, 195-196.
- Weber K.A., Urrutia M.M., Churchill P.F., Kukkadapu R.V., and Roden E.E. (2006) Anaerobic redox cycling of iron by freshwater sediment microorganisms. *Environmental Microbiology* **8**, 100-113.

4. Increased rates of dissimilatory nitrate reduction to ammonium (DNRA) under aerobic conditions in a periodically hypoxic estuary are linked to the availability of iron



*Part of this chapter has been submitted for publication in *Geochimica et Cosmochimica Acta*: Roberts, K.L, Kessler, A.J, Grace, M.R and Cook, P.L.M (2013) 'Increased rates of DNRA under aerobic conditions in a periodically anoxic estuary are linked to the availability of iron'*

4.1 Abstract

The Yarra River estuary is a salt wedge estuary prone to hypoxia in the bottom waters during low flow events. Nitrate reduction pathways were examined using the ^{15}N isotope pairing technique in intact sediment cores and slurries, to review the behaviour of denitrification and dissimilatory nitrate reduction to ammonium (DNRA) with respect to NO_3^- and available reductants. Increasing the NO_3^- concentration in slurries from $10 \mu\text{mol L}^{-1}$ to $240 \mu\text{mol L}^{-1}$ did not change the relative contribution of denitrification and DNRA, with DNRA making up $28 \pm 4 \%$ of total NO_3^- reduction. In addition, in the intact sediment cores, no significant NO_3^- storage was observed in the sediment. Most of the NH_4^+ produced via DNRA diffused into the water column, suggesting NO_3^- storing-sulfur oxidising bacteria do not play a key role in determining rates of DNRA in the Yarra River estuary.

In 50 % (v:v) sediment slurries an increase in pH from 7.47 (control) to 8.37 (treatment) caused no significant difference in DNRA rates or the denitrification : DNRA ratio. Furthermore, no significant differences were observed between the control and Fe^{2+} treatments due to the high background concentration of Fe^{2+} in the control treatment. To counter this, slurries were diluted to 5 % (v:v). DNRA then correlated well with Fe^{2+} consumption and the ratio of DNRA to Fe^{2+} consumption was $1 : 4 \pm 2$ and $1 : 10 \pm 6$ for the control and iron treatments, respectively. Long term Fe^{2+} slurry experiments support the hypothesis that DNRA is driven by Fe^{2+} oxidation in the Yarra River estuary.

4.2 Introduction

Nitrogen is a key limiting nutrient in the marine environment and increasing inputs from anthropogenic sources have led to an increasing incidence of eutrophication and hypoxia ($< 100 \mu\text{mol-O}_2 \text{ L}^{-1}$) in coastal waters (Conley *et al.*, 2007; Diaz and Rosenberg, 2008; Jorgensen and Sorensen, 1988). In addition to detrimental ecological impacts, hypoxia also significantly affects biogeochemical cycling pathways, especially for nitrogen. Hypoxic conditions are known to increase the release of bioavailable nitrogen, primarily in the form of ammonium (NH_4^+), at the expense of nitrogen removal processes such as denitrification (Kemp *et al.*, 2005). The major cause for this change is thought to be a decrease in nitrification resulting in less nitrate (NO_3^-) available for denitrification (Roberts *et al.*, 2012). In addition, stronger reducing conditions that accompany hypoxia are thought to favour dissimilatory NO_3^- reduction to NH_4^+ (DNRA) over denitrification, although the controls on this process remain poorly understood.

Four key factors are thought to control the balance between NO_3^- reduction via denitrification and DNRA: (1) NO_3^- availability, (2) temperature, (3) organic carbon loading, and (4) availability of reductants such as sulfide (S^{2-}) or iron (II) (Fe^{2+}).

The affinity of denitrifiers or nitrate ammonifiers for NO_3^- can determine whether NO_3^- is converted to N_2 or NH_4^+ under varying oxygen and NO_3^- concentrations. Unlike denitrifiers, nitrate ammonifiers possess constitutive enzymes; where the enzyme is constantly produced irrespective of substrate concentration. Therefore, nitrate ammonifiers are able to survive under variable NO_3^- concentrations, potentially outcompeting denitrification when NO_3^- is sporadically available (Jorgensen, 1989). In salt marsh sediments, King and Nedwell (1985) observed the proportion of DNRA increased up to 50 % of total NO_3^- reduction when NO_3^- concentrations were low, a finding supported by several other researchers (Childs *et al.*, 2002; Nizzoli *et al.*, 2010; Ogilvie *et al.*, 1997). Under low NO_3^- concentrations, nitrate ammonifiers are energetically favoured, producing more energy per mole of NO_3^- than denitrifying bacteria (Gibbs free energy (ΔG^0); denitrification generates $\sim 560 \text{ KJ mol}^{-1}$ and DNRA generates $\sim 600 \text{ KJ mol}^{-1}$ at pH 7 and 25°C from Dong *et al.* (2011); Childs *et al.*, 2002; Nizzoli *et al.*, 2010).

Seasonal variation in temperature can determine the species composition of a microbial community (King and Nedwell, 1984; Ogilvie *et al.*, 1997; Tison *et al.*, 1980). In estuarine sediments, Ogilvie *et al.* (1997) observed a shift in the heterotrophic microbial population from nitrate ammonifiers at warm water temperatures (20 °C) to denitrifiers at lower temperatures (5 °C). Studies have reported that the NO₃⁻ affinity of nitrate ammonifiers is more efficient than that of denitrifying bacteria at temperatures above 10 °C, whilst below these temperatures denitrifiers utilise NO₃⁻ more efficiently (King and Nedwell, 1984; Ogilvie *et al.*, 1997). Likewise, in the tropical Cisadane estuary, Indonesia, Dong *et al.* (2011) observed that the rate of DNRA was ~10 fold greater than denitrification when NO₃⁻ was in excess. In that study, the high rates of DNRA were explained by the higher affinity of nitrate ammonifiers for NO₃⁻ at tropical temperatures (Dong *et al.*, 2011).

Heterotrophic DNRA is carried out by fermentative bacteria and is observed in environments with high labile organic carbon availability (Tiedje, 1988; Yin *et al.*, 2002). Cole and Brown (1980) observed the accumulation of acetate and formate with NO₂⁻ reduction to NH₄⁺ in strains of *E. coli* sp., a pathway later confirmed by Bonin (1996). In soils, the addition of labile organic carbon increased DNRA from 2 to 25 % of total NO₃⁻ reduction when the C/N ratio was high (Fazzolari *et al.*, 1998). This finding was supported by Yin *et al.* (2002), who noted that soils with high organic carbon inputs were able to support a large heterotrophic population of bacteria, of which ~20 % were nitrate ammonifiers compared to only ~6 % in carbon depleted soils. Under these conditions, > 50 % of the NO₃⁻ added was converted to NH₄⁺ and organic nitrogen at the expense of denitrification (Yin *et al.*, 2002).

Chemoautotrophic DNRA has also been reported and is largely controlled by available reductants such as S²⁻ and Fe²⁺. DNRA has long been linked to S²⁻ oxidation with slurry experiments showing that NH₄⁺ production associated with S²⁻ oxidation accounted for up to 30 % of total NO₃⁻ reduction (Brunet and Garcia-Gil, 1996). Intact sediment core incubations have also shown DNRA is the dominant NO₃⁻ reduction pathway in highly sulfidic sediments (An and Gardner, 2002). A number of sulfur-oxidizing bacteria, for example *Thioploca* sp. and *Beggiatoa* sp., can store and reduce NO₃⁻ to NH₄⁺ as a secondary metabolic pathway (Otte *et al.*, 1999; Schulz and Jorgensen, 2001). In the presence of *Beggiatoa* sp. in Aarhus Bay,

Denmark, DNRA was the predominant pathway of NO_3^- reduction; however, in the absence of sulfur oxidising bacteria, DNRA ceased (Sayama *et al.*, 2005).

Numerous studies have linked iron oxidation to NO_3^- reduction yielding N_2 as the main product (Benz *et al.*, 1998; Nealson and Saffarini, 1994; Straub *et al.*, 1996). However, studies linking Fe^{2+} oxidation to NH_4^+ production via DNRA have been more limited. It has been shown that DNRA can be coupled to Fe^{2+} oxidation in wetland and river floodplain sediments and that *Geobacter sp.* and *Betaproteobacteria* mediate this process (Coby *et al.*, 2011; Weber *et al.*, 2006). Most recently, Hou *et al.* (2012) inferred that Fe^{2+} could be a controlling factor on DNRA based on a strong correlation between $^{15}\text{N-NH}_4^+$ production and reactive iron oxide concentrations in Texas coastal sediments. Estuaries typically have high inputs of colloidal iron (Hart and Davies, 1981; Nealson and Saffarini, 1994) which can result in very high Fe^{2+} concentrations within sediment porewaters, suggesting that Fe-driven DNRA could be an important process.

The Yarra River estuary is prone to periodic hypoxia in the bottom waters during low summer flows due to its typical salt wedge structure. As discussed in Chapter Two (2.6.4), the importance of DNRA relative to denitrification increased in the presence of oxygen in the water column, despite DNRA being expected to occur under more reducing and low NO_3^- conditions (Chp. 2 Fig 2.10). In that study, it was hypothesised that NO_3^- concentration was a possible control on DNRA, with organic carbon availability ruled out as a possible explanatory factor. The purpose of this study was to investigate these unexpected findings further and explore the response of DNRA to changing NO_3^- concentration, pH conditions and reductant availability. Specifically four research questions were addressed:

- (1) How do denitrification and DNRA behave with respect to NO_3^- concentration?
- (2) Does increasing pH affect DNRA rates?
- (3) Are NO_3^- -storing sulfur oxidising bacteria important in the Yarra River estuary?
- (4) Does the availability of Fe^{2+} or S^{2-} change the relative contributions of denitrification and DNRA to total NO_3^- reduction?

4.3 Methods

4.3.1 Site description and sampling

Sediment samples were collected from three sites: Morell Bridge, Scotch College and Bridge Road in the Yarra River estuary, Melbourne, Australia from 2010 to 2013 (*see* section 2.4.1 and Fig 2.1 for site details). Sediment cores were collected in 27.5 x 6.6 cm polyethylene cylinders and stoppered. Bottom water was collected using a bilge pump or a 5 L Niskin bottle. Sediment cores were transferred to a temperature-controlled water bath. Each core was mixed using a magnetic stirrer (~40 rpm) suspended ~2 cm above the sediment surface to prevent disturbance of the sediment.

4.3.2 Slurry preparation

Unless specified otherwise, sediment slurries were prepared by removing the surface 1 cm of sediment from the core after extrusion. The 1 cm slice was immediately mixed with bottom water at a ratio of 1:1 (v:v).

4.3.3 NO₃⁻ slurries

Sediment samples and water were collected on the 15th May 2012 at the Scotch College site. The sediment cores were covered with bottom water from the site and aerated overnight before slurries were prepared the following day. Five slurries were prepared for each treatment; for denitrification, 8 mL of slurry was sealed in a 12.5 mL exetainer and for DNRA, 18 mL of slurry was sealed in a 30 mL gas tight glass bottle. Slurries were purged with He (high purity helium, Air Liquide, Australia) for ~5 minutes, intermittently shaking to ensure all the oxygen was removed from the slurry. The headspace volume was ~36 % and ~40 % of the total volume of the gas tight vials, for the denitrification and DNRA slurries respectively.

Various additions of 0.5 mmol L⁻¹ ¹⁵N-NO₃⁻ were added to the slurry to give final concentrations of ~10, 30, 60, 100 and 200 μmol-¹⁵N L⁻¹. Five slurries were prepared for each treatment and mixed on a shaker table at 125 rpm for the duration of the incubation period. To stop bacterial activity, 250 μL and 500 μL ZnCl₂ (50 %

w:v) was added to the denitrification and DNRA slurries, respectively. The total incubation period was < 2 hours. Denitrification and DNRA samples were pre-treated with 50 μL of air to increase the background concentration of ^{14}N in the analysis; this was done so that excess ^{15}N could be calculated from the ratios of $^{14}\text{N}/^{15}\text{N}$. For DNRA, the accumulation of $^{15}\text{N-NH}_4^+$ over time was determined after a 2 mol L^{-1} KCl 1:1 (v:v) extraction. Samples were pre-treated with 90 μg natural abundance NH_4^+ to increase the background concentration of nitrogen before $^{15}\text{N-NH}_4^+$ was collected via the ammonium diffusion method (ADM) and analysed by GC-IRMS (*see* 4.3.8 Analytical Methods).

4.3.4 pH adjusted slurries

Sediment samples were collected on the 6th March 2013 from Scotch College and five slurries were prepared for each treatment. Denitrification and DNRA were prepared in the same 12.5 mL exetainer and then purged for ~5 minutes with He to remove all oxygen. To examine the impact of pH on denitrification and DNRA, two pH treatments were examined: pH 7.37 (control – pH measured after slurring) and pH 8.37 (treatment - pH adjusted with NaOH). A 200 μL aliquot of 0.5 mmol L^{-1} $^{15}\text{N-NO}_3^-$ was then added to each slurry. Samples were then shaken at 125 rpm in the dark throughout the incubation period. The incubation ceased upon the addition of 250 μL ZnCl_2 (50 % w:v) to individual slurries at ~10, 20, 30, 50 and 70 minutes.

Denitrification samples were pre-treated as described in 4.3.3. After $^{15}\text{N-N}_2$ analysis, $^{15}\text{N-NH}_4^+$ was extracted from the slurry with a 2 mol L^{-1} KCl 1:1 (v:v) extraction, and converted to $^{15}\text{N-N}_2$ using the hypobromite method and analysed via GC-IRMS (*see* 4.3.8 Analytical Methods).

4.3.5 NO_3^- storage and Sulfur oxidising bacteria

Sediment cores were collected on the 16th February, 13th April, 11th May and 15th June 2010 at Morell Bridge, Scotch College and Bridge Road sites. The sediment samples were treated as described in Chapter Two section 2.4.4 and denitrification and DNRA determined as described in section 2.4.5. However, the

final stage of the isotope pairing technique where the sediment sample is slurried was omitted for these four months and the sediment was kept intact and frozen.

The frozen sediment was sliced into 0.5 cm intervals for the first 2.0 cm and 1.0 cm intervals down to 5.0 cm using a thin blade band saw. A ~3 g sub-sample of the sediment was immediately used to extract NO_3^- and $^{15}\text{NH}_4^+$ with 40 mL of 2 mol L^{-1} KCl and 500 μL ZnCl_2 (50 % w:v). A 12 mL sub-sample of the supernatant was filtered (0.45 μm ; 30 mm polypropylene housing; Bonnet) for NO_3^- and frozen until analysis via flow injection analysis (FIA). An unfiltered sample for $^{15}\text{N-NH}_4^+$ was immediately processed to collect the $^{15}\text{N-NH}_4^+$ via the ADM and then analysed via GC-IRMS (*see* section 4.3.8). Samples were duplicated for each slice and triplicate cores were analysed.

4.3.6 Fe^{2+} and S^{2-} slurries

Sediment cores were collected on the 25th March 2013 at the Scotch College site. Cores were circulated with aerated bottom water from the site until slurry preparation. The concentration of Fe^{2+} was tested in the sediment after extruding a core and slicing the core into 1.0 cm depth intervals down to 4.0 cm. The slice was placed in a 50 mL Falcon tube and centrifuged for 5 minutes at 2000 rpm. The supernatant was filtered and 1.0 mL fixed with 0.5 mL ferrozine for analysis of Fe^{2+} via UV-visible spectrometry (*see* section 4.3.8).

Slurries for DNRA and denitrification were prepared as described in section 4.3.4. Five treatments were prepared: a control treatment containing NO_3^- only (final concentration ~600 $\mu\text{mol L}^{-1}$ $^{15}\text{N-NO}_3^-$), two Fe^{2+} (in the form of Ferrous Sulfate monohydrate, Prolabo) treatments (~600 $\mu\text{mol L}^{-1}$ $^{15}\text{N-NO}_3^-$ with ~60 $\mu\text{mol L}^{-1}$ and ~900 $\mu\text{mol L}^{-1}$ Fe^{2+} target concentration) and two S^{2-} (in the form of Sodium Sulfide nonahydrate, Sigma Aldrich) treatments (~600 $\mu\text{mol L}^{-1}$ $^{15}\text{N-NO}_3^-$ with ~60 $\mu\text{mol L}^{-1}$ and ~900 $\mu\text{mol L}^{-1}$ S^{2-} final concentration). The samples were mixed on a shaker table at 125 rpm in the dark throughout the incubation period. Five replicate slurries were prepared for the time series and the incubation was terminated upon the addition 250 μL ZnCl_2 (50 % w:v) at ~10, 20, 30, 50 and 70 minutes. Rates of denitrification and DNRA were determined from the accumulation of $^{15}\text{N-N}_2$ and $^{15}\text{N-NH}_4^+$ over time respectively as described in section 4.3.4.

4.3.7 Fe²⁺ long term slurries

Sediment samples were collected on May 9th 2013 from the Scotch College site. Cores were aerated in bottom water from the site overnight until the preparation of slurries. Slurries comprising 5 % (v:v) wet sediment were prepared with site bottom water and the top 1 cm of sediment. A volume of 15 mL slurry was sealed in a 20 mL gas tight glass vial and purged with He for ~5 minutes to remove all oxygen. Two treatments were prepared, a control treatment with added ¹⁵N-NO₃⁻ only (1 mmol L⁻¹ final concentration), and an Fe²⁺ treatment with both ¹⁵N-NO₃⁻ (1 mmol L⁻¹ final concentration) and Fe²⁺ addition (~5 mmol L⁻¹ concentration).

The incubation was carried out over 8 days and samples were collected at time = 0, 3, 12 and 24 hours and time = 2, 3, 4, 6 and 8 days thereafter. Throughout the incubation period, samples were shaken in the dark at 180 rpm at ~22 °C. As it has been shown that NO₂⁻ spontaneously oxidises Fe²⁺ at acidic pH (Klueglein and Kappler, 2013), the anoxic slurry was centrifuged at 1000 rpm for 2 minutes and the supernatant analysed for Fe²⁺ before extraction of the sediment with HCl to avoid this potential artefact (Klueglein and Kappler, 2013; Weber *et al.*, 2001). Before the sample was uncapped, a 1.5 mL gas sample was collected from the headspace and introduced into an exetainer containing ultrapure water. The slurry was then opened and an unfiltered water sample was collected rapidly in a 3 mL exetainer for ¹⁵N-NH₄⁺ and preserved with 100 µL ZnCl₂ (50 % w:v). The remaining water was filtered (0.2 µm pore size, Advantec) immediately for analysis of NO_x (NO₂⁻ + NO₃⁻), NO₂⁻ and NH₄⁺, and of this, 0.5 and 0.1 mL filtered subsamples were preserved in ferrozine for the analysis of Fe²⁺ for the control and Fe treatments respectively. Nutrient samples were frozen until analysis (*see* section 4.3.8).

The remaining sediment was homogenized and ~0.2 g weighed into a centrifuge tube containing 20 mL 0.5 mol L⁻¹ HCl, to determine the amount of easily reducible iron in the sediment (HCl extractable Fe²⁺; Lovley and Phillips, 1986). The sample was shaken at 200 rpm for 2 hours, then filtered and 0.5 and 0.1 mL subsamples preserved with ferrozine for the control and Fe treatments respectively.

For the determination of ²⁹N₂ and ³⁰N₂, a 100 µL subsample of the gas collected was injected into a purged exetainer containing 1.5 mL helium headspace

and 50 μL of air to increase the background of ^{14}N as described previously. Samples for $^{15}\text{N-NH}_4^+$ were determined via the hypobromite method (*see* section 4.3.8).

4.3.8 Analytical methods

Nutrient samples (NO_x , NO_2^- and NH_4^+) were analysed via flow injection analysis (FIA; Lachat Quickchem 8000 Flow injection Analyser, spectrophotometric detector). Standards (0 - 1 mg-N L^{-1}), spikes and reference materials were within acceptable limits and analysed following the procedures in Standard Methods for Water and Wastewater (2005).

Iron was determined via the ferrozine method (Stookey, 1970; Voillier *et al.*, 2000). Standards were prepared in the range 0 - 1 mg-Fe L^{-1} and triplicate absorbance readings taken at 632 nm using a UV-Visible Spectrophotometer (GBC UV Visible Spectrophotometer - 918). All reagents were prepared as described in Voillier *et al.* (2000). Porewater and slurry samples for iron were filtered and fixed with 0.5 mL ferrozine immediately to preserve Fe^{2+} in the sample; if the expected concentration of Fe^{2+} was high, the amount of ferrozine was doubled. After the analysis of Fe^{2+} via UV-Visible Spectrometry, total Fe was measured; 1 mL of hydroxylamine hydrochloride was added to the sample already containing Ferrozine and allowed to react ~20 minutes before the addition of 0.25 mL of ammonium acetate buffer. After all reagents were added, the samples were left for at least 1 hour for colour development before analysis. Dilution by reagents was taken into consideration in calculations along with the volume of sample removed for Fe^{2+} analysis.

Denitrification was determined from the accumulation of $^{29}\text{N}_2$ and $^{30}\text{N}_2$ over time. After pre-treatment, samples for $^{15}\text{N-N}_2$ were analysed via a gas chromatograph coupled to a mass spectrometer (Sercon GC with He carrier coupled to a 20-22 continuous flow isotope ratio mass spectrometer or a Shimadzu GCMS-QP5050).

DNRA was determined from the accumulation of $^{15}\text{N-NH}_4^+$ over time. $^{15}\text{N-NH}_4^+$ was collected using two different techniques, the ADM and the hypobromite method. $^{15}\text{N-NH}_4^+$ was captured in an acid trap using the ADM (pre-treatment described in sections 4.3.3, 4.3.4 and 4.3.6) before analysis via GC-IRMS

fitted to an elemental analyser at 1050 °C (Sigman *et al.*, 1997). For the slurries described in sections 4.3.7 and 4.3.8, the hypobromite method was used to convert $^{15}\text{N-NH}_4^+$ to $^{15}\text{N-N}_2$ (Rysgaard and Risgaard-Petersen, 1997). A subsample of the extracted $^{15}\text{N-NH}_4^+$ supernatant was sealed in a 3 mL exetainer and purged with helium to remove background N_2 . Then 60 μL of 16 mol L^{-1} NaOH was added to the 3 mL exetainer containing the sample, shaken, then 60 μL of hypobromite added. Volumes of reagents were increased proportionally if the sample was collected in a 12.5 mL exetainer. The samples were shaken for 24 hours before analysis to ensure all the NH_4^+ was converted to N_2 , then analysed via a gas chromatograph coupled to an isotope ratio mass spectrometer (Sercon GC with He carrier coupled to a 20 - 22 continuous flow isotope ratio mass spectrometer). Both the ADM and hypobromite method achieved $\geq 90\%$ recovery of $^{15}\text{N-NH}_4^+$.

4.3.9 Statistical analyses

Regressions and the Michaelis-Menten kinetic model were performed using the Systat software Sigmaplot 12.0. The Analysis of Covariance using a Type 3⁵ sum of squares test was carried out in the statistical program SAS and significance was determined at the 95 % confidence interval.

⁵ Analysis of covariance was used to test for differences in the slope of ^{15}N production over time between treatments. Type 3 sums of squares tests were used to test the main effects of treatment and time on ^{15}N in the presence of an interaction term (i.e. treatment \times time).

4.4 Results

4.4.1 NO₃⁻ slurries

DNRA and denitrification rates both increased to a maximum with increasing NO₃⁻ concentration (Fig 4.1). Denitrification increased to a maximum rate (V_{\max}) of 43.5 $\mu\text{mol L-slurry}^{-1} \text{h}^{-1}$ whereas DNRA reached a V_{\max} 26.4 $\mu\text{mol L-slurry}^{-1} \text{h}^{-1}$ (Fig 4.1). The half saturation constants (K_m) for denitrification and DNRA were 49.0 $\mu\text{mol-NO}_3^- \text{L}^{-1}$ and 85.9 $\mu\text{mol-NO}_3^- \text{L}^{-1}$, respectively. The kinetics for both denitrification ($R^2 = 0.98$, $p < 0.01$) and DNRA ($R^2 = 0.91$, $p < 0.05$) followed the Michaelis–Menten kinetic model (Fig 4.1; Michaelis and Menten, 1913). The denitrification : DNRA ratio was not significantly affected by NO₃⁻ concentration (Denitrification : DNRA = $-0.006(^{15}\text{N-NO}_3^-) + 3.15$, $df = 4$, $R^2 = 0.45$, $p = 0.22$). DNRA averaged 28 ± 4 % of total NO₃⁻ reduction over the NO₃⁻ concentration range.

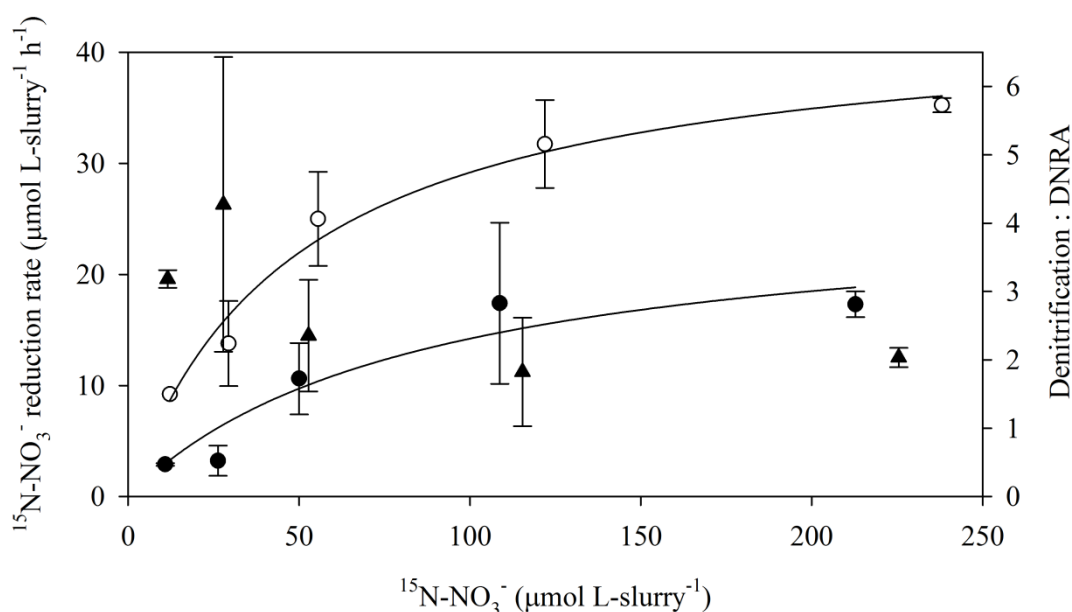


Figure 4.1 $^{15}\text{N-NO}_3^-$ reduction ($\mu\text{mol L slurry}^{-1} \text{h}^{-1}$) with respect to NO₃⁻ concentration ($\mu\text{mol L}^{-1}$). Denitrification (\circ) and DNRA (\bullet) follow the Michaelis–Menten kinetic model and increase with respect to NO₃⁻ concentration ($p < 0.01$ and $p < 0.05$, respectively). Denitrification : DNRA (\blacktriangle) with respect to $^{15}\text{N-NO}_3^-$ concentration.

4.4.2 pH adjusted slurries

DNRA was the dominant NO_3^- reduction pathway in both the control and pH treatments with rates of 28 ± 3 and $24 \pm 2 \mu\text{mol L-slurry}^{-1} \text{h}^{-1}$, respectively (Fig 4.2). Denitrification ($^{15}\text{N-N}_2$) was only 19.3 ± 0.2 and 19.2 ± 0.1 % of total NO_3^- reduction for the control and pH treatment, respectively (Fig 4.2). Analysis of covariance (ANCOVA), using the type 3 test showed no significant difference in rates (slope) of denitrification and DNRA when comparing the control and pH treatment (DNRA, $df = 1$, $F = 1.78$, $p \gg 0.05$; denitrification, $df = 1$, $F = 1.45$, $p \gg 0.05$). The denitrification : DNRA ratios for the control (0.24 ± 0.04) and pH (0.24 ± 0.02) were not significantly different ($df = 8$, $p \gg 0.05$).

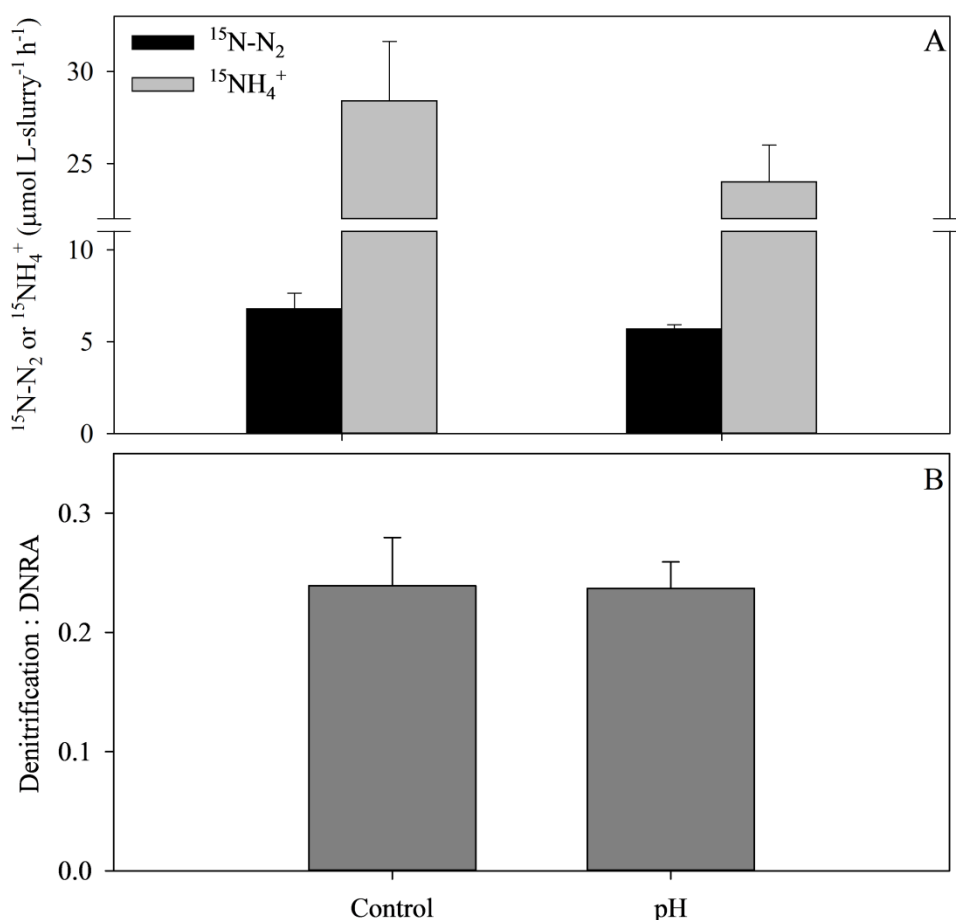


Figure 4.2 (A) Denitrification ($^{15}\text{N-N}_2$) and DNRA ($^{15}\text{N-NH}_4^+$) potential ($\mu\text{mol L-slurry}^{-1} \text{h}^{-1}$) for the control (pH 7.37) and pH (pH 8.37) treatment and (B) Denitrification : DNRA ratios for the control and pH treatments.

4.4.3 NO₃⁻ storage and Sulfur oxidising bacteria

There was no significant storage of NO₃⁻ with sediment depth. Concentrations of up to 50 μmol L⁻¹ NO₃⁻ were only observed on two occasions in May at Scotch College and Morell Bridge sites and decreased sharply with depth (Fig 4.3C, E). In May at Scotch College, the production of ¹⁵N-NH₄⁺ was highest in the sediment coinciding with the high NO₃⁻ in the surface of the sediment. However, on all other occasions, ¹⁵N-NH₄⁺ was highest in the water column (Fig 4.3D). The highest rates of DNRA were observed in February 2010 when the concentration of NO₃⁻ in the sediment was low (Fig 4.3). In addition, during these months visual inspection of the sediment showed that no white layer had developed on the surface indicating sulfur oxidising bacteria were not present in significant numbers.

4.4.4 Fe²⁺ and S²⁻ slurry experiments

The concentration of Fe²⁺ in the sediment porewater was ~100 μmol-Fe²⁺ L⁻¹ before slurry preparation. DNRA (¹⁵N-NH₄⁺) was the dominant process in the 1:1 sediment slurries, making up > 80 % of total NO₃⁻ reduction in all of the treatments (Fig 4.4). The denitrification : DNRA ratio was 0.23 ± 0.02, 0.20 ± 0.01, 0.21 ± 0.02, 0.21 ± 0.02 and 0.14 ± 0.02 for the control, low Fe²⁺, high Fe²⁺, low S²⁻ and high S²⁻ treatments, respectively (Fig 4.4).

Analysis of covariance using the type 3 sum of squares test showed no significant difference in the rates (slopes) of DNRA from the control, Fe²⁺ and S²⁻ treatments (time*treatment, *df* = 4, *F* = 2.82, *p* > 0.05). However a significant difference in the denitrification rates was observed (time* treatment, *df* = 4, *F* = 3.57, *p* < 0.05) owing to the high S²⁻ treatment. Removal of the sulfide treatments and comparison of the two Fe²⁺ treatments with the control resulted in a marginally significant difference between denitrification slopes (time*treatment, *df* = 2, *F* = 4.37, *p* = 0.05). Comparison of the individual treatments with the control indicated rates of both denitrification and DNRA for the high (600 μmol L⁻¹) S²⁻ treatment were significantly different from the control (DNRA, *df* = 1, *F* = 7.59, *p* < 0.05; Denitrification *df* = 1, *F* = 7.47, *p* < 0.05). For the high S²⁻ treatment, DNRA was 44 ± 7 μmol L-slurry⁻¹ h⁻¹ and denitrification was 6.3 ± 0.2 μmol L-slurry⁻¹ h⁻¹ compared to the control rates of 31 ± 2 μmol L-slurry⁻¹ h⁻¹ and 7.1 ± 0.2 μmol L-

slurry⁻¹ h⁻¹, respectively (Fig 4.4). Comparison of DNRA in the individual Fe²⁺ treatments with the control showed no significant difference, (100 μmol-Fe²⁺ L-slurry⁻¹, *df* = 1, *F* = 1.58, *p* > 0.05; 600 μmol-Fe²⁺ L-slurry⁻¹, *df* = 1, *F* = 0.03, *p* > 0.05).

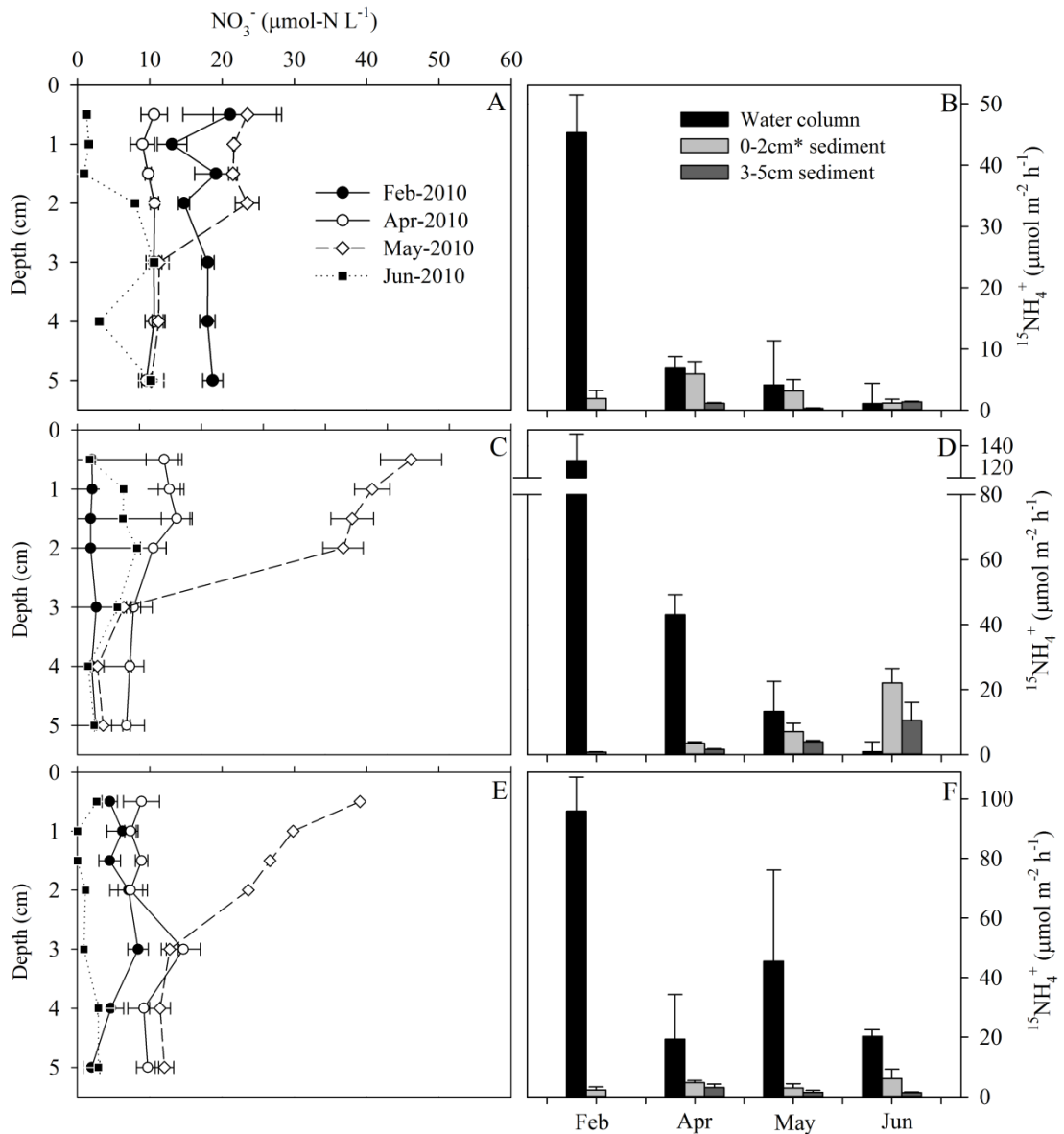


Figure 4.3 NO₃⁻ concentration profiles with sediment depth for February, April, May and June 2010 for (A-B) Bridge Road, (C-D) Scotch College and (D-E) Morell Bridge. The ¹⁵N-DNRA rate was determined for the portions of sediment 0 - 2 cm, 3 - 5 cm and the water column. *February was calculated as a combined rate over the 0 - 5 cm sediment slice.

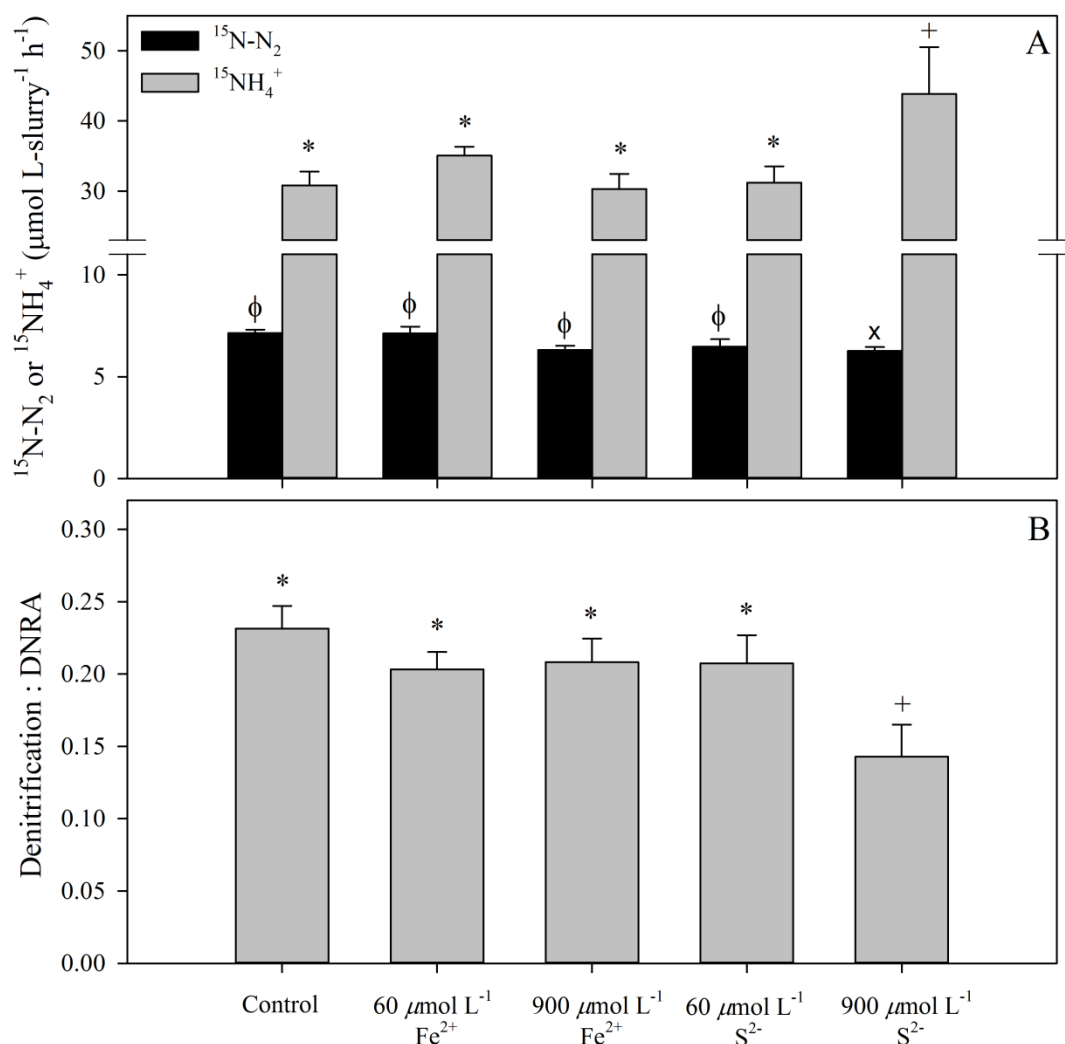


Figure 4.4 (A) Denitrification ($^{15}\text{N-N}_2$) and DNRA ($^{15}\text{N-NH}_4^+$) potential ($\mu\text{mol L-slurry h}^{-1}$) for the control, Fe^{2+} and S^{2-} treatments, and (B) Denitrification : DNRA ratios for the control, Fe^{2+} and S^{2-} treatments. No significant difference compared to the control is denoted by * or ϕ and significant difference compared to the control denoted by + or \times .

4.4.5 Fe^{2+} long term slurries

The $^{15}\text{N-NH}_4^+$ production in both the control and Fe treatment were comparable, reaching maximum concentrations of 55 and 60 $\mu\text{mol L-slurry}^{-1}$ after 48 hours, respectively (Fig 4.5). The rate of $^{15}\text{N-NH}_4^+$ production over the first 48 hours for the control was $1.15 \mu\text{mol L-slurry}^{-1} \text{h}^{-1}$ ($^{15}\text{N-NH}_4^+ = 1.15(\text{h}) + 2.45$, $R^2 = 0.97$, $p < 0.01$; Fig 4.6A) and the rate for the Fe treatment was $1.24 \mu\text{mol L-slurry}^{-1} \text{h}^{-1}$ ($^{15}\text{N-NH}_4^+$

$\text{NH}_4^+ = 1.24(\text{h}) + 3.46$, $R^2 = 0.95$, $p < 0.01$; Fig 4.5B). The $^{15}\text{N-NH}_4^+$ concentration plateaued in both treatments suggesting DNRA ceased after 48 hours. Over the first 48 hours, denitrification (illustrated by the $^{15}\text{N-N}_2$ concentration) was comparable to DNRA in the control ($^{15}\text{N-N}_2 = 1.08(\text{h}) - 0.22$, $R^2 = 1.00$, $p < 0.001$; $^{15}\text{N-NH}_4^+ = 1.15(\text{h}) + 2.47$, $R^2 = 0.97$, $p < 0.01$; Fig 4.5A, C) and half the rate of $^{15}\text{N-NH}_4^+$ production in the Fe treatment ($^{15}\text{N-N}_2 = 0.66(\text{h}) - 0.31$, $R^2 = 0.99$, $p < 0.001$; $^{15}\text{N-NH}_4^+ = 1.23(\text{h}) + 3.46$, $R^2 = 0.95$, $p < 0.01$; Fig 4.5B, D). After 2 days the denitrification rate increased ~6 and 13 fold in the control and Fe treatment, respectively, becoming the dominant NO_3^- reduction pathway (Fig 4.5C, D).

NO_x consumption was $2.27 \mu\text{mol L-slurry}^{-1} \text{h}^{-1}$ ($^{15}\text{N-NO}_3^- = 2.27(\text{h}) + 877$, $R^2 = 0.89$, $p < 0.05$) in the first 48 hours for the control and $2.16 \mu\text{mol L-slurry}^{-1} \text{h}^{-1}$ ($^{15}\text{N-NO}_3^- = 2.26(\text{h}) + 756$, $R^2 = 0.70$, $p = 0.08$) for the Fe treatment (Fig 4.5E, D). NO_x consumption increased significantly after 48 hours, following the denitrification trend in both the control and Fe treatment. The NO_2^- concentration spiked before denitrification increased, reaching ~ 75 % of total NO_x at day 3 and 4 for the control and Fe treatment, respectively.

HCl-extractable Fe^{2+} decreased in the first 48 hours at a rate of $4.53 \mu\text{mol L-slurry}^{-1} \text{h}^{-1}$ and $7.21 \mu\text{mol L-slurry}^{-1} \text{h}^{-1}$ for the control ($\text{Fe}^{2+(\text{HCl})} = -4.53(\text{h}) + 2535$, $R^2 = 0.52$, $p = 0.17$) and Fe ($\text{Fe}^{2+(\text{HCl})} = -7.21(\text{h}) + 2829$, $R^2 = 0.43$, $p = 0.23$) treatments respectively (Fig 4.5G, H). For the Fe treatment, the HCl-extractable Fe^{2+} increased after 48 hours which corresponded to the cessation of DNRA activity, however, for the control treatment, HCl-extractable Fe^{2+} plateaued. The Fe^{2+} concentration in the water column of the control treatment followed a similar trend to the HCl-extractable Fe^{2+} and remained $< 75 \mu\text{mol L}^{-1}$. The consumption rate of water column Fe^{2+} was $0.44 \mu\text{mol L-slurry}^{-1} \text{h}^{-1}$ for the control ($\text{Fe}^{2+} = -0.44(\text{h}) + 41.6$, $R^2 = 0.89$, $p < 0.05$) and $5.45 \mu\text{mol L-slurry}^{-1} \text{h}^{-1}$ for the Fe ($\text{Fe}^{2+} = -5.45(\text{h}) + 974$, $R^2 = 0.64$, $p = 0.10$) treatment (Fig 4.5E, F). The Fe^{2+} concentration in the water column increased after 48 hours with the trend comparable to the HCl-extractable Fe^{2+} .

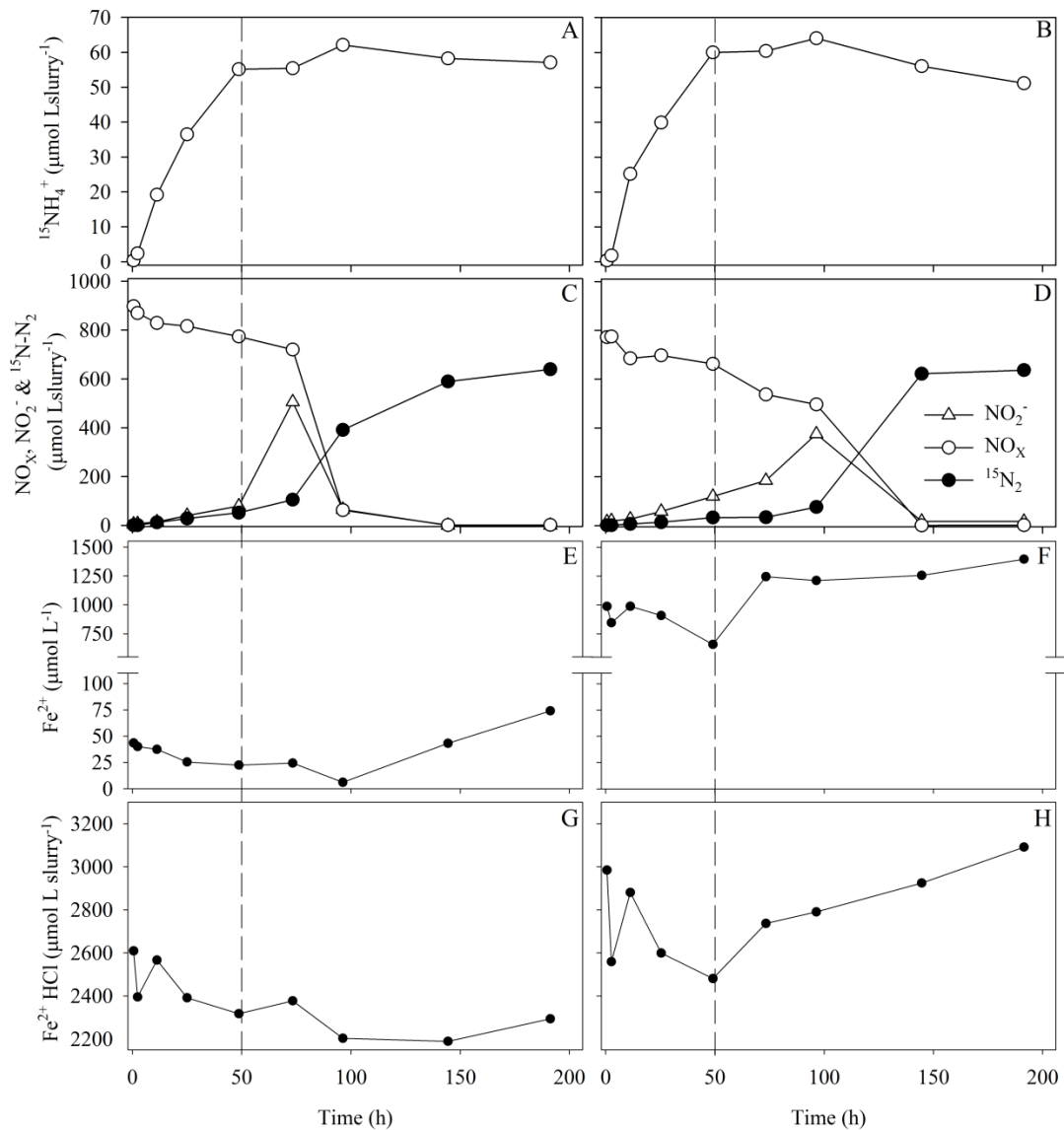


Figure 4.5 $^{15}\text{N-NH}_4^+$, NO_x , NO_2^- , $^{15}\text{N-N}_2$ ($\mu\text{mol L-Slurry}^{-1}$) with respect to time for the control (A, C) and Fe treatment (B, D). Dissolved Fe^{2+} ($\mu\text{mol L}^{-1}$) in the water column and 0.5 mol L^{-1} HCl-extractable Fe^{2+} ($\mu\text{mol L-slurry}^{-1}$) over time (h) in 5 % estuarine slurries in the control (E, G) and Fe treatment (F, H). The dotted line represents the point at which rates of $^{15}\text{N-NH}_4^+$, $^{15}\text{N-N}_2$ production and NO_x and Fe^{2+} consumption were determined.

4.5 Discussion

4.5.1 The influence of NO_3^- on DNRA

Several studies have observed the highest rates of DNRA when NO_3^- is limiting (Childs *et al.*, 2002; King and Nedwell, 1985; Nizzoli *et al.*, 2010). For example, Childs *et al.* (2002) found diminished rates of denitrification in the Gulf of Mexico and hypothesised the decrease was due to a competitive advantage of DNRA under the hypoxic, NO_3^- -limited conditions. In contrast, observations of DNRA in the Yarra River estuary showed the highest rates of DNRA when conditions were aerobic and NO_3^- was present at moderate concentrations. Similarly, in the Cisadane estuary, Indonesia, DNRA increased ~10-fold the rate of increase of denitrification when there was a surplus of NO_3^- . However, this DNRA rate increase was explained by the higher affinity of nitrate ammonifiers for NO_3^- at high temperatures (Dong *et al.*, 2011; Ogilvie *et al.*, 1997). Unlike the Cisadane estuary, the Yarra River estuary is a temperate estuary and DNRA was observed over a range of temperatures (14 - 22 °C, Chp. 2). The concentration of NO_3^- is typically $< 30 \mu\text{mol L}^{-1}$ in the bottom waters of the Yarra River estuary, however, to account for influxes of NO_3^- during high flow events (when DNRA was observed) and nitrification within the sediment, the NO_3^- concentration range tested in incubation experiments was 10 to $240 \mu\text{mol L}^{-1}$. Both denitrification and DNRA followed similar Michaelis-Menten kinetics with respect to NO_3^- concentration. Only a weak negative correlation ($p = 0.22$) was observed between the denitrification : DNRA ratio and increasing NO_3^- concentration (Fig. 4.1, black triangles). However, this weak correlation is not strong enough to be considered the primary factor regulating DNRA in the Yarra River estuary and does not explain the very low denitrification : DNRA ratios observed under oxic conditions in intact cores (Figs. 2.10 and 3.1).

4.5.2 pH influence on nitrate reduction pathways

The pH of the sediment can determine the availability of reductants such as Fe^{2+} and S^{2-} for NO_3^- reduction pathways. For example, increasing the pH increases the number of negative sites on the sediment surface and results in enhanced cation (Fe^{2+}) adsorption (McLean and Bledsoe, 1992). Furthermore the speciation of sulfide (H_2S , HS^- or S^{2-}) is heavily dependent on pH (Snoeyink and Jenkins, 1980). Because

the Yarra River estuary is a salt wedge estuary, the bottom waters can be saline or fresh depending on freshwater inflow and a change in salinity can lead to a change in pH (Fig.4.6). DNRA was observed in the Yarra River estuary under oxic conditions (low salinity) and therefore the pH under these conditions would be 6.5 - 7.5 (Fig. 4.6). Under anoxic conditions (high salinity), pH would increase to 7.0 - 8.5 (Fig. 4.6). In laboratory experiments sediment cores were purged with air or argon (Ar) to achieve the desired oxygen concentration; purging with Ar alone rather than an Ar : CO₂ mix can increase the pH of the water column to above 8. Modelled data in Chapter Three (Fig 3.7) showed the water column pH did not significantly influence the pH in the sediment beyond the first few millimetres. However, to ensure a change in pH would not influence rates of denitrification, DNRA or the availability of reductants for these processes, the effect of pH on NO₃⁻ reduction pathways was examined in slurries. The results here show a change in pH from 7.47 to 8.37 (a pH similar to anoxic intact cores) did not significantly influence rates of denitrification or DNRA and did not change the denitrification: DNRA ratio (Fig. 4.2).

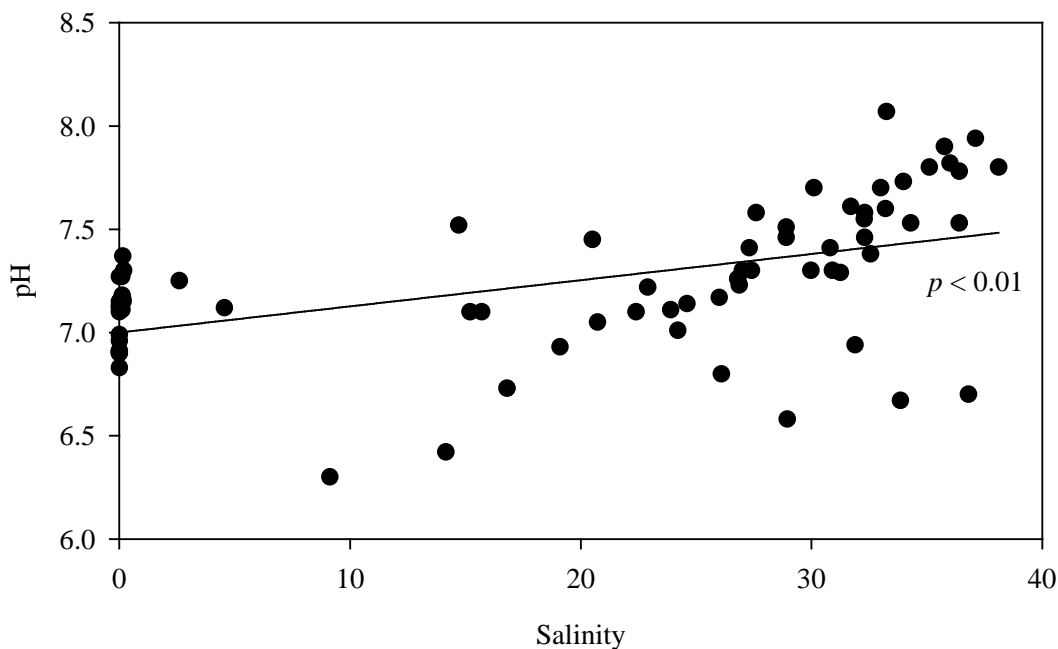


Figure 4.6 pH range in the bottom waters of the Yarra River estuary over the observational period from September 2009 to March 2011 (Chp. 2) with respect to salinity. The pH increases significantly with salinity ($pH = 0.01(\text{salinity}) + 7.00$, $R^2 = 0.25$, $p < 0.01$).

4.5.3 NO₃⁻ storage and Sulfur oxidising bacteria

Several studies have linked the competitive advantage of DNRA over denitrification to the presence of sulfide in the sediment (An and Gardner, 2002; Brunet and Garcia-Gil, 1996). Two mechanisms can explain the dominance of DNRA over denitrification under these conditions:

- (1) Denitrification is inhibited by high S²⁻ concentrations, and
- (2) Sulfur oxidising bacteria (*Thioploca* sp. and *Beggiatoa* sp.) can carry out DNRA as a secondary metabolic pathway (Otte *et al.*, 1999; Schulz and Jorgensen, 2001).

In the Yarra River estuary, white bacterial mats were observed on the sediment surface during the summer of 2009 - 2010 (hypoxic bottom waters, Chp. 2), however, rates of DNRA during these months were low (Chp. 2, Fig. 2.7). Several studies (Ahmad *et al.*, 1999; Hinck *et al.*, 2007; McHatton *et al.*, 1996) propose that sulfur oxidising bacteria such as *Beggiatoa* or *Thioploca* sp. have NO₃⁻ storage capabilities in cellular vacuoles. These motile bacteria are able to accumulate NO₃⁻, collected from the sediment surface or the water column, and move it into the anoxic zone where available reductants such as S²⁻ can then be used to convert the NO₃⁻ to NH₄⁺ (DNRA). In the Yarra River estuary, DNRA was observed under oxic conditions, perhaps suggesting that this translocation mechanism is important. In a study of Eckenförde Bay, Germany the presence of *Beggiatoa* sp. in the sediment moved the peak in ¹⁵N-NH₄⁺ production down to ~2.0 cm depth in comparison to ~0.5 cm in the absence of *Beggiatoa* sp. (Preisler *et al.*, 2007). Moreover, Fossing *et al.* (1995) observed *Thioploca* sp. were able to store NO₃⁻ to concentrations of up to 500 mmol L⁻¹ down to depths > 5 cm. In this study, no significant storage of NO₃⁻ was observed in sediment (Fig. 4.3). At all sites, DNRA occurred at the sediment surface with ~70 % of the ¹⁵N-NH₄⁺ produced diffusing into the water column (Fig 4.3). Based on these findings, DNRA under oxic conditions in the Yarra River estuary is unlikely to be linked to NO₃⁻ storing sulfur oxidising bacteria.

4.5.4 Fe²⁺ and S²⁻

Intact core profiles of denitrification and DNRA in the Yarra River estuary showed DNRA coincided with Fe²⁺ in the sediment (Fig 3.4). However, the addition of Fe²⁺ to 50 % (v:v) sediment slurries did not stimulate DNRA (Fig 4.4). Freshwater inflow into the Yarra River estuary contains high concentrations of particulate material and colloidal iron that coagulate and settle on convergence with seawater, resulting in high concentrations of iron within the sediment porewater (Hart and Davies, 1981). The concentration of Fe²⁺ in the porewater before slurry preparation was ~100 $\mu\text{mol-Fe}^{2+} \text{ L}^{-1}$. This Fe²⁺ concentration is an underestimate as it does not include easily extractable Fe²⁺ from the sediment surface, which can make up more than 90 % of Fe²⁺ in the Yarra River estuary⁶. It is therefore probable that stimulation of DNRA was not observed in 50 % (v:v) slurries because the addition of Fe²⁺ to the slurry did not increase the pool of Fe²⁺ to concentrations significantly greater than the control.

Concerning the intact sediment core profiles, DNRA did not occur at high rates in the presence of sulfide, however in the slurry incubations DNRA increased by ~40 % in the presence of high S²⁻ concentrations. From these slurries it is difficult to elucidate whether S²⁻ addition decreased competition between denitrification and DNRA due to the inhibition of denitrification or whether DNRA was stimulated by S²⁻ despite the high background concentration of Fe²⁺ (porewater and easily reducible sediment bound Fe²⁺). In these slurries it is unlikely the addition of S²⁻ in the presence of high Fe²⁺ concentrations remained available and not bound as FeS. To differentiate these possible mechanisms and to account for the high background concentration of Fe²⁺, slurries were diluted to 5 % (v:v) and long term incubation experiments were undertaken, as discussed in section 4.5.5.

4.5.5 DNRA linked to availability of Fe²⁺

The slurry experiments presented in this chapter support the observations shown in the intact sediment profiles presented in Chapter Three (Fig. 3.5) which

⁶ Estimated from both porewater and HCl-extractable Fe²⁺ from the long term Fe²⁺ slurry experiments.

indicated DNRA was coupled to Fe²⁺ in the sediment under oxic conditions in the water column.

In slurries, the accumulation and decomposition of NO₂⁻ after NO₃⁻ addition can lead to artefacts when interpreting trends in Fe²⁺ consumption. Under acidic conditions, NO₂⁻ decomposes to NO₂ and NO which are powerful oxidants and can readily re-oxidise Fe²⁺ to insoluble Fe³⁺ (Klueglein and Kappler, 2013; Weber *et al.*, 2001). This problem was avoided by centrifuging the sample when conditions were anoxic and the supernatant immediately fixed with ferrozine. The remaining sediment sample was then extracted with HCl. The concentrations of NO₂⁻ in the extractant over the first 48 hours were < 0.7 and 0.5 μmol L⁻¹ in the control and iron treatments, respectively, and over the total incubation NO₂⁻ did not exceed 5 μmol L⁻¹. Under anaerobic conditions, Klueglein and Kappler (2013) found 15 - 50 % of Fe²⁺ was oxidised by decomposition products of NO₂⁻ over the concentration range 0.5 - 4 mmol-NO₂⁻ L⁻¹; the concentration of NO₂⁻ in this study was < 1 % of these concentrations tested. Consequently, the decomposition of NO₂⁻ and subsequent oxidation of Fe²⁺ is unlikely to be an artefact in this study.

The addition of NO₃⁻ to estuarine slurries resulted in the immediate onset of DNRA which remained the dominant process for the first 48 hours of the incubation. In this period of DNRA activity, both dissolved Fe²⁺ and HCl-extractable Fe decreased, suggesting NH₄⁺ production is linked to Fe²⁺ oxidation. Upon cessation of NH₄⁺ production, Fe²⁺ concentrations changed little, or increased slightly in the control and Fe treatments, respectively (Fig. 4.5). The ratios of Fe²⁺ consumption to NH₄⁺ production in the slurries were 1 : 4 ± 2 and 1 : 10 ± 6 for the control and iron treatments, respectively. Although these ratios are not strictly consistent with the expected stoichiometry of 1 : 8 (Eq. 2), it is clear Fe²⁺ plays an important role in NH₄⁺ production.



No significant difference in the rates of DNRA was observed between the control and iron slurry treatments. As discussed previously, the most likely reason for this is the large pool of Fe²⁺ present in the slurries before Fe²⁺ addition. The addition of Fe²⁺ to the iron treatment only increased the pool of total filterable and HCl-extractable Fe²⁺ by ~ 35 %. In both treatments DNRA activity ceased after 48

hours and a shift in NO_3^- reduction was observed, with denitrification becoming the dominant process after day 3 (Fig. 4.5). The cause of this shift from DNRA to denitrification remains uncertain. However, it is most likely that the significant disruption of the sediment caused by slurring led to a rapid and unpredictable shift in the microbial community. It is possible the turnover of the microbial community initially present led to a release of labile organic carbon, which stimulated denitrification.

The NO_3^- -dependent oxidation of Fe^{2+} described in Weber *et al.* (2006) led to the formation of crystalline Fe^{3+} oxide phases, such as goethite. This is in contrast to a number of previous studies that have linked NO_3^- reduction and Fe^{2+} oxidation to the production of iron oxy-hydroxides (Benz *et al.*, 1998; Coby *et al.*, 2011; Straub *et al.*, 1996). For both the control and iron slurry treatments, only 2% of the Fe^{2+} was re-oxidised to iron oxy-hydroxides (Figs. 4.5 and 4.7), suggesting this is an unlikely product of Fe-driven DNRA. Crystalline Fe^{3+} is a more probable product of Fe-driven DNRA in the Yarra River estuary and requires further investigation to confirm this hypothesis.

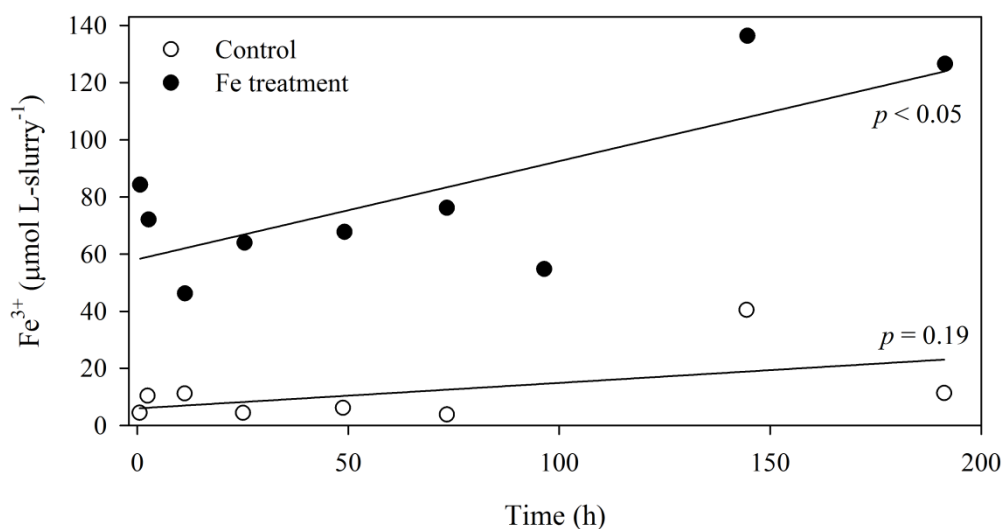


Figure 4.7 Formation of Fe^{3+} (Fe(III) oxy-hydroxides; $\mu\text{mol L-slurry}^{-1}$) with respect to time for the control and Fe treatments. No significant Fe^{3+} formation was observed in the control ($\text{Fe}^{3+} = 0.1(\text{time}) + 6.0$, $R^2 = 0.27$, $p = 0.19$) while significant formation of Fe^{3+} was observed in the Fe treatment ($\text{Fe}^{3+} = 0.3(\text{time}) + 58.2$, $R^2 = 0.56$, $p < 0.05$).

Iron is found in the cytochrome of a number of metallo-enzymes involved in NO_3^- reduction (Stolz and Basu, 2002; Tavares *et al.*, 2006). An alternate hypothesis to the role of Fe^{2+} as an electron donor in enzymatic Fe-driven DNRA is the use of Fe^{2+} in metallo-enzymes to catalyse the reaction with an alternate electron donor such as carbon. Klueglein and Kappler (2013) observed an increase in the number of BoFeN1 (NO_3^- reducer and Fe^{2+} oxidiser) cells in the presence of Fe^{2+} and proposed that the Fe^{2+} aided in increasing the number of enzymes used in NO_3^- reduction coupled to acetate oxidation. The immediate consumption of Fe^{2+} observed in this study is not consistent with the hypothesis proposed by Klueglein and Kappler (2013). In that study, a lag time was observed in Fe^{2+} oxidation coincident with an increase in bacterial cell mass and no significant change was observed in Fe^{2+} in the first day. In the present study, the addition of $^{15}\text{N-NO}_3^-$ resulted in the immediate oxidation of Fe^{2+} and production of $^{15}\text{N-NH}_4^+$ (Fig. 4.5G, H). Although the involvement of Fe^{2+} in metallo-enzymes cannot be ruled out in this study, this mechanism seems less plausible in the Yarra River estuary.

The results here support the findings of the intact sediment profiles that showed DNRA coincided with Fe^{2+} in the sediment. Fe-driven DNRA may be significant in the Yarra estuary, however the global importance of this process remains uncertain. It may be a significant process in non-sulfidic sediments including freshwater lakes, wetlands and estuarine systems which accumulate large amounts of iron through aggregation and sedimentation of colloidal material (Hart and Davies, 1981). In large rivers such as the Amazon and Mississippi, significant amounts of Fe may be deposited on the continental shelf, leading to high rates of Fe reduction and Fe^{2+} accumulation within the porewaters (Aller *et al.*, 1986; Powell and Wilson-Finelli, 2003; Sholkovitz, 1993). There appears to be circumstantial evidence in the literature to support this hypothesis. In Copano Bay, Texas, iron oxide concentrations were significantly correlated with $^{15}\text{N-NH}_4^+$ production (Hou *et al.*, 2012). Moreover, a recent study has shown that the highest accumulation of $^{15}\text{N-NH}_4^+$ after $^{15}\text{N-NO}_3^-$ addition was observed in sediments from the Mississippi delta, which had the highest concentrations of Fe^{2+} in the porewater (Behrendt *et al.*, 2013). It is therefore possible that Fe-driven DNRA may occur at globally significant rates within these diagenetic ‘hotspots’. Clearly, further research is required to systematically investigate this hypothesis.

4.6 Concluding Remarks

In summary, slurry experiments confirmed observations in intact core profiles (Fig. 3.4), linking DNRA to Fe^{2+} oxidation. The concentration of NO_3^- was not a primary regulatory factor on the denitrification : DNRA ratio in the Yarra River estuary. This ratio, and DNRA rates, were also largely unaffected by an increase in pH from 7.47 to 8.37. NO_3^- storing sulfur oxidising bacteria are unlikely to be an important mechanism for DNRA in the Yarra River estuary because there was no significant NO_3^- storage or $^{15}\text{N-NH}_4^+$ production with sediment depth. An initial comparison of denitrification and DNRA in 50 % (v:v) slurries indicated Fe^{2+} did not play a significant role in determining DNRA rates. This finding was attributed to the original high concentration of Fe^{2+} in the porewater, so that the addition of more Fe^{2+} to the treatments did not significantly increase the Fe^{2+} pool. Therefore, no discernible difference in DNRA rates was observed between the control and Fe treatments. Slurries were then diluted to 5 % (v:v) to decrease the background Fe^{2+} concentration. Results from these slurries supported the hypothesis of Fe-driven DNRA. The ratio of Fe^{2+} consumption to $^{15}\text{N-NH}_4^+$ production was $1 : 4 \pm 2$ and $1 : 10 \pm 6$ in the control and iron treatments, respectively. Iron availability appears to be the factor determining the relative contributions of denitrification and DNRA to total NO_3^- reduction in the Yarra River estuary. Finally, in environments with high Fe inputs such as major river deltas, DNRA maybe a more important process than previously considered.

4.7 References

- Ahmad A., Barry J.P., and Nelson D.C. (1999) Phylogenetic affinity of a wide, vacuolate, nitrate-accumulating *Beggiatoa* sp. from Monterey Canyon, California. *Applied and Environmental Microbiology* **65**, 270-277.
- Aller R.C., Mackin J.E., and Cox Jr R.T. (1986) Diagenesis of Fe and S in Amazon inner shelf muds: apparent dominance of Fe reduction and implications for the genesis of ironstones. *Sedimentary Processes on the Amazon Continental Shelf* **6**, 263-289.
- An S. and Gardner W.S. (2002) Dissimilatory nitrate reduction to ammonium (DNRA) as a nitrogen link, versus denitrification as a sink in a shallow estuary (Laguna Madre/ Baffin Bay, Texas). *Marine Ecology Progress Series* **237**, 41-50.
- APHA (2005) *APHA-AWWA-WPCF, Standard Methods for the Examination of Water and Wastewater*. American Public Health Association, American Water Works Association and Water Environment Federation, Washington.
- Behrendt A., De Beer D., and Stief P. (2013) Vertical activity distribution of dissimilatory nitrate reduction in coastal marine sediments. *Biogeosciences Discussions* **10**, 8065-8101.
- Benz M., Brune A., and Schink B. (1998) Anaerobic and aerobic oxidation of ferrous iron at neutral pH by chemoheterotrophic nitrate reducing bacteria. *Archives of Microbiology* **169**, 159-165.
- Bonin P. (1996) Anaerobic nitrate reduction to ammonium in two strains isolated from coastal marine sediment: A dissimilatory pathway. *FEMS Microbiology Ecology* **19**, 27-38.
- Brunet R.C. and Garcia-Gil L.J. (1996) Sulfide-induced dissimilatory nitrate reduction to ammonia in anaerobic freshwater sediments. *FEMS Microbiology Ecology* **21**, 131-138.
- Childs C.R., Rabalais N.N., Turner R.E., and Proctor L.M. (2002) Sediment denitrification in the Gulf of Mexico zone of hypoxia. *Marine Ecology Progress Series* **240**, 285-290.
- Coby A.J., Picardal F., Shelobolina E., Xu H., and Roden E.E. (2011) Repeated anaerobic microbial redox cycling of iron. *Applied and Environmental Microbiology* **77**, 6036-6042.

- Cole J.A. and Brown C.M. (1980) Nitrite reduction to ammonia by fermentative bacteria: a short circuit in the biological nitrogen cycle. *FEMS Microbiology Letters* **7**, 65-72.
- Conley D.J., Carstensen J., Aertebjerg G., Christensen P.B., Dalsgaard T., Hansen J.L.S., and Josefson A.B. (2007) Long-term changes and impacts of hypoxia in Danish coastal waters. *Ecological Applications* **17**, S165-S184.
- Diaz R.J. and Rosenberg R. (2008) Spreading dead zones and consequences for marine ecosystems. *Science* **321**, 926-929.
- Dong L.F., Sobery M.N., Smith C.J., Rusmana I., Phillips W., Stott A., Osborn A.M., and Nedwell D.B. (2011) Dissimilatory reduction of nitrate to ammonium, not denitrification dominates benthic nitrate reduction in tropical estuaries. *Limnology and Oceanography* **56**, 279-291.
- Fazzolari E., Nicolardot B., and Germon J.C. (1998) Simultaneous effects of increasing levels of glucose and oxygen partial pressures on denitrification and dissimilatory nitrate reduction to ammonium in repacked soil cores. *European Journal of Soil Biology* **34**, 47-52.
- Fossing H., Gallardo V.A., Jorgensen B.B., Huttel M., Nielsen L.P., Schulz H., Canfield D.E., Forster S., Glud R.N., Gundersen J.K., Kuver J., Ramsing N.B., Teske A., Thamdrup B., and Ulloa O. (1995) Concentration and transport of nitrate by the mat-forming sulphur bacterium *Thioploca*. *Letters to Nature* **374**, 713-715.
- Hart B.T. and Davies H.R. (1981) Trace metal speciation in the freshwater and estuarine regions of the Yarra River, Victoria. *Estuarine, Coastal and Shelf Science* **12**, 353-374.
- Hinck S., Neu T.R., Lavik G., Mussmann M., De Beer D., and Jonkers H.M. (2007) Physiological adaptation of a nitrate-storing *Beggiatoa* sp. to diel cycling in a phototrophic hypersaline mat. *Applied and Environmental Microbiology* **73**, 7013-7022.
- Hou L., Liu M., Carini S.A., and Gardner W.S. (2012) Transformation and fate of nitrate near the sediment-water interface of Copano Bay. *Continental Shelf Research* **35**, 86-94.
- Jorgensen K.S. (1989) Annual pattern of denitrification and nitrate ammonification in estuarine sediment. *Applied and Environmental Microbiology* **55**, 1841-1847.

- Jorgensen K.S. and Sorensen J. (1988) Two annual maxima of nitrate reduction and denitrification in estuarine sediment (Norsminde Fjord, Denmark). *Marine Ecology Progress Series* **48**, 147-154.
- Kemp W.M., Boynton W.R., Adolf J.E., Boesch D.F., Boicourt W.C., Brush G., Cornwell J.C., Fisher T.R., Glibert P.M., Hagy J.D., Harding L.W., Houde E.D., Kimmel D.G., Miller W.D., Newell R.I.E., Roman M.R., Smith E.M., and Stevenson J.C. (2005) Eutrophication of Chesapeake Bay: historical trends and ecological interactions. *Marine Ecology Progress Series* **303**, 1-29.
- King D. and Nedwell D.B. (1984) Changes in the nitrate-reducing community of an anaerobic saltmarsh sediment in response to seasonal selection by temperature. *Journal of General Microbiology* **130**, 2935-2941.
- King D. and Nedwell D.B. (1985) The influence of nitrate concentration upon the end-products of nitrate dissimilation by bacteria in anaerobic salt marsh sediment. *FEMS Microbiology Ecology* **31**, 23-28.
- Klueglein N. and Kappler A. (2013) Abiotic oxidation of Fe(II) by reactive nitrogen species in cultures of the nitrate-reducing Fe(II) oxidizer *Acidovorax* sp. BoFeN1 – questioning the existence of enzymatic Fe(II) oxidation. *Geobiology* **11**, 180-190.
- Lovley D.R. and Phillips E.J.P. (1986) Organic matter mineralization with reduction of ferric iron in anaerobic sediments. *Applied and Environmental Microbiology* **51**, 683-689.
- McHatton S.C., Barry J.P., Jannasch H.W., and Nelson D.C. (1996) High nitrate concentrations in vacuolate, autotrophic marine *Beggiatoa* spp. *Applied and Environmental Microbiology* **62**, 954-958.
- McLean J.E. and Bledsoe B.E. (1992) Ground Water Issues - Behaviour of metals in soils. United States Environmental Protection Agency, Office of Solid Waste and Emergency Response, Office of Research and Development.
- Michaelis L. and Menten M.L. (1913) Die kinetik der invertinwirkung. *Biochemische Zeitschrift* **49**, 333-369.
- Nealson K.H. and Saffarini D. (1994) Iron and Manganese in anaerobic respiration: environmental significance, physiology, and regulation. *Annual review of Microbiology* **48**, 311-343.
- Nizzoli D., Carraro E., Nigro V., and Viaroli P. (2010) Effect of organic enrichment and thermal regime on denitrification and dissimilatory nitrate reduction to ammonium (DNRA) in hypolimnetic sediments of two lowland lakes. *Water Research* **44**, 2715-2724.

- Ogilvie B.G., Rutter M., and Nedwell D.B. (1997) Selection by temperature of nitrate-reducing bacteria from estuarine sediments: species composition and competition for nitrate. *FEMS Microbiology Ecology* **23**, 11-22.
- Otte S., Kuenen J.G., Nielsen L.P., Paerl H.W., Zopfi J., Schulz H., Teske A., Strotmann B., Gallardo V.A., and Jorgensen B.B. (1999) Nitrogen, carbon, and sulfur metabolism in natural *Thioploca* samples. *Applied and Environmental Microbiology* **65**, 3148-3157.
- Powell R.T. and Wilson-Finelli A. (2003) Importance of organic Fe complexing ligands in the Mississippi River plume. *Estuarine, Coastal and Shelf Science* **58**, 757-763.
- Preisler A., de Beer D., Lichtschlag A., Lavik G., Boetius A., and Jorgensen B.B. (2007) Biological and chemical sulfide oxidation in a *Beggiatoa* inhabited marine sediment. *The ISME Journal* **1**, 341-353.
- Roberts K.L., Eate V.M., Eyre B.D., Holland D.P., and Cook P.L.M. (2012) Hypoxic events stimulate nitrogen recycling in a shallow salt-wedge estuary: The Yarra River estuary, Australia. *Limnology and Oceanography* **57**, 1427-1442.
- Rysgaard S. and Risgaard-Petersen N. (1997) A sensitive method for determining nitrogen-15 isotope in urea. *Marine Biology* **128**, 191-195.
- Sayama M., Risgaard-Petersen N., Nielsen L.P., Fossing H., and Christensen P.B. (2005) Impact of bacterial NO₃⁻ transport on sediment biogeochemistry. *Applied and Environmental Microbiology* **71**, 7575-7577.
- Schulz H.N. and Jorgensen B.B. (2001) Big Bacteria. *Annual review of Microbiology* **55**, 105-137.
- Sholkovitz E.R. (1993) The geochemistry of rare earth elements in the Amazon River estuary. *Geochimica et Cosmochimica Acta* **57**, 2181-2190.
- Sigman D.M., Altabct M.A., Michener R., McCorkle D.C., Fry B., and Holmes R.M. (1997) Natural abundance-level measurement of the nitrogen isotopic composition of oceanic nitrate: an adaptation of the ammonia diffusion method. *Marine Chemistry* **57**, 227-242.
- Snoeyink V.L. and Jenkins D. (1980) *Water Chemistry*. John Wiley & Sons, New York.
- Stolz J.F. and Basu P. (2002) Evolution of nitrate reductase: molecular and structural variations on a common function. *ChemBioChem* **3**, 198-206.

- Stookey L.L. (1970) Ferrozine - A new spectrophotometric reagent for iron. *Analytical Chemistry* **42**, 779-781.
- Straub K.L., Benz M., Shinck B., and Widdel F. (1996) Anaerobic, nitrate-dependent microbial oxidation by ferrous iron. *Applied and Environmental Microbiology* **62**, 1458-1460.
- Tavares P., Pereira A.S., Moura J.J.G., and Moura I. (2006) Metalloenzymes of the denitrification pathway. *Journal of Inorganic Biochemistry* **100**, 2087-2100.
- Tiedje J.M. (1988) Ecology of denitrification and dissimilatory nitrate reduction to ammonium, in: Zehnder, A.J.B. (Ed.), *Biology of Anaerobic Microorganisms*. Wiley, New York, pp. 179-244.
- Tison D.L., Pope D.H., and Boylen C.W. (1980) Influence of seasonal temperature on the temperature optima of bacteria in sediments of Lake George, New York. *Applied and Environmental Microbiology* **39**, 675-677.
- Voillier E., Inglett P.W., Hunter K., Roychoudhury A.N., and Van Cappellen P. (2000) The ferrozine method revisited: Fe(II)/Fe(III) determination in natural waters. *Applied Geochemistry* **15**, 785-790.
- Weber K.A., Picardal F.W., and Roden E.E. (2001) Microbially catalyzed nitrate-dependent oxidation of biogenic solid-phase Fe(II) compounds. *Environmental Science and Technology* **35**, 1644-1650.
- Weber K.A., Urrutia M.M., Churchill P.F., Kukkadapu R.V., and Roden E.E. (2006) Anaerobic redox cycling of iron by freshwater sediment microorganisms. *Environmental Microbiology* **8**, 100-113.
- Yin S.X., Chen D., Chen L.M., and Edis R. (2002) Dissimilatory nitrate reduction to ammonium and responsible microorganisms in two Chinese and Australian paddy soils. *Soil Biology and Biogeochemistry* **34**, 1131-1137.

5. Discussion and Concluding Remarks



A conceptual model (Fig. 5.1) draws together the key findings of this study and will be referred to throughout this concluding chapter. In this study, the nitrogen cycle was examined in detail in the Yarra River estuary. Three specific research questions were proposed in the introduction:

- (1) Does bottom water hypoxia within the Yarra River estuary promote the recycling or removal of nitrogen?
- (2) What are the main mechanisms of nitrogen removal or recycling during hypoxic conditions?
- (3) Does oxygen concentration influence the relative contribution of NO_3^- reduction pathways within the estuary, and if so, what is the controlling mechanism behind this shift?

Two approaches were taken to address these research questions:

- a) *Observational approach:* NO_3^- reduction pathways, nutrient fluxes and *in situ* nutrient concentrations were determined in the salt wedge region of the estuary prone to bottom water hypoxia from September 2009 to March 2011 (Chp. 2).
- b) *Experimental approach:* Intact core and slurry experiments were used to determine the controls (O_2 , pH, NO_3^- , S^{2-} and Fe^{2+}) on the relative contribution of denitrification and DNRA to total NO_3^- reduction (Chp. 3 and 4).

5.1 Chapter summaries

5.1.1 **Chapter Two:** *Hypoxic events stimulate nitrogen recycling in a shallow salt-wedge estuary: The Yarra River estuary, Australia*

Chapter Two used both water column profiles of oxygen and salinity in addition to logged data to examine the cause and duration of hypoxia within the Yarra River estuary. The estuary exhibits a typical salt wedge structure and low freshwater inflow was the controlling factor on bottom water hypoxia, inducing salinity stratification and isolation of the bottom waters.

The production or consumption of *in situ* nutrients under changing oxygen conditions was determined using the deviation from conservative mixing; during hypoxia the estuary was a source of dissolved organic nitrogen (DON) and NH_4^+ . Several studies have hypothesised less efficient and rapid mineralisation rates can result in an increase in DON under hypoxic conditions and this is the likely cause of elevated DON in the Yarra River estuary (Burdige 2001; Burdige and Zheng 1998, Hansen and Blackburn 1991). To remove the influence of residence time and remineralisation rate on NH_4^+ concentration, DIC : NH_4^+ ratios were used – an approach justified in Chapter Two. The DIC : NH_4^+ ratios for both *in situ* water column concentrations using deviations from conservative mixing and sediment fluxes confirmed there was a net efflux of NH_4^+ from the sediment under hypoxic conditions (Fig. 2.8). Under hypoxic conditions, ~40 % of NH_4^+ produced was sourced from the sediment. As conditions approached anoxia ($\text{O}_2 < 10 \mu\text{mol L}^{-1}$), ~60 and 100 % of NH_4^+ from the *in situ* concentrations and sediment flux measurements, respectively, was sourced from the sediment. In the presence of oxygen, nitrification removed NH_4^+ through coupled nitrification-denitrification. However, under hypoxic conditions, the cessation of nitrification disconnected the link between nitrogen removal (nitrification-denitrification coupling) and mineralisation leading to an efflux of NH_4^+ from the sediment.

The ^{15}N isotope pairing technique was used to determine the impact of bottom water hypoxia on two NO_3^- reduction pathways, denitrification and DNRA, that remove or recycle nitrogen, respectively. Denitrification was the dominant NO_3^- reduction pathway under hypoxic conditions. Surprisingly, DNRA increased in the

presence of oxygen. Under hypoxic conditions, DNRA was $< 1\%$ of total NO_3^- reduction but increased up to $39 \pm 11\%$ in the presence of oxygen in the water column (Fig. 2.10). In this chapter, I hypothesised oxygen and NO_3^- were the most likely controlling variables on DNRA rates.

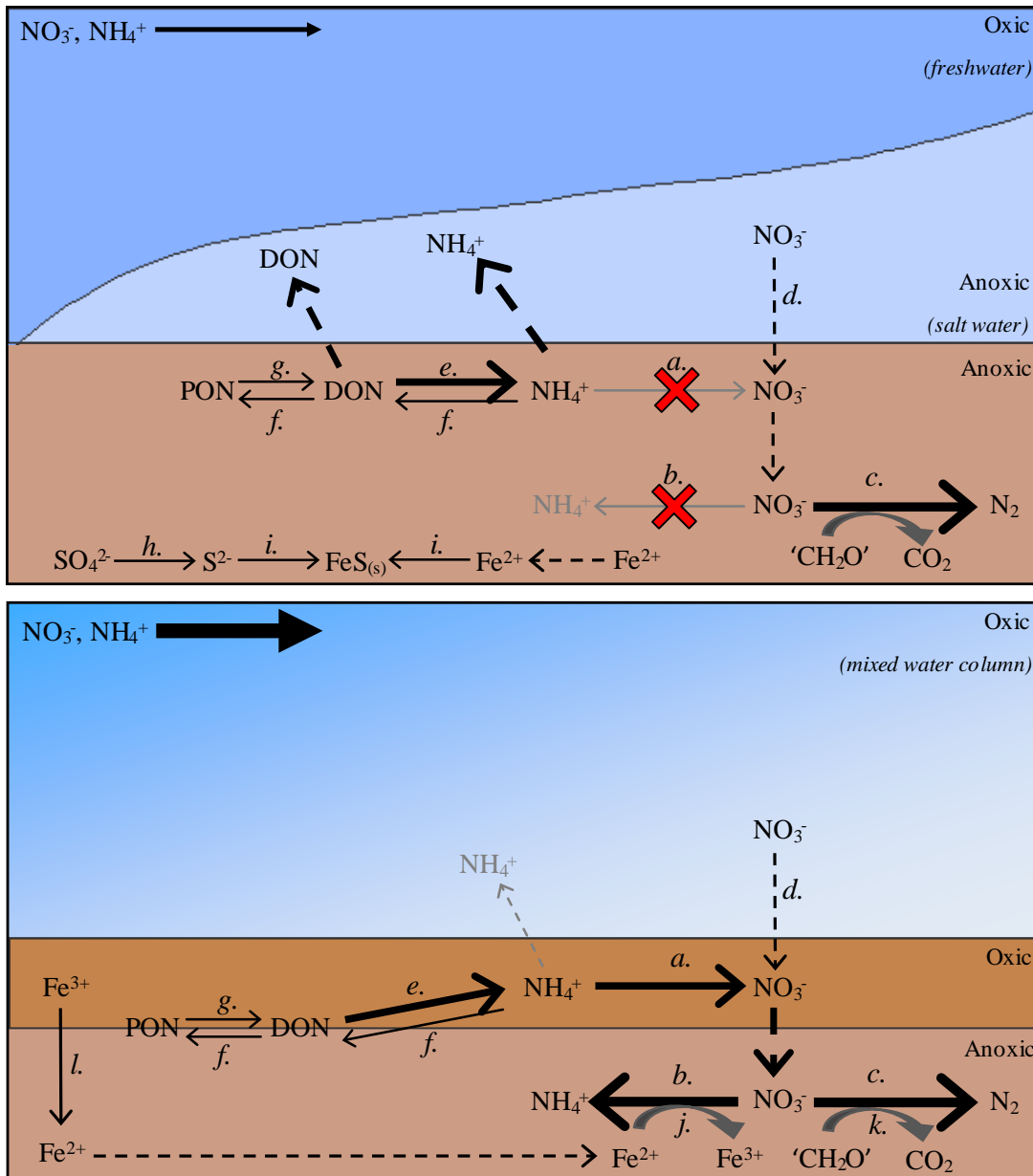


Figure 5.1 Conceptual model of the nitrogen cycle in the Yarra River estuary under stratified hypoxic conditions and well mixed oxic conditions. a) nitrification, b) DNRA, c) denitrification, d) diffusion, e) mineralisation, f) assimilation, g) decomposition, h) sulfate reduction, i) precipitation of $\text{FeS}_{(s)}$, j) Fe^{2+} oxidation, k) carbon oxidation and l) Fe^{3+} reduction.

5.1.2 Chapter Three: *Denitrification and DNRA in sediment profiles combining the isotope pairing technique and diffusive equilibrium in thin layer gels*

Chapter Three investigated the behaviour of denitrification and DNRA under varied oxygen conditions in intact sediment cores to determine whether the observations in Chapter Two, regarding increased DNRA in the presence of oxygen, could be replicated experimentally. Manipulation of oxygen conditions in sediment cores supported the findings in Chapter Two; under hypoxic conditions, denitrification was the dominant NO_3^- reduction process. After oxygen was introduced into the water column, DNRA increased from $< 1\%$ under hypoxic conditions to $\sim 18\%$ of total NO_3^- reduction in the presence of oxygen.

To investigate these findings in more detail, depth profiles of denitrification (N_2O or $^{15}\text{N-N}_2$) and DNRA ($^{15}\text{N-NH}_4^+$) in the sediment were examined using diffusive equilibrium in thin layer (DET) gels alongside the measurement of O_2 , NO_3^- , total NH_4^+ , Fe^{2+} , S^{2-} and pH using either DET gels or microelectrodes under varied oxygen conditions.

Profiles of denitrification under hypoxic and oxic conditions confirmed both the observational data and oxygen experiments in intact cores. In the profiles, the denitrification : DNRA ratio was high under hypoxic conditions and decreased in the presence of oxygen in the water column owing to an increase in DNRA (Fig 3.3, 3.4). In the September profiles, DNRA only occurred under sub-oxic ($< 20\%$ O_2 saturation) conditions and oxic conditions. When oxygen was introduced into the water column, the S^{2-} in the sediment decreased. The occurrence of DNRA under oxic or sub-oxic conditions was not explained by the presence or absence of S^{2-} . As such, I hypothesised that the presence of Fe^{2+} under these conditions is the controlling mechanism on DNRA.

Profiles measured in January-February 2013 confirmed the hypothesis of Fe^{2+} oxidation coupled to DNRA (Chp. 4). Under aerobic conditions in the water column Fe^{3+} oxides form in aerobic surficial sediments and at the oxic-anoxic boundary layer of the sediment Fe^{3+} is reduced to free Fe^{2+} . In the Yarra River estuary under oxic conditions in the water column, a peak in Fe^{2+} concentration was observed in the anaerobic layer of sediment and was in good agreement with the DNRA profile (Fig. 3.4). The increase in $^{15}\text{N-NH}_4^+$ production in the presence of

Fe^{2+} can explain the decrease in the denitrification : DNRA ratio observed in both the profile experiments and the observational data under oxic conditions in the water column (Fig 5.1). In the absence of oxygen in the water column, the development of free sulfide in the sediment, a by-product of sulfate reduction, can bind to Fe^{2+} , precipitating FeS , thereby removing Fe^{2+} (Fig. 3.7) and reducing DNRA rates.

In this chapter, two denitrification profile methods were used: the acetylene block method (N_2O) measured via a N_2O microelectrode and the isotope pairing technique ($^{15}\text{N}\text{-N}_2$) measured, after calibration, in DET gels (Fig. 3.6). The $^{15}\text{N}\text{-N}_2$ method was more representative of total denitrification. The benefits of the $^{15}\text{N}\text{-N}_2$ method included: (1) simultaneous measurement of NO_3^- reduction in the same core and (2) the inclusion of both nitrification and water column- NO_3^- driven denitrification. Under anoxic conditions, the N_2O method was representative of total denitrification; however, the main drawbacks of this method were: (1) the profile is measured in a separate core to DNRA, and (2) it only measures water column- NO_3^- driven denitrification due to the inhibition of nitrification by acetylene and therefore leads to an underestimation of denitrification in the presence of oxygen.

5.1.3 Chapter Four: *Increased rates of dissimilatory nitrate reduction to ammonium (DNRA) under aerobic conditions in a periodically hypoxic estuary are linked to the availability of iron*

Chapter Four investigated the factors potentially controlling denitrification, and in particular DNRA. From the literature, several key factors are thought to control the balance between NO_3^- reduction via denitrification or via DNRA: NO_3^- availability, temperature, organic carbon loading, pH and available reductants such as S^{2-} or Fe^{2+} . From the observational data in this thesis, carbon and temperature were excluded as possible predictors of DNRA. The hypothesis in Chapter Three of Fe-driven DNRA was examined in more detail in slurry experiments in this chapter. In addition, other potential predictor variables of DNRA such as NO_3^- , S^{2-} and pH were examined in slurries.

To test the hypotheses proposed in Chapter Two, slurry experiments were used to examine the effect of NO_3^- (concentration series 10 - 240 $\mu\text{mol L}^{-1}$ NO_3^-) on DNRA. NO_3^- slurries indicated both denitrification and DNRA exhibited similar

kinetics both conforming to the Michaelis-Menten equation. The denitrification : DNRA ratio remained unchanged over the range of investigated NO_3^- concentrations, indicating NO_3^- concentration did not give DNRA a competitive advantage (Fig. 4.1).

Solution pH can influence the availability of reductants such as S^{2-} or Fe^{2+} . Within the estuarine bottom waters, the pH ranged from 6.50 - 8.30 (Fig. 4.6). To examine if pH had an impact on DNRA rates, the pH was increased from 7.47 to 8.37 in slurries. No significant difference was observed in the denitrification : DNRA ratio. I hypothesised that the fluctuation in pH observed in the water column is buffered by the sediment and the pH will be stable with sediment depth. This hypothesis was supported by modelling data, where an increase of 1 pH unit in the water column was only reflected in the first few millimetres of sediment and did not change significantly with depth (Fig. 3.7). As a result, pH changes within the natural range experienced in the Yarra River estuary will not significantly change rates of DNRA or denitrification. This finding was supported by the slurry experiments.

Available reductants such as S^{2-} or Fe^{2+} can play an important role in determining the contribution of denitrification or DNRA to total NO_3^- reduction. The preparation of 50 % (v:v) sediment slurries did not yield useful results. The addition of S^{2-} or Fe^{2+} at low or high concentrations showed little change from the control treatment or within treatments. The porewaters of the Yarra River estuary contain a high concentration of easily extractable Fe^{2+} . As such, the addition of more Fe^{2+} was negligible compared to the pool of existing Fe^{2+} in the sediment, making it difficult to determine whether the addition of Fe^{2+} had an impact on DNRA when compared to the control.

To overcome this shortcoming, and enable detection of any discernible change between the control and Fe^{2+} treatments, the slurries were diluted to 5 % (v:v) estuarine sediment and the addition of Fe^{2+} repeated over a longer term incubation. The control (NO_3^- only) and Fe^{2+} treatments still contained a large amount of HCl-extractable Fe^{2+} ; however, the control treatment contained $< 50 \mu\text{mol L}^{-1}$ of Fe^{2+} in the water column. The long term Fe^{2+} experiments support the Fe-driven DNRA hypothesis proposed in Chapter Three. In both treatments, the production of $^{15}\text{N-NH}_4^+$ over the first 48 hours coincided with a decrease in Fe^{2+} . After the cessation of $^{15}\text{N-NH}_4^+$ production, Fe^{2+} concentrations plateaued or increased in the control and Fe treatments, respectively.

5.2 Nitrogen cycling in the Yarra River estuary during hypoxia.

The collection of observational data spanned two summers, the first in 2009 - 2010 - a dry summer⁷ exhibiting frequent hypoxia in the bottom waters, and 2010 - 2011 - a wet summer which received regular flushing and re-oxygenation of the bottom waters (Fig 2.3, 2.4, 5.2). As a result, this study provides a unique insight into the behaviour of nitrogen under different flow regimes driven by climate variability opposed to seasonality.

Nitrogen loads into the Yarra River estuary are strongly driven by rainfall and resulting freshwater inflow (Fig 5.2). Over the study period, NO_3^- was 87 ± 2 % and NH_4^+ only 11 ± 2 % of dissolved inorganic nitrogen (NO_3^- and NH_4^+ - DIN) entering the estuary from the catchment; hence understanding the removal of NO_3^- before its released into coastal waters is essential (Fig 5.2). Under hypoxic conditions (summer of 2009 - 2010), there was a net efflux of NH_4^+ from the sediment, driven by the cessation of nitrification and breakdown of nitrification-denitrification coupling (Fig 5.1 and Chp. 2). Under these conditions, the high residence time of the bottom waters within the estuary allow NH_4^+ to accumulate. In the event of high rainfall and resulting freshwater inflow, the bottom waters of the estuary will be transported into Port Phillip Bay along with this accumulated NH_4^+ . As hypoxic conditions generally occur in summer when temperatures are high and conditions are optimal for algal growth, the release of NH_4^+ after a high rainfall event, along with high NO_3^- concentrations from the freshwater inflow, could potentially cause an increase in primary productivity and result in algal growth (Fig 5.2). Although the removal of nitrogen via denitrification occurs under hypoxic conditions, it does not equate to the amount of NH_4^+ released from the sediment (Chp. 2).

Although several studies have examined the nitrogen cycle in detail and observed the co-occurrence of denitrification and DNRA (An and Gardner, 2002; Bonin, 1996; Nizzoli *et al.*, 2010), to my knowledge, this study is the first to examine the relative importance of denitrification and DNRA during hypoxic events in a shallow salt wedge estuary and to identify a mechanism that controls the relative contribution of these two processes under changing oxygen conditions.

⁷ Summer months – December, January and February.

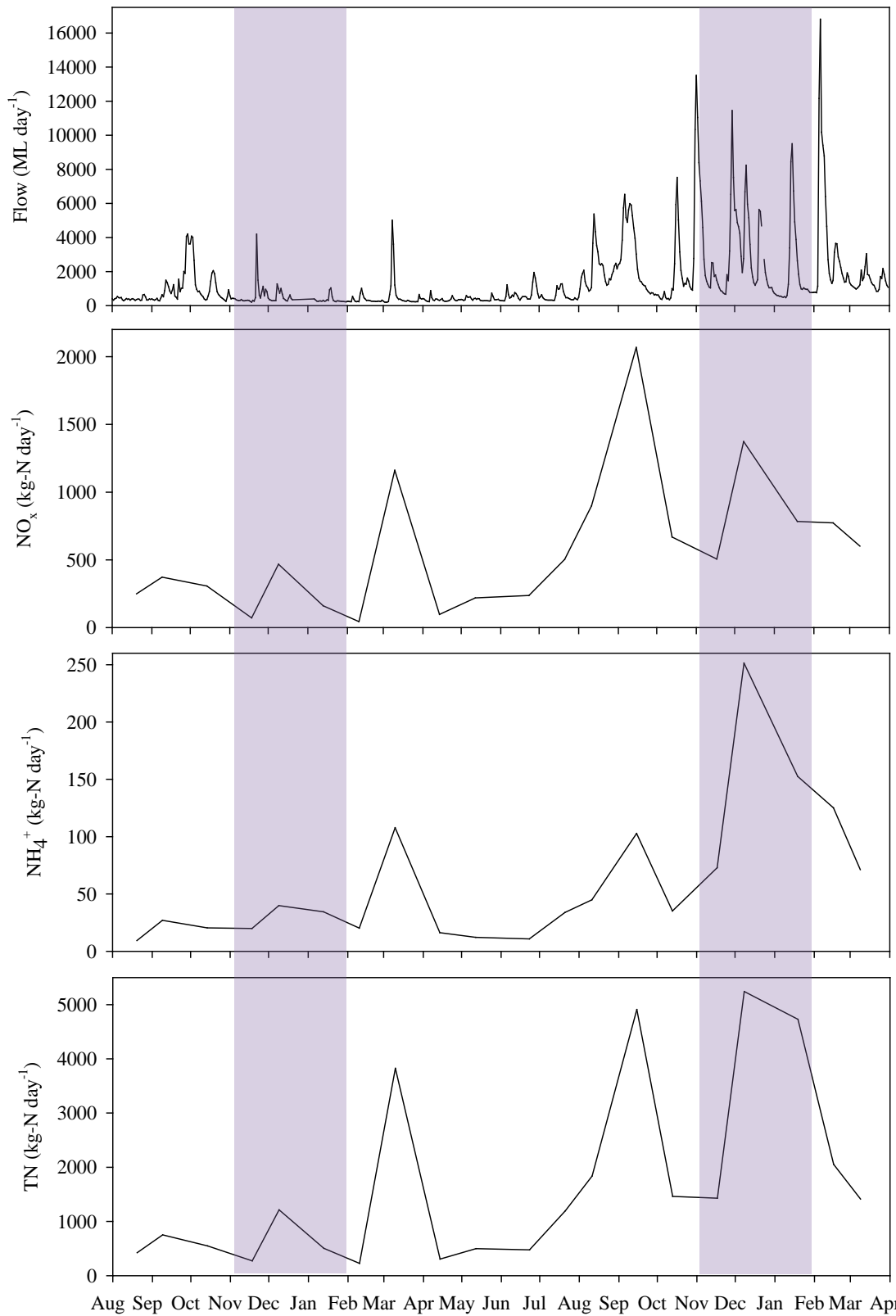


Figure 5.2 Freshwater inflow and nutrient loads entering the estuary; NO_x (NO₃⁻ + NO₂⁻), NH₄⁺ and Total nitrogen (TN; kg-N day⁻¹)⁸. Shading represents summer.

⁸ See appendix for load data and calculation. *Data from Melbourne Water Corporation.*

In the Yarra River estuary, denitrification was the dominant NO_3^- reduction pathway during a hypoxic event. Under these conditions, NO_3^- is effectively removed from the system as N_2 gas. High freshwater inflow replenishes the bottom waters with oxygen and nutrients. Interestingly, under these conditions DNRA increased to rates comparable to denitrification. Although contrary to the current paradigm, increased DNRA rates can be explained by the presence of Fe^{2+} in sediment. The reasoning for the exclusion of alternate hypotheses is summarised in Table 5.1. The coupling of Fe^{2+} oxidation and NO_3^- reduction to NH_4^+ has been described in Weber *et al.* (2006), however, to my knowledge this is the first study to observe this process in intact estuarine sediments. In the Yarra River estuary, the nitrogen cycle is strongly coupled to both the sulfur and iron cycles (Fig. 5.3). Both slurry and intact core experiments confirm the link between Fe^{2+} oxidation and DNRA rates during oxic conditions. As discussed, the absence of DNRA during hypoxia is likely due to the binding of Fe^{2+} in FeS precipitates (Fig 5.3).

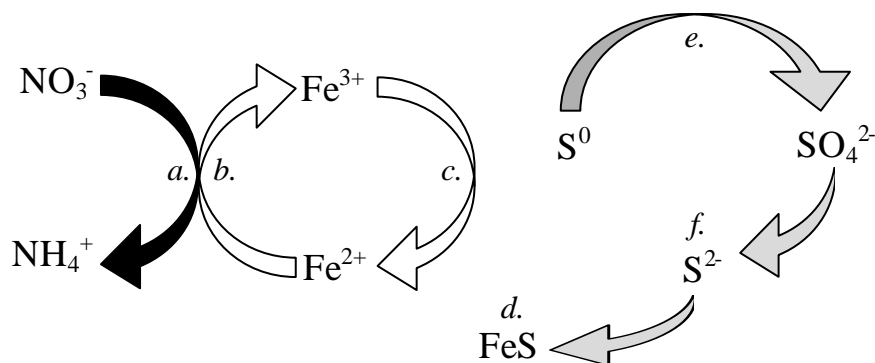


Figure 5.3 Simplified pathways in the iron and sulfur cycles linked to DNRA. a) DNRA, b) Fe^{2+} oxidation, c) Fe^{3+} reduction, d) FeS precipitation, e) sulfur oxidation, f) sulfate reduction.

Freshwater inputs into estuarine systems carry a significant amount of iron both filterable and bound to suspended material, upon reaching saline waters much of the iron is removed through aggregation and sedimentation of colloidal material (Hart and Davies, 1981). In large rivers such as the Amazon and Mississippi, significant amounts of iron may be deposited on the continental shelf, leading to high rates of iron reduction and Fe^{2+} accumulation within the porewaters (Aller *et al.*,

1986; Powell and Wilson-Finelli, 2003; Sholkovitz, 1993). It is therefore possible that Fe-driven DNRA observed in the Yarra River estuary may occur at globally significant rates within these diagenetic hotspots.

DIN makes up 30 - 40 % of total nitrogen input into the Yarra River estuary (Fig. 5.2). Although some total nitrogen will be removed through aggregation and sedimentation of particulate material, much of the bioavailable nitrogen remains in the water column. On the sampling dates⁹ denitrification only removed 1.6 ± 0.6 % of the daily water column NO_3^- load, assuming the majority of the NO_3^- in the estuary was derived from freshwater inputs. Over the sampling period, NO_3^- reduction led to a net removal of total DIN input into the estuary; however the amount removed was only 3.6 ± 0.6 %. These estimates do not include DIN produced within the estuary from mineralisation and therefore the estuary's capacity for nitrogen removal is almost certainly more limited. As discussed in Chapter Two, the high turbidity of the water column and shallow euphotic depth suggest immobilisation of nitrogen through assimilation will also be limited.

The estimates of nitrogen removal in this study are low (3.6 ± 0.6 %) compared to values presented (20 - 50 %) for other estuarine systems (Dong *et al.*, 2000; Ogilvie *et al.*, 1997; Seitzinger, 1988; Soetaert and Herman, 1995). The capacity of an estuary to remove DIN is based not only on oxygen concentration but is also related to the residence time of the water within an estuary (Dettmann, 2001). In the Yarra River estuary, the residence time of the freshwater and saline bottom waters can differ greatly. For example, surface freshwater inflow can have a residence time of less than 1 day under high flow ($> 5000 \text{ ML day}^{-1}$) conditions. However, saline bottom waters can take up to 2 weeks to be renewed under medium flow ($\sim 2000 - 3000 \text{ ML day}^{-1}$) conditions (Beckett *et al.*, 1982). Considering the majority of the nitrogen input into the system is from freshwater inflow, the short residence time of this water decreases the estuary's nitrogen removal capacity (Dettmann, 2001). As such the management of nitrogen loads in the Yarra River estuary relies on reducing catchment derived nitrogen inputs rather than internal nitrogen cycling.

⁹ Sampling dates – 8th September and 8th December 2009; 27th January, 16th February, 13th April, 11th May, 15th June and 15th December 2010; 18th January and 15th March 2011.

Table 5.1 Summary of common hypotheses described in the literature that explain the behaviour of DNRA. The reasoning is provided for the exclusion (×) or supported (✓) hypothesis with respect to the behaviour of DNRA in the Yarra River estuary and (?) represents a plausible or indirect predictor of DNRA.

Predictor		Reasoning	Ref
O_2	?	DNRA predominated under oxic conditions; however, the process occurred in the anoxic sediment as shown in both slurry and intact cores experiments. O_2 is an indirect predictor of DNRA as it controls the availability of reductants.	Chp 2, 3, 4
Organic Carbon	×	The comparison of DNRA rates with the product of respiration, CO_2 (DIC), indicates whether carbon oxidation is coupled to DNRA. No significant relationship was observed between DIC and DNRA, suggesting $^{15}N-NH_4^+$ production was not linked to carbon.	Chp 2
Temperature	×	No relationship was observed between DNRA and temperature. DNRA occurred over a wide range of temperatures (14 - 22°C).	Chp 2, 4
Microbial Type	×	The ^{15}N -DNRA potential was not correlated with oxygen concentration. This suggests that irrespective of O_2 concentration, the potential for DNRA to occur remained unchanged, hence it can be inferred that the microbial population also remained unchanged.	Chp 2
Salinity	×	The increase in sulfate reduction under saline conditions has been used to explain increased rates of DNRA. However, in this study salinity was not an independent variable, but rather was linked to bottom water hypoxia.	Chp 2
NO_3^-	×	Slurry experiments revealed the kinetics of both denitrification and DNRA were similar and the denitrification : DNRA ratio did not significantly change with NO_3^- concentration.	Chp 4
pH	×	pH did not have a significant influence on DNRA rates as shown in the slurry experiments.	Chp 4
S^{2-}	?	Sulfur oxidising bacteria have been previously linked to DNRA. This study hypothesised the main form of DNRA is chemoautotrophic (driven by Fe^{2+}); however, the possible role of S^{2-} cannot be excluded. Slurry experiments demonstrated DNRA occurred in presence of S^{2-} at rates similar to the Fe^{2+} treatment. Fe^{2+} is high in the porewaters of the Yarra River estuary and could not be completely excluded to allow specific testing of S^{2-} .	Chp 3, 4
Fe^{2+}	✓	The presence of Fe^{2+} in both long term slurry experiments and profile experiments showed that DNRA potential increased in the presence of Fe^{2+} . In the oxic profile experiment, the presence of Fe^{2+} correlated well with DNRA in the sediment. The depletion of oxygen resulted in an increase in S^{2-} and disappearance of free Fe^{2+} . It is hypothesized that the absence of DNRA under hypoxic conditions is related to the precipitation of Fe^{2+} as FeS.	Chp 3, 4

5.3 Recommendations for Future Research

Although this study was limited by the usual project time constraints, the current dataset supports the hypothesis of Fe-driven DNRA. Several approaches could be taken to further improve our understanding of this process in the Yarra River estuary, for example: (1) measure the product of Fe^{2+} oxidation, (2) inoculated slurry controls and (3) bacterial studies.

- (1) The by-product of Fe^{2+} oxidation is Fe^{3+} , however, in the present study no significant formation of Fe^{3+} oxy-hydroxides was observed. Weber *et al.* (2006) proposed that goethite was the main by-product of Fe-driven DNRA. To investigate if the formation of goethite occurs in the Yarra River estuary, a $^{15}\text{N}\text{-NO}_3^-$ time series experiment should be performed and along with the production of $^{15}\text{N}\text{-NH}_4^+$ and consumption of Fe^{2+} , the formation of goethite should be examined. Two approaches that could be used to determine the formation of goethite are the dithionite or Ti(III)-citrate-EDTA- HCO_3^- extraction method or X-ray diffraction (Ryan and Gschwend, 1991; Weber *et al.*, 2006).
- (2) A control was used in all slurry experiments. In this study, the control was prepared in the same way as the treated slurries and only NO_3^- was added. In these controls the existing bacterial community could carry out DNRA or denitrification. Although these controls are useful to determine whether a process is stimulated by the addition of an electron donor, they provide little information about underlying abiotic processes. A number of studies have hypothesised that abiotic Fe^{2+} oxidation is linked to NH_4^+ production (Hansen *et al.*, 2001; Hansen *et al.*, 1996). Despite this mechanism being considered unlikely in the Yarra River estuary, as discussed in Chapter Four, to rule out this process, slurry experiments should be repeated with inoculated controls to remove bacteria.
- (3) There are a number of known iron oxidising bacteria that can couple to NO_3^- reduction to Fe^{2+} oxidation. For example, Weber *et al.* (2006) identified the bacteria involved in Fe-driven DNRA as *Geobacter* sp. To understand further the role of both Fe- and S- oxidising bacteria in the

Yarra River estuary, sediment samples should be collected and bacteria identified. Two techniques should be employed in the Yarra River estuary;

- (i) culture-dependent (extraction of DNA from pure culture for PCR and 16S rRNA gene sequence analysis) and
- (ii) culture-independent (extraction of DNA from sediment for fluorescence *in situ* hybridisation (FISH) analysis).

As discussed in Haaijer *et al.* (2012), it is important to employ both techniques when examining Fe- and S- oxidising bacteria to ensure method selection does not exclude important species of bacteria.

Finally, this thesis highlights the role of Fe²⁺ in determining rates of DNRA in the Yarra River estuary, under conditions that have previously not been considered conducive toward this process. The importance of Fe-driven DNRA in systems with similar characteristics (iron-rich freshwater inflow and sediments) to the Yarra River estuary, for example the Mississippi and Amazon deltas, remains uncertain and should be investigated. Detailed surveys of other iron-rich estuarine systems are essential to determine the significance of Fe-driven DNRA to the global nitrogen cycle.

5.4 References

- Aller R.C., Mackin J.E., and Cox Jr R.T. (1986) Diagenesis of Fe and S in Amazon inner shelf muds: apparent dominance of Fe reduction and implications for the genesis of ironstones. *Sedimentary Processes on the Amazon Continental Shelf* **6**, 263-289.
- An S. and Gardner W.S. (2002) Dissimilatory nitrate reduction to ammonium (DNRA) as a nitrogen link, versus denitrification as a sink in a shallow estuary (Laguna Madre/ Baffin Bay, Texas). *Marine Ecology Progress Series* **237**, 41-50.
- Beckett R., Easton A.K., Hart B.T., and McKelvie I.D. (1982) Water movement and salinity in the Yarra and Maribyrnong Estuaries. *Australian Journal of Marine and Freshwater Research* **33**, 401-415.
- Bonin P. (1996) Anaerobic nitrate reduction to ammonium in two strains isolated from coastal marine sediment: A dissimilatory pathway. *FEMS Microbiology Ecology* **19**, 27-38.
- Dettmann E.H. (2001) Effect of water residence time on annual export and denitrification of nitrogen in estuaries: A model analysis. *Estuaries* **24**, 481-490.
- Dong L.F., Thornton D.C.O., Nedwell D.B., and Underwood G.J.C. (2000) Denitrification in sediments of the River Colne estuary, England. *Marine Ecology Progress Series* **203**, 109-122.
- Haaijer S.C.M., Crienen G., Jetten M.S.M., and Op den Camp H.J.M. (2012) Anoxic iron cycling bacteria from an iron sulfide- and nitrate-rich freshwater environment. *Frontiers in Microbiology* **3**, 26.
- Hansen H.C.B., Guldberg S., Erbs M., and Koch C.B. (2001) Kinetics of nitrate reduction by green rusts - effects of interlayer anion and Fe(II):Fe(III) ratio. *Applied Clay Science* **18**, 81-91.
- Hansen H.C.B., Koch C.B., Nancke-Krogh H., Borggaard O.K., and Sorensen J. (1996) Abiotic nitrate reduction to ammonium: key role of green rust. *Environmental Science and Technology* **30**, 2053-2056.
- Hart B.T. and Davies H.R. (1981) Trace metal speciation in the freshwater and estuarine regions of the Yarra River, Victoria. *Estuarine, Coastal and Shelf Science* **12**, 353-374.
- Nizzoli D., Carraro E., Nigro V., and Viaroli P. (2010) Effect of organic enrichment and thermal regime on denitrification and dissimilatory nitrate reduction to

- ammonium (DNRA) in hypolimnetic sediments of two lowland lakes. *Water Research* **44**, 2715-2724.
- Ogilvie B., Nedwell D.B., Harrison R.M., Robinson A., and Sage A. (1997) High nitrate, muddy estuaries as nitrogen sinks: the nitrogen budget of the River Colne estuary (United Kingdom). *Marine Ecology Progress Series* **150**, 217-228.
- Powell R.T. and Wilson-Finelli A. (2003) Importance of organic Fe complexing ligands in the Mississippi River plume. *Estuarine, Coastal and Shelf Science* **58**, 757-763.
- Ryan J.N. and Gschwend P.M. (1991) Extraction of iron oxides from sediments using reductive dissolution by titanium(III). *Clays and Clay Minerals* **39**, 509-518.
- Seitzinger S.P. (1988) Denitrification in freshwater and coastal marine ecosystems: ecological and geochemical significance. *Limnology and Oceanography* **33**, 702-724.
- Sholkovitz E.R. (1993) The geochemistry of rare earth elements in the Amazon River estuary. *Geochimica et Cosmochimica Acta* **57**, 2181-2190.
- Soetaert K. and Herman P.M.J. (1995) Nitrogen dynamics in the Westerschelde estuary (SW Netherlands) estimated by means of the ecosystem model MOSES. *Hydrobiologia* **311**, 225-246.
- Weber K.A., Urrutia M.M., Churchill P.F., Kukkadapu R.V., and Roden E.E. (2006) Anaerobic redox cycling of iron by freshwater sediment microorganisms. *Environmental Microbiology* **8**, 100-113.

6. Appendix

The DVD contains the raw thesis data and plots. Please find corresponding data for each figure in chapter folders.

